

ET
1428

STATIC LOAD VERSUS SETTLEMENT
FOR SQUARE AND RECTANGULAR PLATES ON COHESIONLESS SOIL

THESIS

Presented to the Faculty of Engineering and Architecture of
the American University of Beirut in Partial Fulfilment
of the Requirements

For the Degree of

MASTER OF ENGINEERING

MAJOR - CIVIL

by

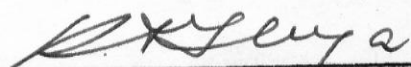
Ahmed Salim Najm, B.C.E.

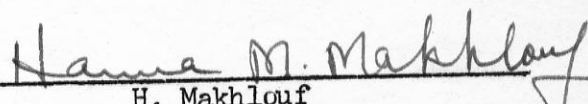
Beirut, Lebanon

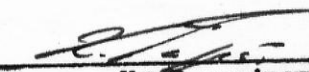
March 1968


STATIC LOAD VERSUS SETTLEMENT
FOR SQUARE AND RECTANGULAR PLATES ON COHESIONLESS SOIL

APPROVED:


Supervising Professor - R. Iliya


H. Makhlouf


H. Papazian


T. Searle

ACKNOWLEDGEMENTS

The author wishes to express his sincerest appreciation and acknowledgement to Professor Raja A. Iliya, Professor of Civil Engineering, under whose direction this research was performed, for his invaluable assistance and encouragement in all phases of the study and in the preparation and review of the manuscript; to Professor Terence R. Searle, Assistant Professor of Civil Engineering, whose helpful suggestions and constructive criticisms contributed greatly to completing this work; and to Professor Hratch Papazian, Assistant Professor of Civil Engineering, for his help in explaining some experimental phenomena and procedures.

Finally, the author wishes to record his thanks and indebtedness to the Soil Mechanics Laboratory Staff for their hearty cooperation.

ABSTRACT

This investigation deals with bearing capacities and settlements of rigid, smooth, square and rectangular plates, under static, vertical loads, on the horizontal surface of dense sand. It discusses the influence of the following factors on ultimate bearing capacity, settlement at the ultimate bearing capacity, and coefficient of subgrade reaction:

- a) The ratio of the dimensions of the cubical soil bed to the width of the square plate
- b) The side length of the square plates
- c) The ratio of the length to the width of the plates
- d) The ratio of the depth of the soil bed to the side length of the square plates

Experimental results are compared with theoretical values.

For this dense state of sand (relative density equal to 0.798) it is found that for square plates the ratio of the dimensions of the cubical soil bed to the width of the plate has to be at least ten so that the soil container may not influence the bearing capacity and settlement. The ultimate bearing capacity is directly proportional to the width of the plates, while the corresponding settlement bears a higher

ABSTRACT

This investigation deals with bearing capacities and settlements of rigid, smooth, square and rectangular plates, under static, vertical loads, on the horizontal surface of dense sand. It discusses the influence of the following factors on ultimate bearing capacity, settlement at the ultimate bearing capacity, and coefficient of subgrade reaction:

- a) The ratio of the dimensions of the cubical soil bed to the width of the square plate
- b) The side length of the square plates
- c) The ratio of the length to the width of the plates
- d) The ratio of the depth of the soil bed to the side length of the square plates

Experimental results are compared with theoretical values.

For this dense state of sand (relative density equal to 0.798) it is found that for square plates the ratio of the dimensions of the cubical soil bed to the width of the plate has to be at least ten so that the soil container may not influence the bearing capacity and settlement. The ultimate bearing capacity is directly proportional to the width of the plates, while the corresponding settlement bears a higher

proportional value. The ultimate bearing capacity as well as the corresponding settlement increases with the increase in the ratio of the length to the width of a rectangular plate. The ratio of the depth of the soil bed to the side length of a square plate in model studies must be at least ten if bottom effects are to be neglected. The minimum settlement of a footing at the ultimate bearing capacity occurs when a sand layer of four times the width of the footing is underlain by solid strata. Finally Terzaghi's coefficients for bearing capacity can be applied conservatively to the sand used in this investigation.

TABLE OF CONTENTS

	Page
Abstract	iv
Symbols and Notations	viii
List of Tables	x
List of Figures	xi
Chapter I, Introduction	1
Art. 1.1 General	1
Art. 1.2 Objectives and Scope of Investigation	1
Art. 1.3 Foundation Elements and Foundation Medium Used	3
Chapter II, Theoretical Considerations	6
Art. 2.1 Introduction	6
Art. 2.2 The Bearing Capacity of Foundations	8
Art. 2.3 Settlement Analysis of Surface Footings	17
Art. 2.4 The Theory of Subgrade Reaction	20
Chapter III, Testing Equipment	23
Art. 3.1 Soil Containers	23
Art. 3.2 Loading Machine	24
Art. 3.3 Vibrator	26

Chapter IV, Description of Tests	31
Art. 4.1 Placing of Sand and Control of Density	31
Art. 4.2 Determination of the Angle of Internal	32
Friction of the Sand	
Art. 4.3 Standard Procedure For Load-Settlement Tests	34
Chapter V, Results and Discussion	36
Art. 5.1 Influence of Dimensions of Soil Container	36
Art. 5.2 Influence of Plate Dimensions	52
Art. 5.3 Influence of Footing Length	62
Art. 5.4 Influence of Depth of Soil Bed	74
Art. 5.5 Experimental Versus Theoretical Results	82
Chapter VI, Conclusions	84
Appendices	87
A. Computations of N_g For Plates	88
B. Computations of the Relative Density of Sand	106
C. Tables of Results From Literature	110
Bibliography	116

SYMBOLS AND NOTATIONS*

- B** Diameter or width of the footing, ft. or in.
- C_a Force of cohesion, lbs.
- C_u Uniformity coefficient.
- c Unit cohesion of the soil, lb/ft^2 .
- D_f The vertical distance between the surface of the ground and the base of the footing, ft.
- D_r Relative density of the sand.
- D_{10} Effective size.
- e Void ratio.
- k_s Coefficient of subgrade reaction tons/ft^3 or lb/in^3 .
- \bar{k}_{s1} Coefficient of subgrade reaction for a 1 x 1 - ft. square plate, tons/ft^3 or lb/in^3 .
- N_c Dimensionless bearing capacity coefficient.
- N_γ Dimensionless bearing capacity coefficient.
- N_q Dimensionless bearing capacity coefficient.
- p Pressure per unit of surface area, lb/ft^2 or lb/in^2 .
- P_p Passive force, lbs.
- q Load per unit of area, lb/ft^2 or lb/in^2 .
- q_0 Ultimate bearing capacity lb/ft^2 or lb/in^2 .
- Q Total vertical force, lb.

- r Ratio of the dimensions of the cubical soil bed to the width of the square plate.
- R Radial force, lbs.
- S Settlement, ft. or in.
- γ Unit weight of soil, lb/ft³.
- ϕ Angle of internal friction, degrees
- ψ Angle of rise of lower boundary of central zone under a loaded strip footing, degrees.

*When these symbols or others are used in a special sense, they are explained on the figure where they appear.

LIST OF TABLES

		Page
1.	Coefficients of subgrade reaction for a 1-ft x 1-ft square plate resting on sand (24)	21
2.	Inner dimensions of boxes used in this investigation	23
3.	Sand dimensions used with 1 x 1 - in. square plate	36
4.	Significant results of loading tests with a square plate in different containers.	48
5.	Significant results of loading tests with square plates.	58
6.	Sand dimensions for rectangular footings	62
7.	Significant results of loading tests with rectangular plates.	68
8.	Experimental versus theoretical results, from Iliya (24)	111
9.	Experimental versus theoretical results, from Selig and Mckee (35).	112
10.	Experimental versus theoretical results, from Meyerhoff (33).	113
11.	Significant results of loading tests with circular plates at the surface, from Vesic (2).	114
12.	Experimental versus theoretical results, from Davis and Woodward (36)	115

LIST OF FIGURES

	Page
1. Foundation elements tested in this investigation . .	4
2. Grain size accumulative curve	5
3. Types of failure	7
4. Prandtl's plastic equilibrium theory for long areas	10
5. Terzaghi's plastic equilibrium theory for continuous footings.	13
6. Coefficients of the Terzaghi expressions for ultimate bearing capacity.	15
7. Pressure distribution under rigid and flexible footings	18
8. General view of the boxes used in this investigation .	25
9. Testing equipment	27
10. Vibrator used	29
11. Relation between density of sand and its angle of inter- nal friction.	33
12. Average load-settlement curve for 1 x 1 - in. square . . plate in box No.1.	37
13. Average load-settlement curve for 1 x 1 - in. square . . box No.2.	38
14. Average load-settlement curve for 1 x 1 - in. square . . plate in box No.3.	39

15.	Average load-settlement curve for 1 x 1 - in. square in box No.4.	40
16.	Average load-settlement curve for 1 x 1 - in. square in box No.5.	41
17.	Average load-settlement curve for 1 x 1 - in. square in box No.6.	42
18.	Average load-settlement curve for 1 x 1 - in. square plate in box No.7.	43
19.	Average load-settlement curve for 1 x 1 - in. square plate in box No.8.	44
20.	Average load-settlement curves for 1 x 1 - in. square plate in the different boxes of sand.	45
21.	Influence of dimensions of soil container on: ultimate bearing capacity, settlement at ultimate bearing capacity and coefficient of subgrade reaction.	49
22.	Average load-settlement curve for $\sqrt{2} \times \sqrt{2}$ - in. square plate.	54
23.	Average load-settlement curve for $\sqrt{3} \times \sqrt{3}$ - in. square plate.	55
24.	Average load-settlement curve for 2 x 2 in. square plate	56
25.	Average load-settlement curves for the different square plates tested.	57

26.	Influence of footing dimensions for square footings on: ultimate bearing capacity, settlement at ultimate bearing capacity and coefficient of subgrade reaction.	59
27.	Average load-settlement curve for 1 x 2 - in. . . . rectangular plate.	64
28.	Average load-settlement curve for 1 x 3 - in. . . . rectangular plate.	65
29.	Average load-settlement curve for 1 x 4 - in. . . . rectangular plate.	66
30.	Average load-settlement curves for the different. . . . rectangular plates tested.	67
31.	Effect of footing length on: ultimate bearing capacity, settlement of ultimate bearing capacity and coefficient of subgrade reaction.	69
32.	Effect of soil depth at ultimate bearing capacity .	75
33.	Effect of soil depth on the settlement of ultimate bearing capacity.	76
34.	Effect of soil depth on coefficient at subgrade . reaction.	77

35.	Terzaghi's solution of the bearing capacity coefficient N_{γ}	91
36.	Diagram of forces	92
37.	Failure surfaces for a strip footing for a rise angle . ψ equal to ϕ .	94
38.	Failure surfaces for a strip footing for a rise angle ψ equal to $45 + \phi/2$.	100

CHAPTER ONE

INTRODUCTION

1.1 General

A foundation is the connecting link between soil and the superstructure. The importance of this link is self-evident, since no structure can endure without an adequate foundation. To serve its purpose, it must be adequately designed to satisfy two requirements; first, failure by plunging into the soil must be avoided, and secondly settlements must be maintained within the limits safely tolerated by the superstructure.

The subject of foundation requires the study of the behavior of the various shapes and sizes of footings under static loading on various types of soil. Such a study requires the use of models, since in general prototypes are too large to be handled in the laboratory. Cohesionless soils only are considered in this investigation.

1.2 Objectives and Scope of Investigation

This research was performed to study the following five objectives:

- a) The minimum size of sand container where the sides of the

box can be considered to have no effect on bearing capacity or settlement i.e. the sand can be considered infinite in the analysis.

- b) Applicability of Terzaghi's coefficients N_γ to local sand.
- c) The effect of varying the size of the footing on ultimate bearing capacity and settlement.
- d) The effect of varying the shape of the footing.
- e) The effect of varying the ratio of the depth of the soil bed to the side length of square footings on ultimate bearing capacity and settlement, keeping in mind that all variables except the one studied are to be kept constant.

To achieve these objectives, cubical boxes of sand of dimensions ranging from 3 - to 12 - times the size of the footing were used. The ultimate bearing capacity was compared with the value obtained using Terzaghi's equations. Four sizes of square plates were studied in cubical boxes of sand of edges six times the size of the plate. Four rectangular plates were investigated using sand boxes having the length and the width six times the corresponding plate dimensions, and a depth of six times the width of the plate. Then for two sizes of square plates the effect of varying the ratio of the depth of the soil bed to the side of the plate (keeping horizontal dimensions six times the side of the plate) on ultimate bearing

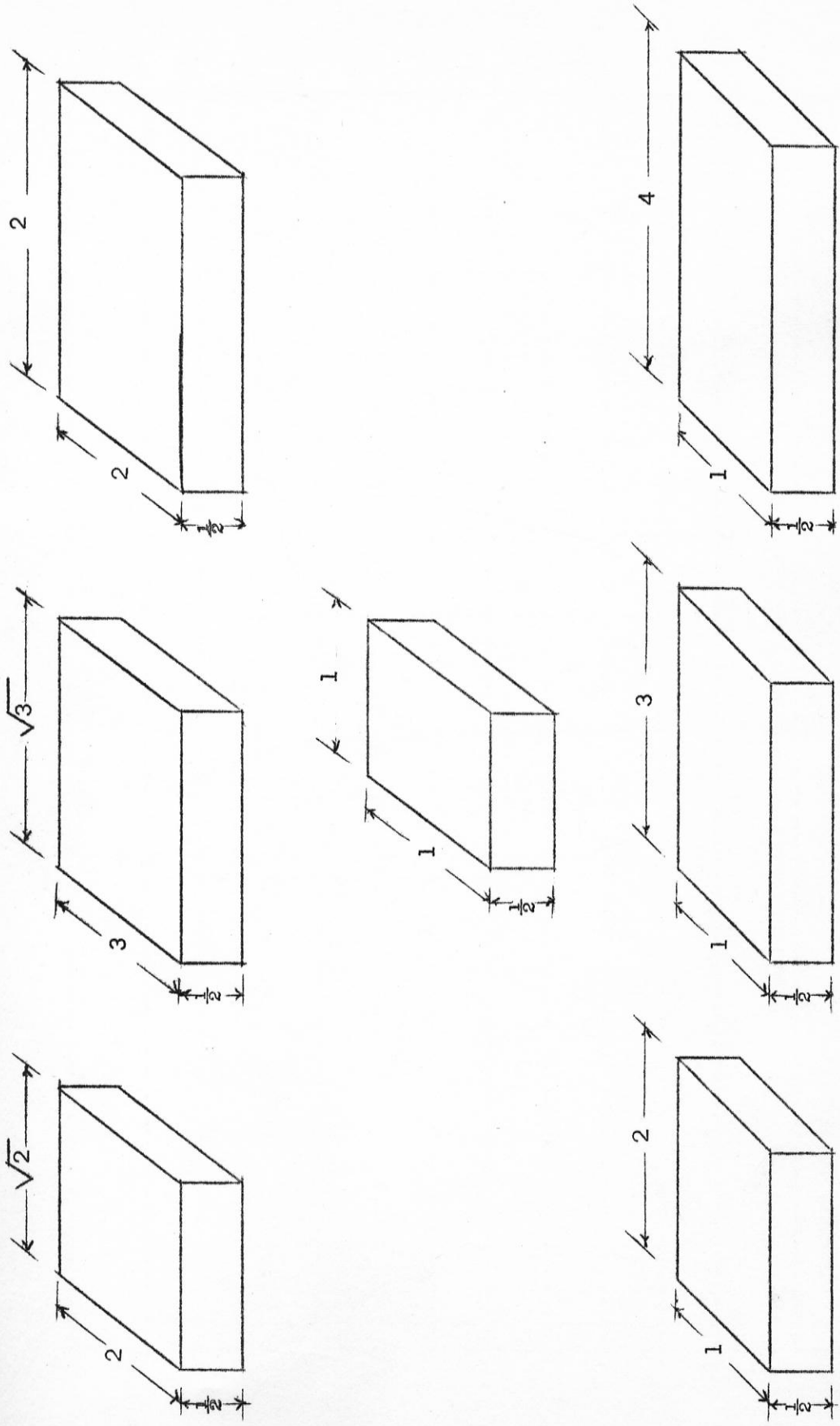
capacity, corresponding settlement, and coefficient of subgrade reaction was studied.

1.3 Foundation Elements and Foundation Medium Used

Square and rectangular plates were selected for the foundation elements. These are shown with their sizes in Fig. 1. They were made of aluminium alloy. Great care was taken to make them as smooth as possible. Being $\frac{1}{2}$ inch thick in such small sizes they were considered to be rigid.

The foundation medium used was local sand. A sufficient amount was brought from Khalde and dried for 24 hours in an electric oven kept at 110°C . The portion passing U.S. Standard Sieve No.20 was kept in covered vessels under normal conditions and was uncovered only during experimenting.

Examined under a magnifying glass, the sand grains showed angular shapes. Moreover, the sand was found to be quite rich in quartz and is of uniform distribution having a uniformity coefficient " C_u " of 1.24. 1.6 percent passed U.S. Standard Sieve No.100 and only 0.3 percent was finer than No.200 Sieve. Mostly it was fine sand of effective size D_{10} of 0.238 mm. The grain size distribution curve of the sand is shown in Fig. 2.



Note - All Dimensions Are In Inches

FIG. 1 FOUNDATION ELEMENTS

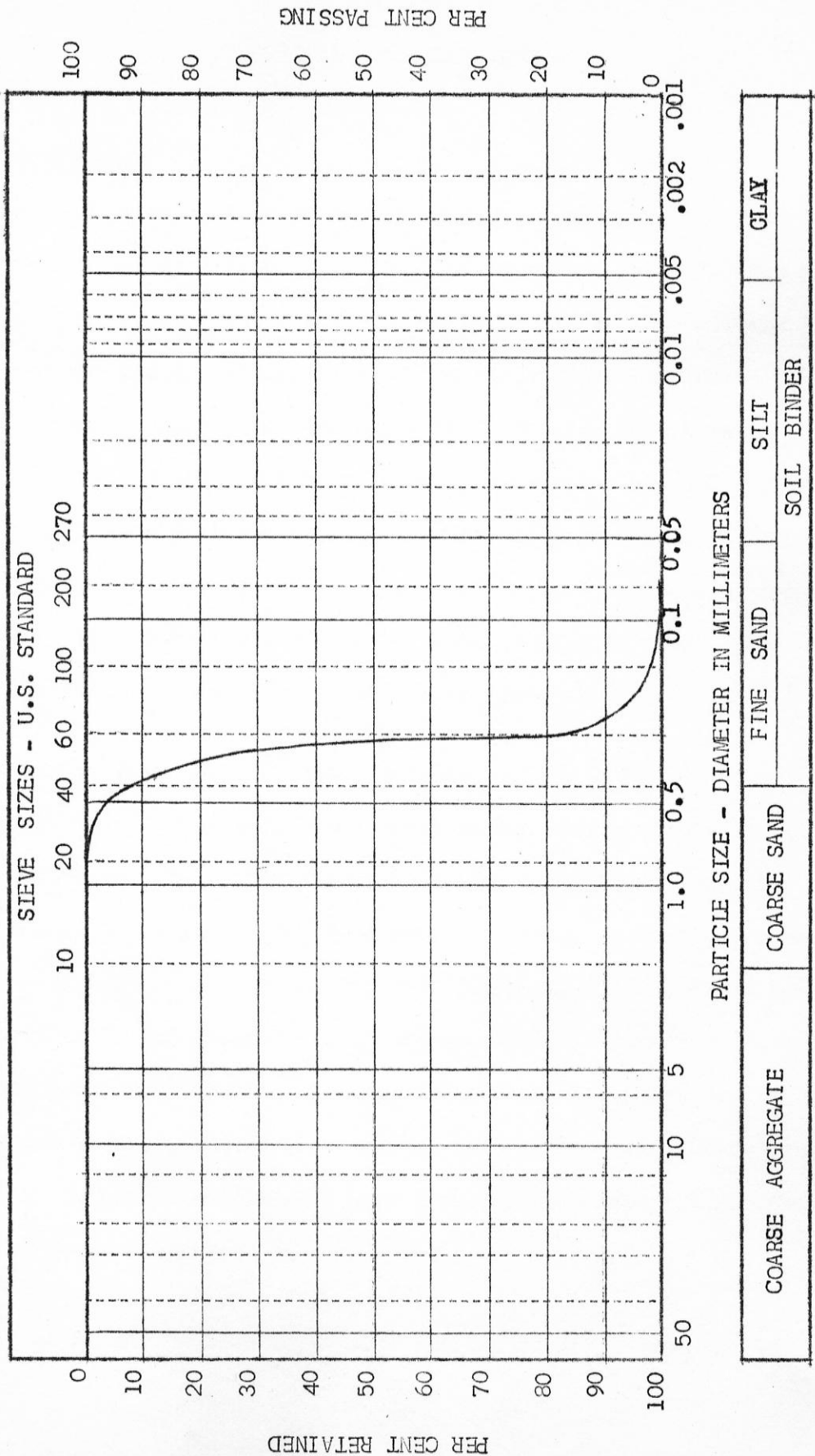


FIG. 2 MECHANICAL ANALYSIS
GRAIN SIZE ACCUMULATIVE CURVE

CHAPTER TWO

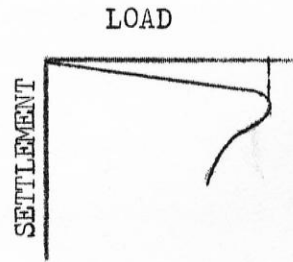
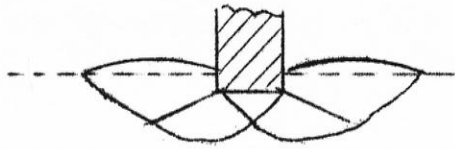
THEORETICAL CONSIDERATIONS

2.1 Introduction

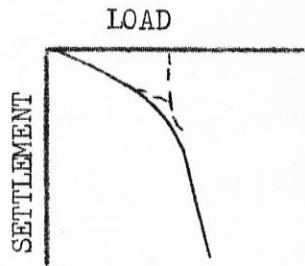
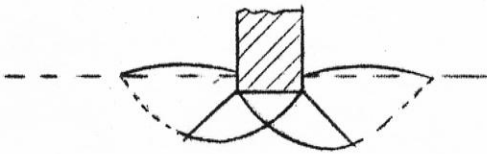
The load settlement relationship of a rigid plate is studied both theoretically and experimentally. Shallow footings, i.e. footings whose width is equal to or greater than the vertical distance D_f between the surface of the ground and the base of the footing are considered (1)*. Under increasing loads such footings exhibit three characteristic types of failure (2). Foundations on relatively dense sand ($D_r > 0.70$) fail suddenly with very pronounced peaks of base resistance (Fig. 3a). The failure is accompanied by the appearance of failure surfaces at the sand surface and by considerable bulging of sheared mass of sand. This phenomenon is described by Terzaghi (1) as "general shear failure."

Foundations on sand of medium density ($0.35 < D_r < 0.70$) do not show a sudden failure (Fig. 3b). But small sudden shears within the sand mass are apparent from observations of load and settlement gages. Simultaneously, bulging of the sand surface starts. However, the peak of base resistance may never be reached. Terzaghi (1) describes this phenomenon as "local shear failure" and specifies arbitrarily, "but in accordance with current conceptions, that the earth support has failed as soon as the load settlement curve passes into a steep and fairly straight tangent". De Beer and Vesic (3) give also the same description (rupture par refoulement incomplet).

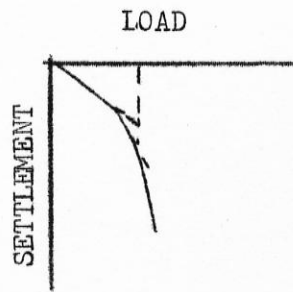
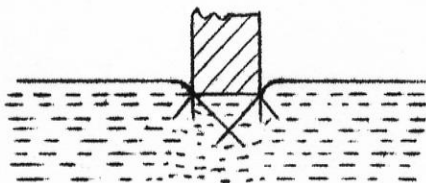
*Numbers in paranthesis refer to papers cited in Bibliography.



(a)



(b)



(c)

FIG. 3 TYPES OF FAILURE

Finally, foundations on relatively loose sand ($D_r < 0.35$) penetrate into the soil without any bulging of the sand surface (Fig. 3c). The base resistance steadily increases as the settlement progresses. Sudden shears can be observed for large settlements. The failure surface, which is vertical or slightly inclined and follows the perimeter of the base, never reaches the sand surface. The phenomenon is essentially "punching shear failure", as described by De Beer and Vesic (3).

Referring to Fig. 3, the early part of the curve is almost a straight line in all types of failure, and it forms the basis of the theory of subgrade reaction.

In this chapter, the theoretical considerations for (a) bearing capacity, (b) settlement analysis and (c) subgrade reaction are briefly discussed.

2.2 The Bearing Capacity of Foundations

A- Introduction

The bearing capacity of foundations is a function of the following factors (5):

1- Mechanical properties of the soil:

- a) Density
- b) Shearing strength
- c) Deformation characteristics
- d) Size and shape of grains
- e) Permeability of the soil

2- Physical characteristics of the foundation

- a) Size
- b) Depth
- c) Shape
- d) Roughness of the base
- e) Rigidity of the base

3- The original stresses in the soil

4- The water conditions in the ground

5- The way in which the foundation is installed

6- The rate and direction of loading

The factors indicate clearly that the wide spread idea that the bearing capacity of a soil depends mainly on the characteristics of the soil in question is incorrect. Although the main difficulty in bearing capacity problems is in indentifying the soil properties yet the previously mentioned factors are to be considered if a correct solution is to be obtained and the attempt in building codes to give bearing capacity values depending on soil characteristics without due allowance to the other factors is totally erroneous.

B- Theory of Bearing Capacity for Shallow Footings.

The solution of the problem of bearing capacity of the base of a footing has been sought in the past primarily by an approach based on the classical work by Prandtl (6,7), and Reissner (8). They presented a solution of the problem of penetration of a rigid stamp into an incompressible (rigid-plastic) solid (Fig. 4). That solution was first applied to the

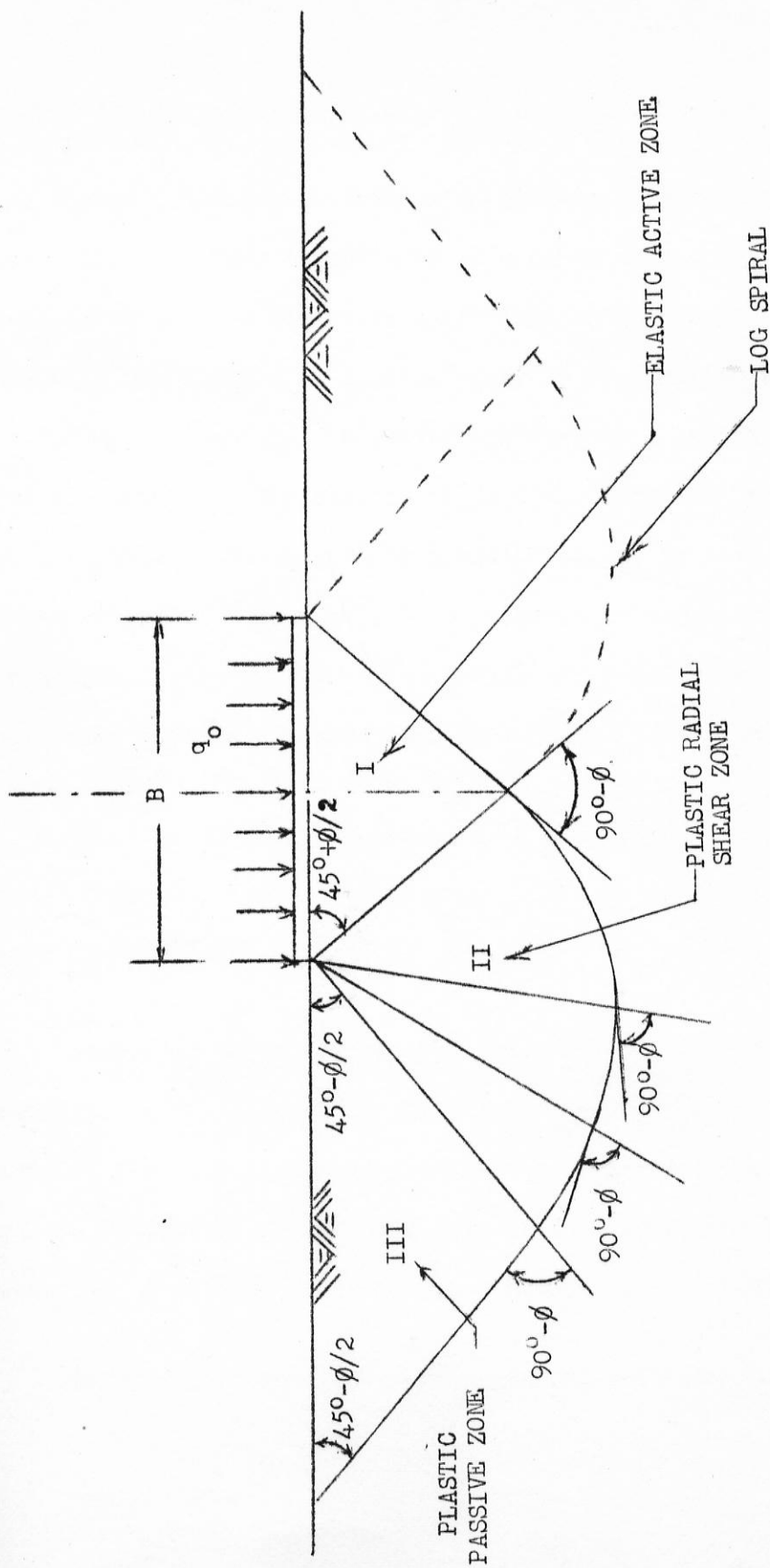


FIG. 4 PRANDTL'S PLASTIC EQUILIBRIUM THEORY FOR LONG AREAS

problem of bearing capacity of soils by Caquot (9) and Buisman (10).

Figure 4 shows a cross-section illustrating Prandtl's plastic equilibrium theory (11) for long loaded area of width B on the surface of soil. The figure shows three zones which exist after failure is reached. Zone I moves downward with the footing as a unit. Zone II is plastic in which radial planes are failure planes and the curved boundary is a logarithmic spiral provided that the weight of the soil is neglected. Zone III is forced by passive pressure upward and outward as a unit. It may be noted that all failure planes are at $45 \pm \frac{\phi}{2}$ to principal planes. On the basis of these assumptions and applicability of Coulomb's Law (12) to shearing strength of soils, Prandtl's expression for the ultimate bearing capacity of any soil is (11):

$$q_o = \left(\frac{c}{\tan \phi} + \frac{1}{2} \gamma B \sqrt{K_p} \right) (K_p e^{\pi \tan \phi} - 1)$$

where $K_p = \frac{1 + \sin \phi}{1 - \sin \phi}$

Because of their compressibility, soils do not show close agreement with Prandtl's hypothesis, which was originally set up for metals, and in actual cases of footings loaded to failure the region corresponding to Zone III is much narrower than is shown in Fig. (4). However the general concepts of the mechanics of failure given by this theory are reasonably correct.

Terzaghi (1) presented a more general solution for the ultimate

bearing capacity of long rectangular rough footings. Figure 5 shows the failure zones and surfaces assumed by this theory. He observed (13) that the ultimate normal load that could be applied to the soil surface could be approximately estimated by superposing the limit stresses obtained for the following cases: (a) for weightless soil whose ability to sustain a surface stress depends only on the presence of a surcharge, (b) for soil having weight, in the absence of surcharge, and (c) for soil lacking weight, but possessing cohesion. Following his method, the normal stress due to item (b) is considered to vary linearly with distance from the edge of the footing. Because the basic system of equations describing the yield problem is nonlinear, such a superposition method does not lead to a correct solution, but in many instances it enables one to find an approximate answer without the labor involved in solving the problem by numerical methods. Sokolovski (14) studied the superposition of these individual limiting conditions and concluded that the total stresses obtained at yield by summing the stresses at yield in the separate cases (a) through (c) above satisfy the appropriate equations of equilibrium. However, because of the non-linearity of the equations he found that the yield condition for the superimposed stresses is that holding for a material whose angle of friction is smaller than the angle employed in obtaining the component stress states. Thus, for most materials, the superposition solution will not correspond to the solution which would be found by means of a single "exact" analysis in which all material properties were included; the superposition solution yields a conservative result.

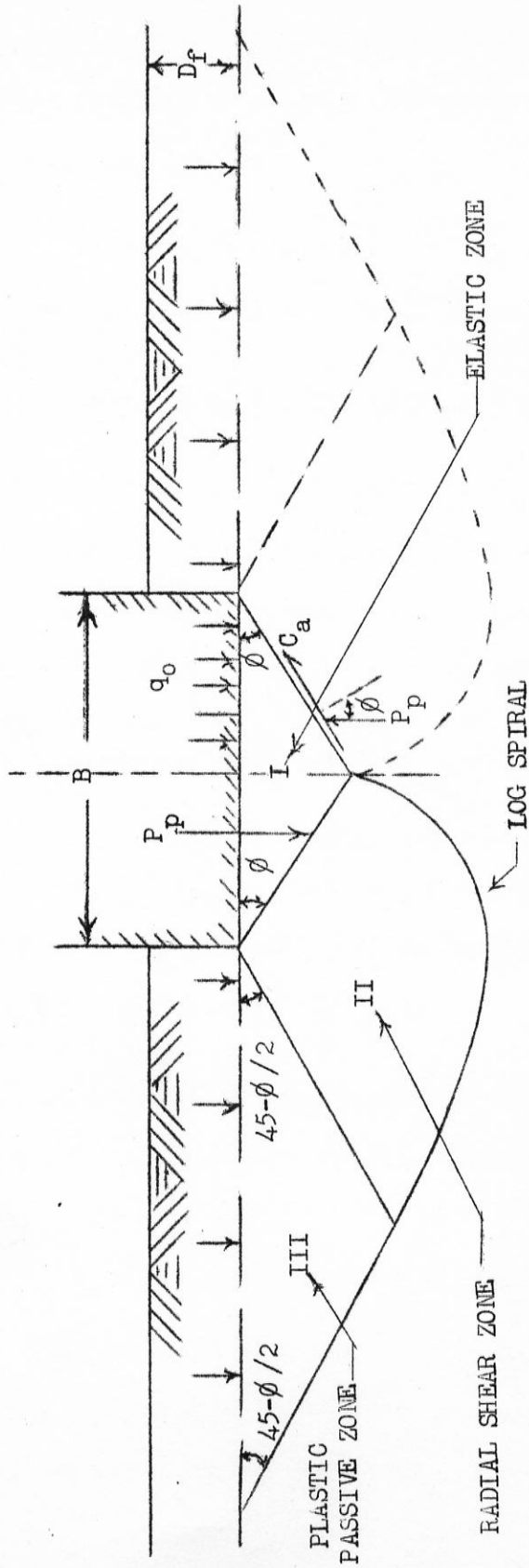


FIG. 5 TERZAGHI'S PLASTIC EQUILIBRIUM THEORY FOR CONTINUOUS FOOTINGS

Terzaghi's expression for the ultimate bearing capacity of long rectangular footings at or below the surface of any soil conforming to general shear is (1):

$$q_o = c (N_c) + \gamma B (\frac{1}{2} N_\gamma) + \gamma D_f (N_q)$$

and for any soil conforming to local shear the expression is

$$q_o = c (\frac{2}{3} N'_c) + \gamma B (\frac{1}{2} N'_\gamma) + \gamma D_f (N'_q)$$

In these equations the N coefficients, which are enclosed in parentheses, depend only on the friction angle and are given by the curves of Fig. 6 (11). (Appendix A shows the procedure and calculations of N_γ using $\phi = 45.2^\circ$ which corresponds to the angle of internal friction of the sand used in this investigation).

For a purely cohesive soil and surface footings the previous expressions become

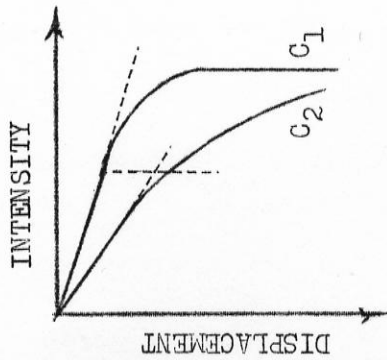
$q_o = c (N_c)$ and $q_o = c (\frac{2}{3} N'_c)$ respectively. For a purely cohesionless soil and surface footings they reduce to $q_o = \gamma B (\frac{1}{2} N_\gamma)$ and $q_o = \gamma B (\frac{1}{2} N'_\gamma)$ respectively.

From an analysis of experimental data Terzaghi obtained the following expressions for the ultimate bearing capacity for round and square shallow footings:

$$q_o = 1.3 c (N_c) + 0.6 \gamma B (\frac{1}{2} N_\gamma) + \gamma D_f (N_q) \quad \text{and}$$

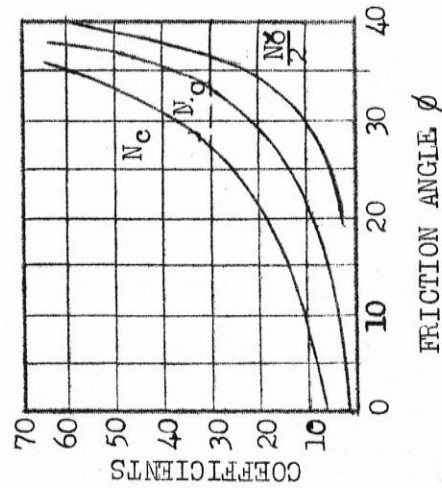
$$q_o = 1.3 c (N_c) + 0.8 \gamma B (\frac{1}{2} N_\gamma) + \gamma D_f (N_q) \quad \text{respectively.}$$

Wherein N_c , N_q , and N_γ represent the bearing capacity factors for continuous footings, supported by the same soil. For a purely cohesive soil with surface

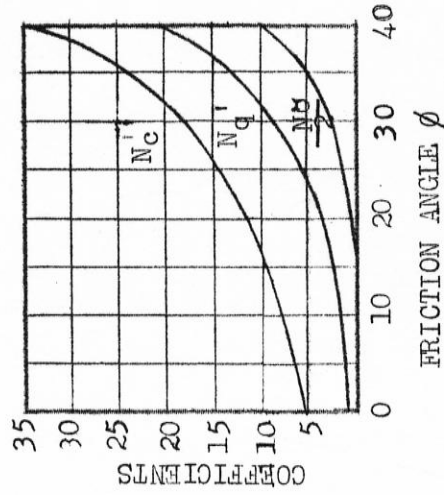


c_1 , general shear
 Use chart (b)
 c_2 , local shear
 Use chart (c)

(a)



(b)



(c)

FIG. 6 COEFFICIENTS OF THE TERZAGHI EXPRESSIONS FOR ULTIMATE BEARING CAPACITY

footings the previous expressions reduce to $q_0 = 1.3 c (N_c)$ in both cases, independently of the size of the footing. If the soil is purely cohesionless with footings on the surface, the expressions reduce to $q_0 = 0.6 \gamma B(\frac{1}{2} N_\gamma)$ and $q_0 = 0.8 \gamma B(\frac{1}{2} N_\gamma)$ respectively, directly proportional to the width of the footing.

If the soil is loose or very compressible, the bearing capacity factors N must be replaced by the values N' (Fig. 6c).

Many theories using the same general approach but different shear patterns have been presented in the literature (5, 13, 16, 17, 18). Another possible approach to the problem originated by the work of Bishop, Mill and Mott, (20), Skempton, Yassin and Gibson (21) and Ladnyi (26), who have considered the problem of expansion of a spherical or cylindrical cavity inside an infinite mass of an ideal solid. In such a case there exists around the cavity a highly stressed zone where the material, by assumption, behaves as a rigid-plastic solid. Outside that zone it behaves as an ideal elastic (or linearly deformable) solid. In spite of this, the approach of Prandtl and Terzaghi is still the predominant one. Theories following that approach offer only slight modifications to the theories of Prandtl and Terzaghi. Therefore, only these two theories are discussed and employed later as the basis for comparison with the experimentally observed data.

2.3 Settlement Analysis of Surface Footings

The pressure distribution under a footing depends on whether a rigid or a flexible footing is concerned, and for the same footing it varies with the type of soil whether it is a cohesive or cohesionless soil.

For a rigid footing resting on the surface of soil where no tilting is allowed, the settlement must be uniform. The pressure distribution under such footings is shown in Fig. 7 (a,b) for both cohesionless and cohesive soils (11).

In sand, under uniform settlement, the high resistance to compression in the soil below the centre of the footing, as compared to the lack of resistance to compression below the edge must result in a relatively large pressure under the centre and no pressure at the edge as shown in Fig. 7a. Owing to the lack of rigidity in sand, the shearing strains developed at the edges of the footings require little or no force to be produced. While in a cohesive soil large vertical forces are required to furnish the shearing strains. For an elastic material, the distribution shown by the theory of elasticity indicates an infinite stress at the edge of the footing. Actually an infinite stress cannot occur, but the stress at the edges may be much larger than that at the center (Fig. 7b).

For a flexible footing on the surface of a cohesionless soil, carrying a uniformly distributed load, the pressure distribution is also uniform resulting in larger settlement at the edges than at the center of the footing because below the center of the footing the soil

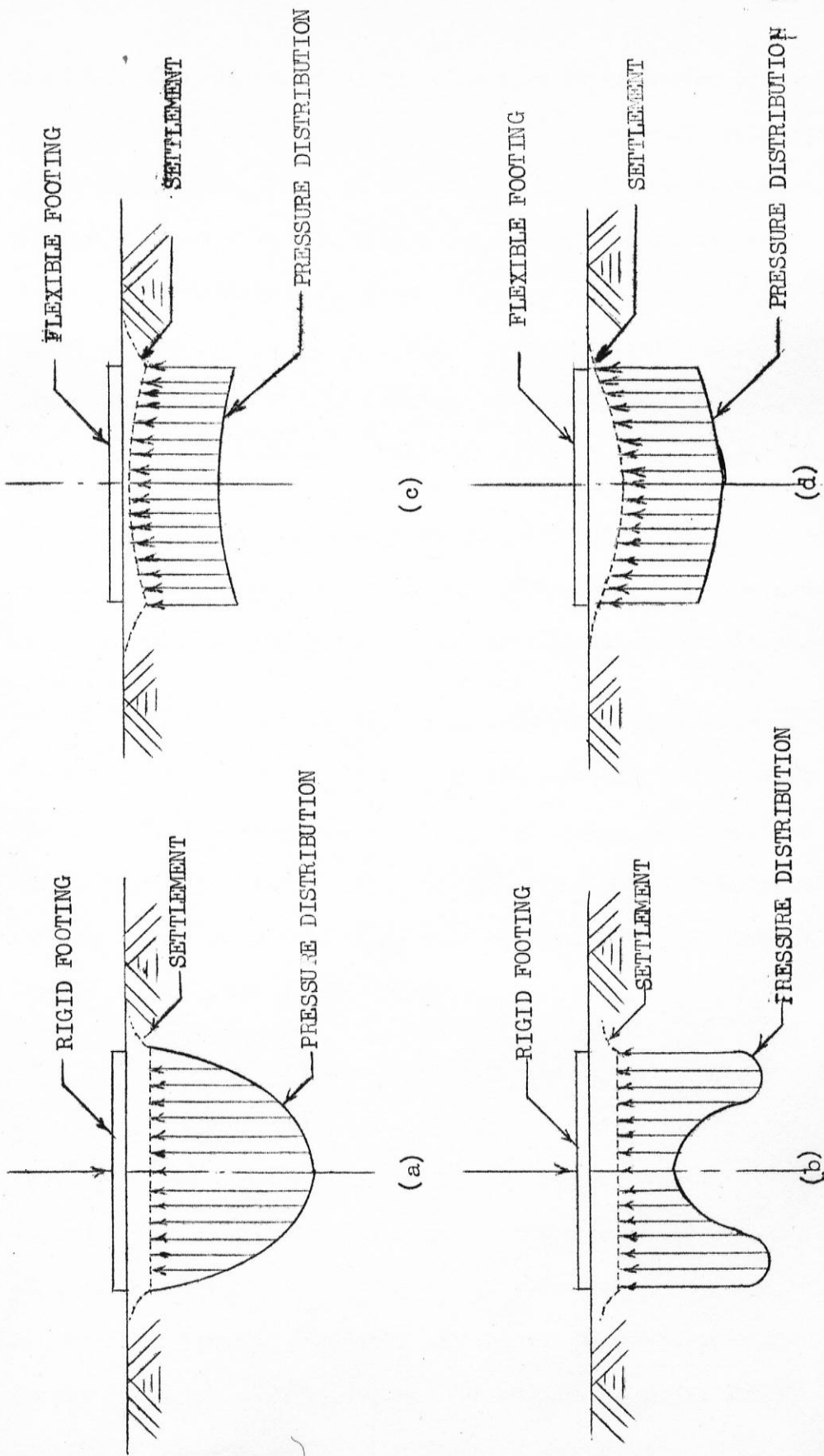


FIG. 7 PRESSURE DISTRIBUTION UNDER: RIGID FOOTINGS ON (a) SAND, (b) CLAY, AND FLEXIBLE FOOTINGS ON (c) SAND, (d) CLAY.

develops strength and rigidity as fast as it is loaded whereas it takes larger settlements for the required strength to develop at the edges (Fig. 7c). If the soil is highly cohesive the uniform surface distribution transmits a bell-shaped distribution of pressure to the subsurface layer. The greater stress below the center of the footing at this subsurface layer must cause a greater compressive strain at this location with much greater settlement under the center than under the edge of the footing. (Fig. 7d).

In estimating the settlement of a foundation on a clay soil, it is important to realize that the total movement is composed of the immediate settlement and the consolidation settlement.

The immediate settlement is that due to the compression of the solid matter i.e. it is the elastic settlement. However, Meyerhoff (23) considers the initial settlement to contain an elastic portion and a plastic one with the plastic deformation forming $\frac{1}{3}$ to $\frac{1}{2}$ of the total movements, depending upon loading with respect to ultimate bearing capacity.

The theory of settlement for saturated clay appears in Iliya's dissertation (24). Skempton (17) has shown that the greater part of the settlement is due to strains in the clay within a depth of not more than four times the diameter below the base of the footing. At greater depths of thick clays, the stresses are less than about 5 percent of the net foundation pressure. No comparable theory exists for a cohesionless soil; however, as discussed later, certain aspects of the settlement of a plate on cohesionless soil were considered in this investigation.

2.4 The Theory of Subgrade Reaction

A definite characteristic of many plate loading tests is the early straight line portion extending to intensities of roughly one third or one half of the ultimate intensity. The ratio between the stress and the settlement of points on the line has a definite constant value. This ratio is called coefficient of settlement or coefficient of subgrade reaction. The latter term is used in the field of pavement design. It is a function of the elastic properties of the subgrade as well as the dimensions of the loaded area (25).

Terzaghi's theory (4) of subgrade reaction is based on the following simplifying assumptions:

- a- The modulus of subgrade reaction k_s is independent of the pressure, and
- b- It has the same value for every point of the surface acted upon by the contact pressure.

For a rigid foundation where settlement is the same at all points and with assumption (b) the pressure should be uniform, which is contrary to reality.

In spite of the discrepancy between theory and reality, the theory of subgrade reaction can be used safely in the design of footings. The errors are within the margin of safety and on the conservative side.

For a highly cohesive soil contact settlement is proportional to the width of the footing (11), consequently the coefficient of subgrade reaction k_s is inversely proportional to the width of the

footing. This agrees well with experiments done by Goodman, Hegedus and Liston (26) and Skempton (27,17). For a cohesionless soil strength as well as settlement increases with the size of the footing, so k_s may be expected to vary less than in the case of a cohesive soil.

Terzaghi (4) gives values of \bar{k}_{s1} in tons per cu. ft. for 1 x 1 ft. square footing resting on clay and sand; but since this investigation deals with sand only \bar{k}_{s1} value of sand are given in table 1.

TABLE 1. (24)

Values of \bar{k}_{s1} in Tons/ft³

Relative Density of Sand	Loose	Medium	Dense
Dry or moist sand, limiting values	20 - 60	60 - 300	300 - 1000
Dry or moist sand, proposed value	40	130	500

Moreover he considers that the value k_{s1} for a beam with a width of 1 ft. resting on sand is roughly equal to that of a square plate, 1 ft. wide. For a beam with a width B feet k_s is determined by the equation:

$$k_s = \bar{k}_{s1} \frac{(1 + B)^2}{4 B^2}$$

The use of the theory of subgrade reaction has limitations due to the simplifying assumptions used in the derivation and values obtained are often too far from reality. A comparison of the theoretical values with values obtained in this investigation appears in chapter five.

CHAPTER THREE

TESTING EQUIPMENT

3.1 Soil Containers

The soil beds were placed in boxes made out of $\frac{3}{4}$ in. plywood covered from the inside with Formica. Hence the surfaces of the boxes were considered smooth and due to the low loads met and short lengths of boxes, any deformation of the boxes during loading was neglected. Boxes were provided with handles to facilitate transferring them from the place of the vibrator to that of the loading machine without any disturbance.

Eleven boxes were needed for the investigation. To refer to them easily each box was given a number. The following table shows the numbers and inner dimensions of the boxes.

Table 2

<u>Box No.</u>	<u>Inner Dimensions (Length x Width x Height, inches)</u>
1	3 x 3 x 6
2	4 x 4 x 7
3	5 x 5 x 8
4	6 x 6 x 13
5	7 x 7 x 10

<u>Box No.</u>	<u>Inner Dimensions (Length x Width x Height, inches)</u>
6	8.5 x 8.5 x 17
7	10.4 x 10.4 x 17
8	12 x 12 x 15
9	12 x 6 x 9
10	18 x 6 x 9
11	24 x 6 x 9

3.2 Loading Machine

The loading was applied electrically by the use of triaxial apparatus (Soil Test T-114). The triaxial chamber was taken off and all accessories not pertaining to loading were shut off. Hence the essential elements remaining were: the structural frame, the electric loading system, and the proving ring assembly for measurement of loads.

The structural frame is quite rigid and capable of supporting the heaviest box **used.**

The loading system is an electrically driven Transmission Unit which actuates the loading screw **through** a chain drive. This is provided with the Control Switch (load-off-release) which is located in a prominent position on the frame. The Speed Control Dial is connected to the transmission unit through a flexible shaft mounted on the frame and which can be adjusted to develop the desired speed. A set of Limit Switches

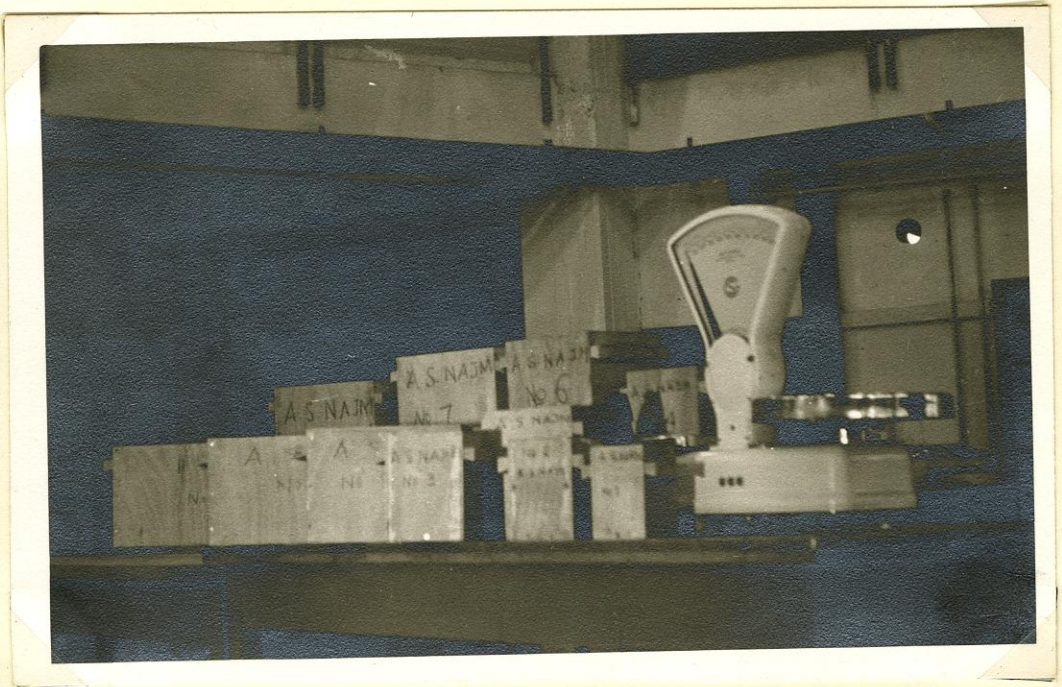


FIG. 8 GENERAL VIEW OF THE BOXES

are mounted on the feed screws to prevent damage to the apparatus through over-run of the loading screw.

The Proving Ring Assembly is attached to the loading screw.

A proving ring (Soil Test No.9988) with sensitivity for measuring down to 0.48 lbs., was fitted on the loading piston. The loading screw has an adjustable stroke of more than 6 in. range which is sufficient to produce ample settlement in all the foundation elements used. The settlement measurements were made with two extensometers with one half and two inches of travel. A division of the first corresponds to 0.0001" and that of the second to 0.001". This measure was taken to be able to record settlements accurately and to account for the larger settlements in the case of the larger footings. (See Fig. 9).

3.3 Vibrator

As the foundation soil had to be in a dense state vibration was a necessity. Syntron Semi-Noiseless Electric Vibrator was used (Fig. 10). This vibrator is made up of essentially two pieces of equipment - a vibrator, which is a pulsating electro-magnet, and a controller for operating the vibrator.

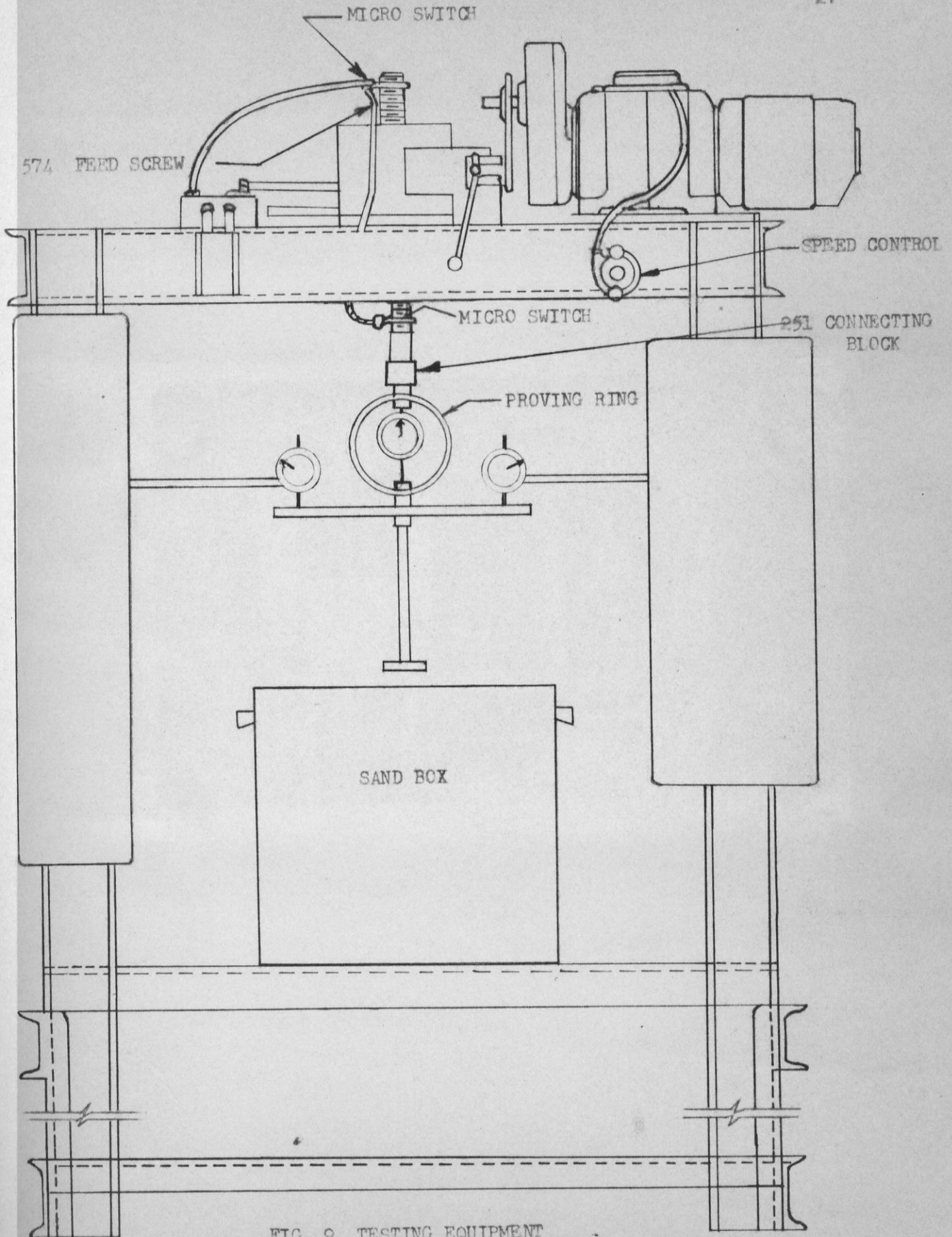


FIG. 9 TESTING EQUIPMENT

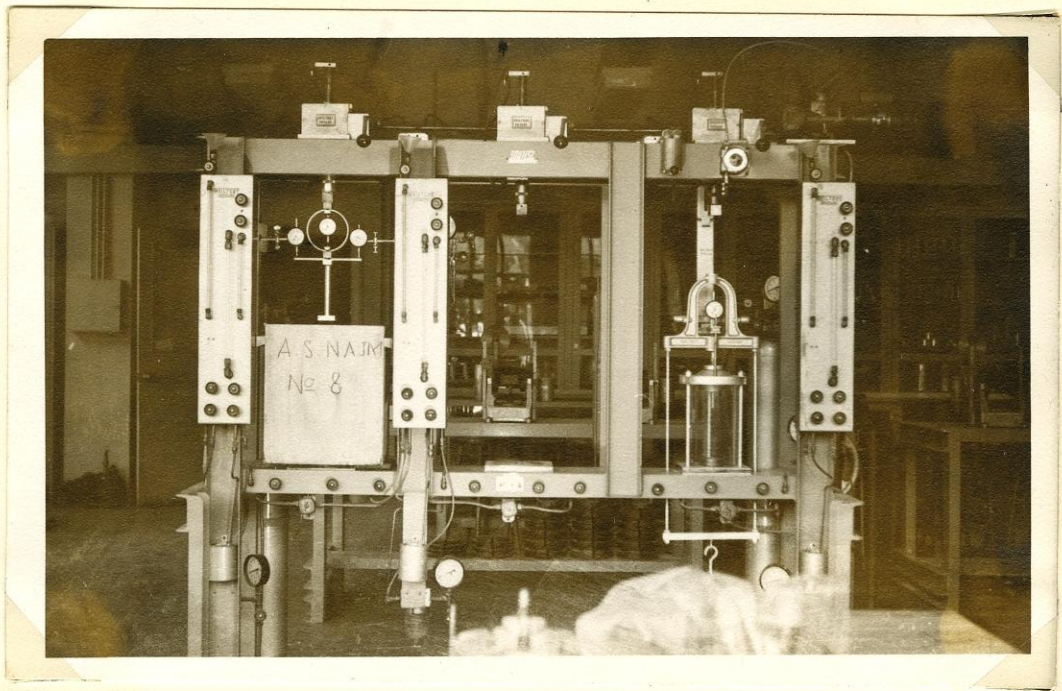


FIG. 9 TESTING EQUIPMENT



FIG. 10 VIBRATOR

Too much vibration tends to pack the material, consequently, the rheostat knob in the control should not be turned any higher than is actually required to move the material.

CHAPTER FOUR

DESCRIPTION OF TESTS

4.1 Placing of Sand and Control of Density

Density of the soil foundation is one of the critical factors affecting the load-settlement curves. Hence it has to be highly controlled for every test if comparable results are desired for the different shapes and sizes of footings.

The sand, being a cohesionless material, is best densified through vibration. For this the vibrator mentioned in Art. 3.3 was used.

Due to the different places of vibration and loading it was felt that if the relative density D_r of the sand was on the high side and if great care in transferring the boxes was taken, little or no disturbance of the sand after vibration will occur. So it was decided to use a density " γ " of 107 lb. per cu. ft. giving D_r equal to 0.798. Having decided on the density, and having fixed the dimensions of sand desired for the particular plate, it was possible to calculate the weight of the sand to put in any particular box for that particular plate in a given test. After deciding on the depth of the soil bed in a given box the height of sand was marked on the inside faces of that box by sticking

colored paper. To keep the faces smooth the paper extended from the top of the box to the desired height.

The amplitude of the vibrator was regulated for every weight of sand. The time of vibration was recorded as a check and the surface of the sand was watched until it reached the edge of the colored paper. Before every vibration, the box was emptied to disturb the structure of the sand. Due to the uniform nature of the investigated sand (Fig.2) layering during vibration was not felt to be a problem. As a check, sand put in different layers in box No.4 gave the same result as that obtained from the above mentioned procedure.

4.2 Determination of the Angle of Internal Friction of the Sand

Vacuum-triaxial tests were run on samples from the sand under investigation. These samples were 1.5 in. in diameter and 3.0 in. in height. The testing procedure recommended by Lambe (28) was followed. The densities of the sand varied from 97.4 to 113.1 lb./ft.³ The lateral pressure was obtained by applying a vacuum to the soil that varied up to a maximum of 11.41 psi. The test speeds were 0.06 in. per minute.

Figure 11 shows the relation between the density and the angle of internal friction. For a density of 107 lb./ft.³, (the density of the sand used in this investigation) the angle of

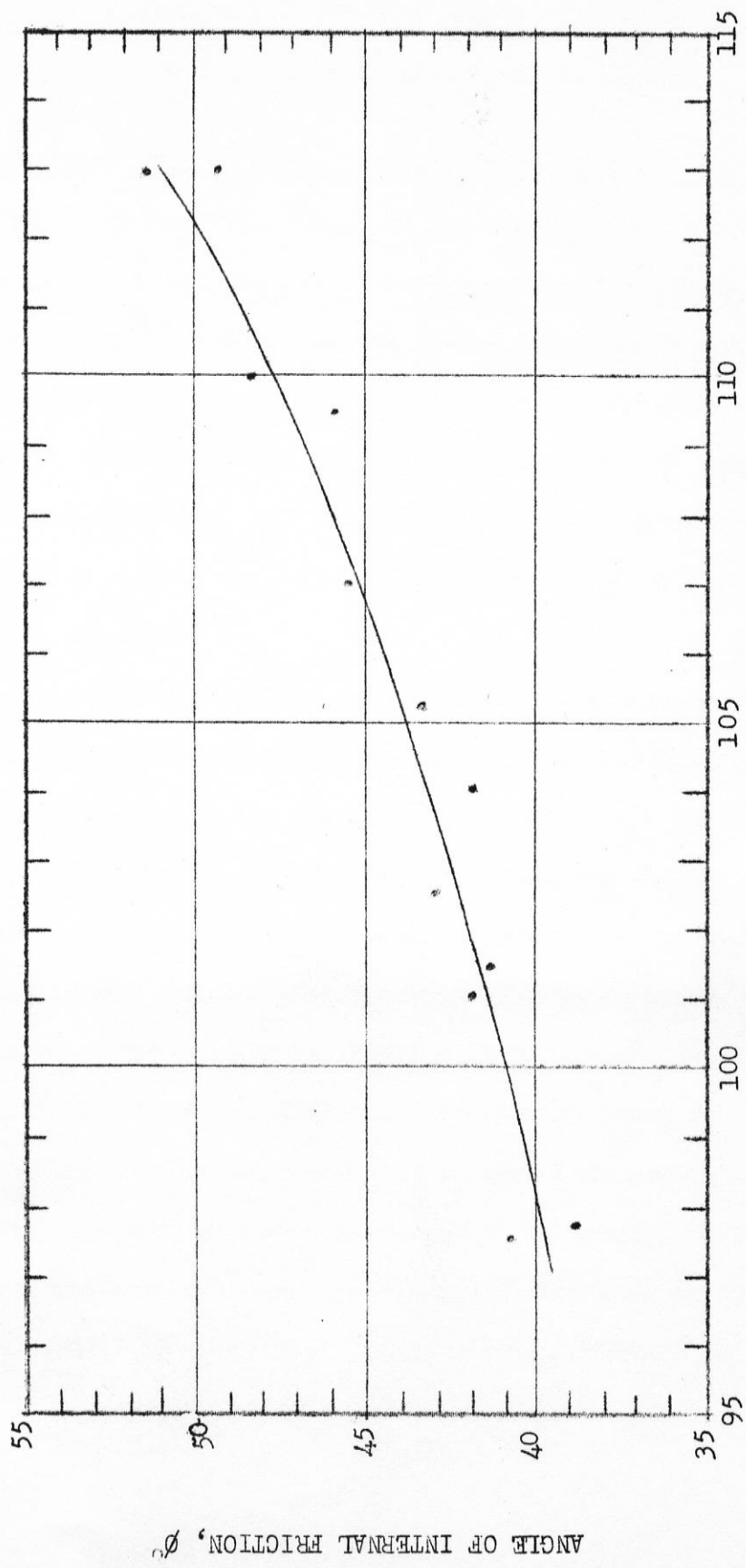


FIG. 11 RELATION BETWEEN DENSITY OF SAND AND ITS ANGLE OF INTERNAL FRICTION.

ANGLE OF INTERNAL FRICTION, ϕ

DENSITY OF SAND (LBS. PER CU. FT.)

internal friction ϕ is approximately equal to 45.2° .

4.3 Standard Procedure for Load-Settlement Tests

Due to the uniform vibration and horizontality of the table of the vibrator the surface of sand was obtained horizontal with little effort by keeping the box in the center of the table. This is important to get because the initial position of a footing with respect to the surface of sand has a great effect on the load-settlement curve (29, 30, 31). Great care was exercised to bring the footing element to just touch the surface of the sand without applying any load.

The speed of the motor of the loading machine was set to 0.06 in. per minute to correlate with that of the triaxial compression machine, the load and settlement dials were set to zero and the testing was started. The accepted loading rate in triaxial compression tests on cohesionless soils for static loading effects is that causing a strain of from $\frac{1}{4}$ to 2 percent per minute (32) being 2 percent for the machine used. This gives a speed rate of 0.06 in. per minute. Triaxial compression tests on one type of cohesionless soil showed only a 10 percent increase in strength when the duration of time from the start of loading to the time of maximum compressive stress was decreased from 1000 seconds to 0.01 seconds (32). No difference in results was observed for rates of

loading between $\frac{1}{4}$ and 2 percent per minute. Hence the results of this investigation are considered in the static load conditions, unaffected by the slow rates of loading.

The loading was continued after failure till the upper surface of the footing was level with the sand surface. Then the loading was stopped, the box emptied to disturb the structure of the sand and filled with the same sand again and the whole process of vibrating and loading using the same plate was repeated until a sufficient number of curves was obtained from which the average curve shown in this report was derived. Sometimes, when doubtful results were obtained, eight tests were performed. However, no fewer than four tests for any condition, were performed.

CHAPTER FIVE

RESULTS AND DISCUSSION

5.1 Influence of Dimensions of Soil Container

The load-settlement curves of the 1 x 1 in. square plate in boxes one through eight are studied and these are shown in figures 12 through 19. The sand dimensions in the different boxes are shown in the following table* :

Table 3

<u>Box No.</u>	<u>Sand Dimensions(Length X Width X Depth,inches)</u>
1	3 x 3 x 3
2	4 x 4 x 4
3	5 x 5 x 5
4	6 x 6 x 6
5	7 x 7 x 7
6	8.5 x 8.5 x 8.5
7	10.4 x 10.4 x 10.4
8	12 x 12 x 12

Vibration and loading follow the standard procedures (Art. 4.3).

The ratio of the settlement to the width of the plate was used in plotting the results of the load test for better comparison purposes. Figure 20 shows the curves of figures 12 through 19.

*Note: When a box number is mentioned in this article (5.1) the sand dimensions in that box are as indicated in table 3.

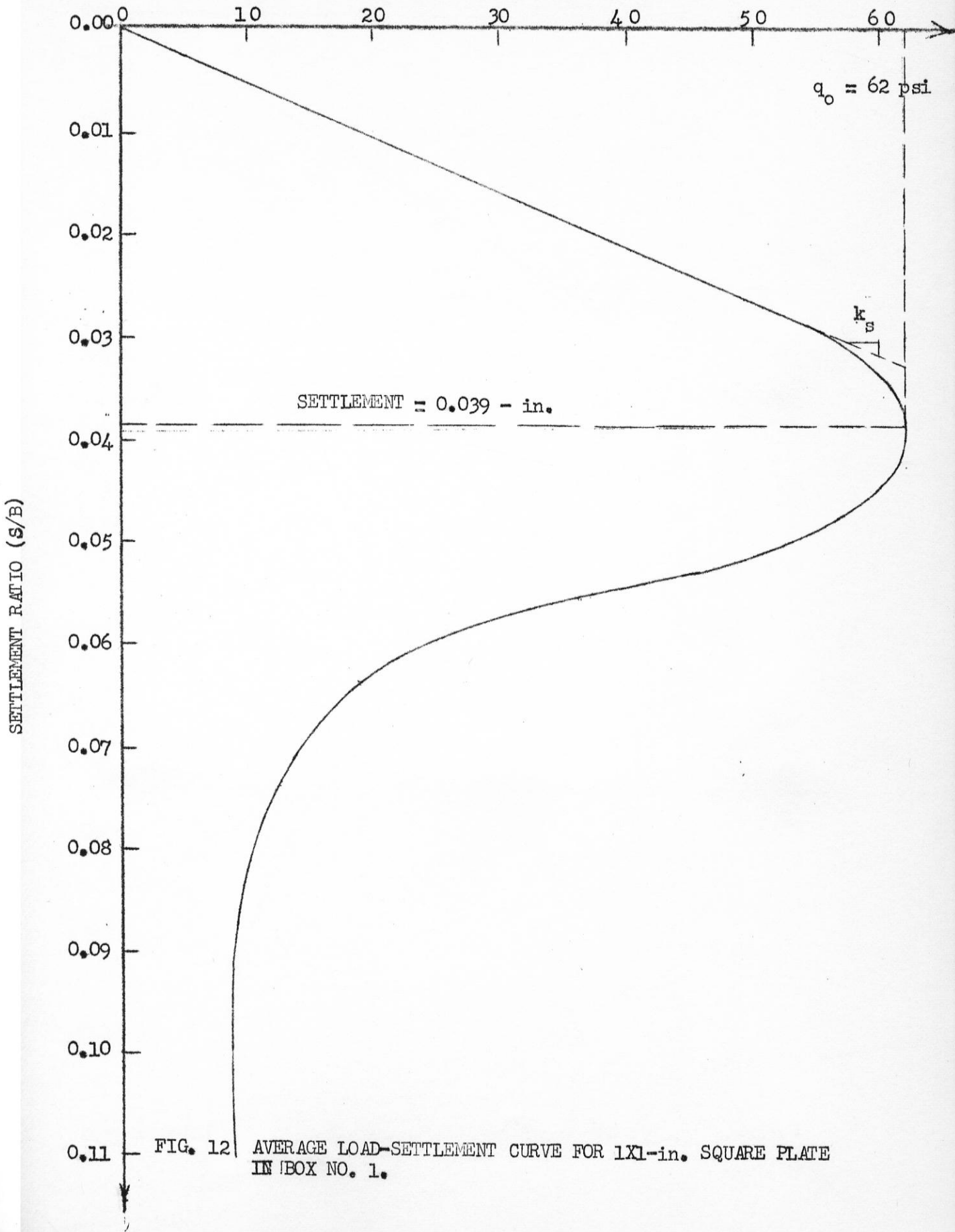


FIG. 12 AVERAGE LOAD-SETTLEMENT CURVE FOR 1x1-in. SQUARE PLATE IN BOX NO. 1.

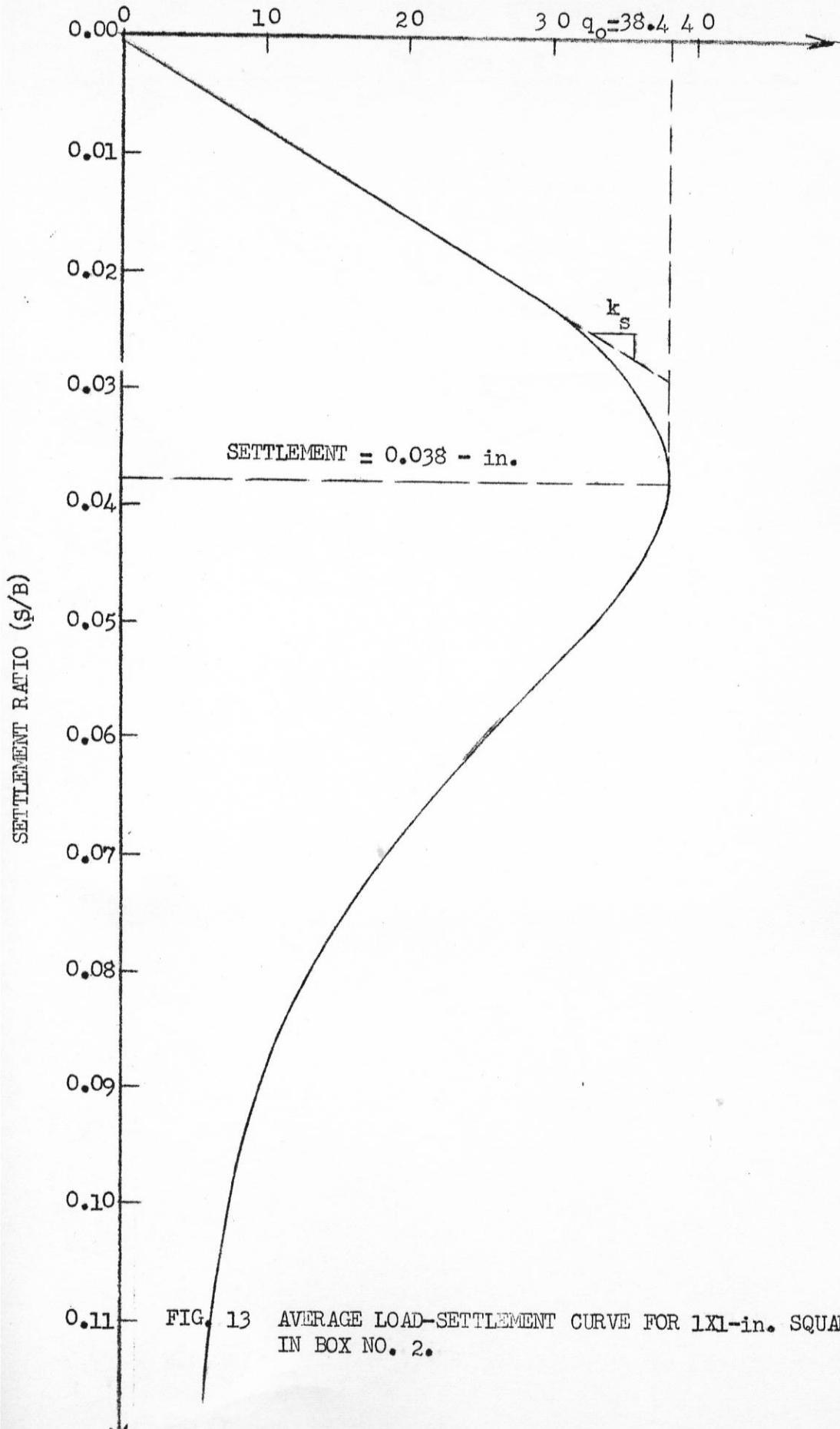


FIG. 13 AVERAGE LOAD-SETTLEMENT CURVE FOR 1X1-in. SQUARE IN BOX NO. 2.

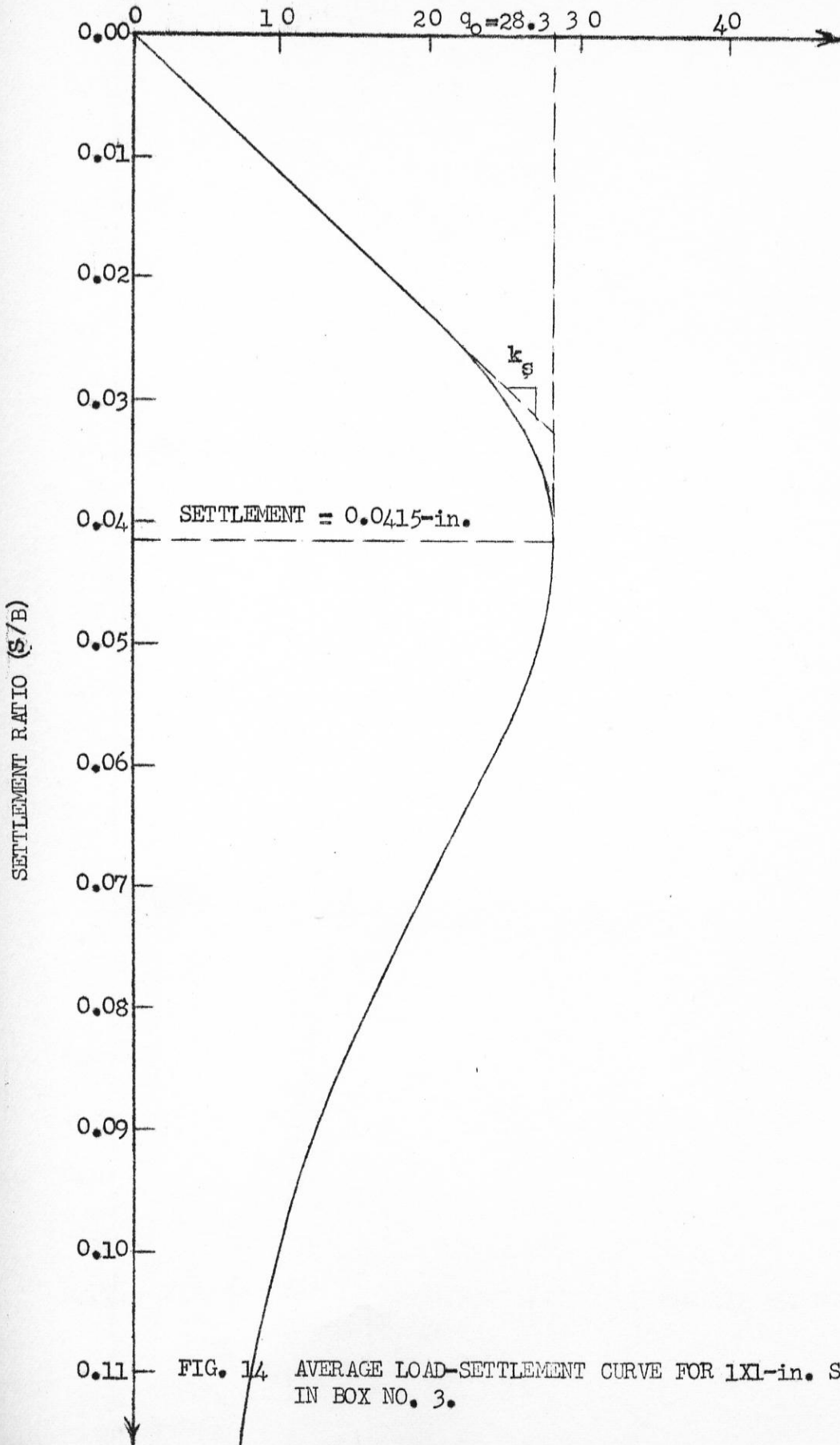


FIG. 14. AVERAGE LOAD-SETTLEMENT CURVE FOR 1x1-in. SQUARE PLATE IN BOX NO. 3.

BEARING PRESSURE (psi)

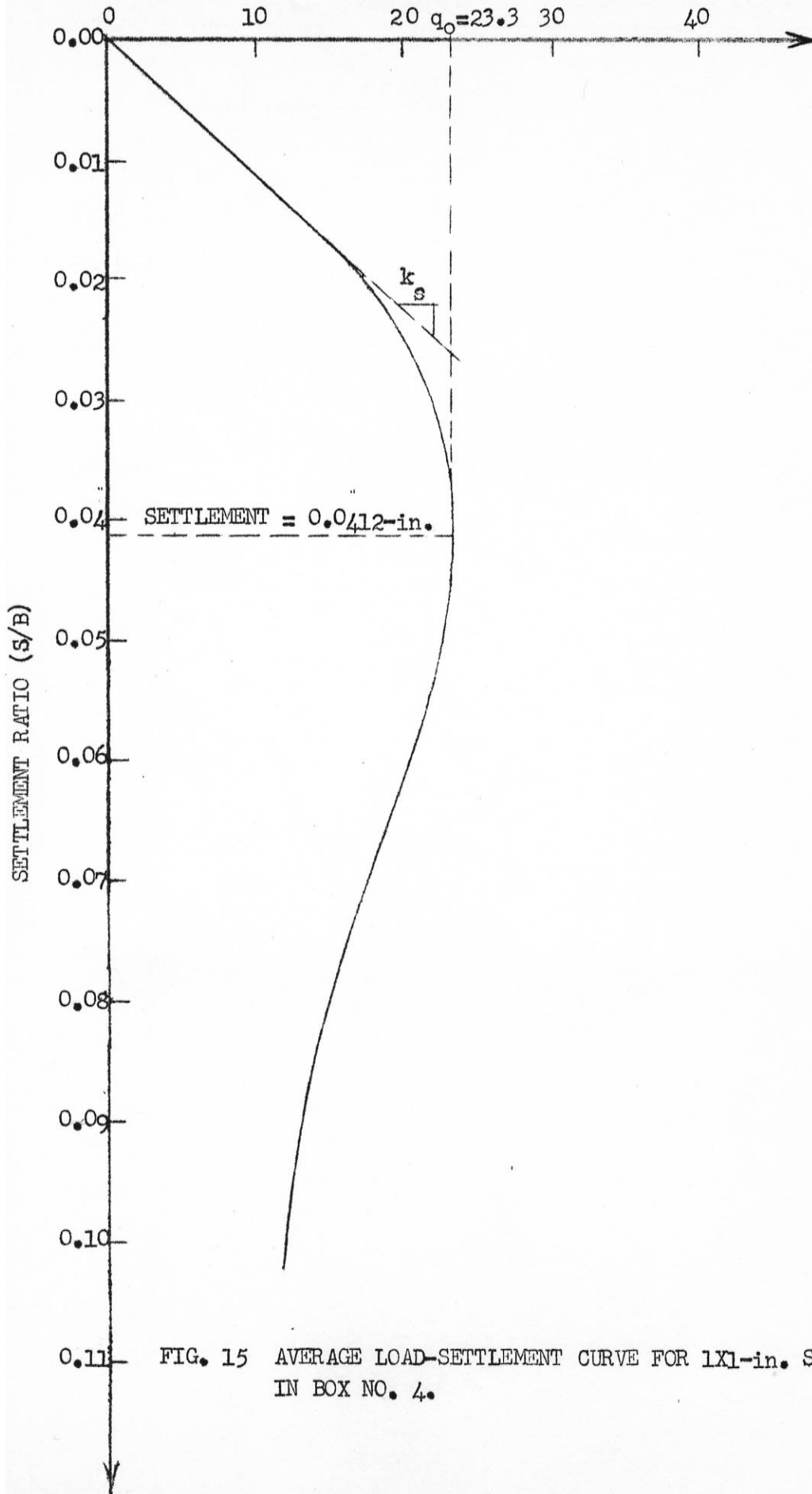


FIG. 15 AVERAGE LOAD-SETTLEMENT CURVE FOR 1x1-in. SQUARE PLATE IN BOX NO. 4.

SETTLEMENT RATIO (s/B)

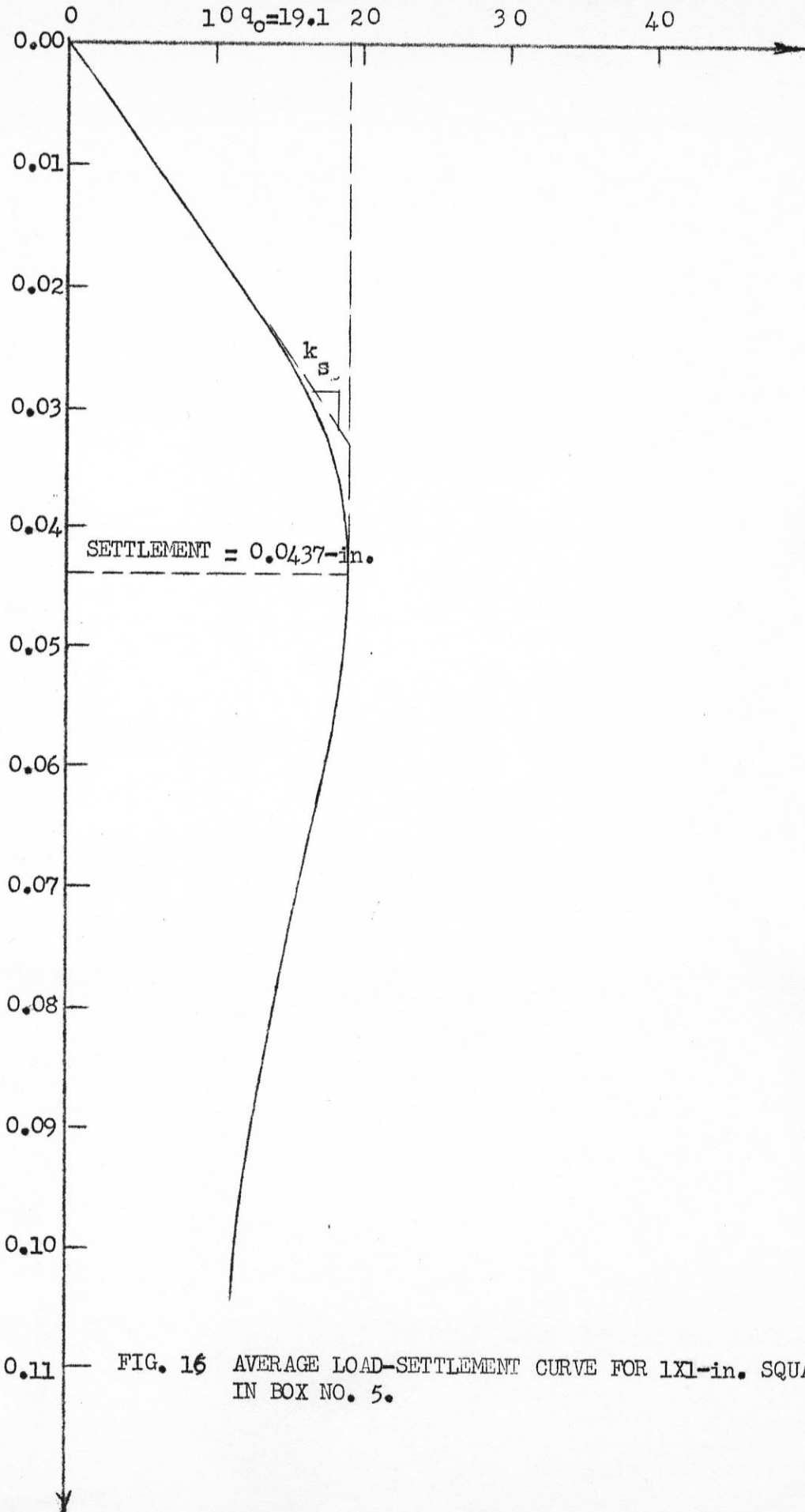


FIG. 16 AVERAGE LOAD-SETTLEMENT CURVE FOR 1x1-in. SQUARE PLATE IN BOX NO. 5.

BEARING PRESSURE (psi)

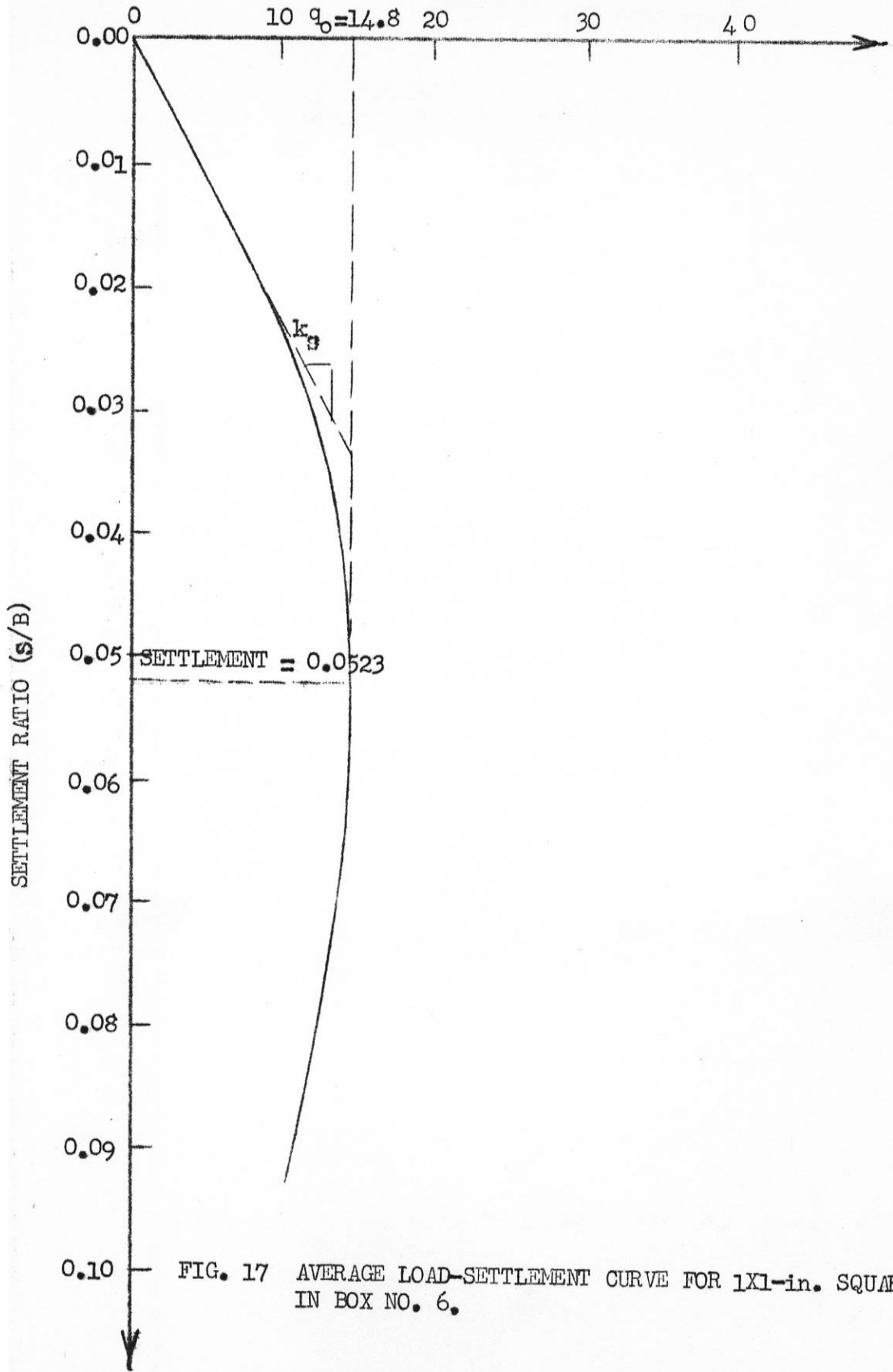


FIG. 17 AVERAGE LOAD-SETTLEMENT CURVE FOR 1x1-in. SQUARE PLATE IN BOX NO. 6.

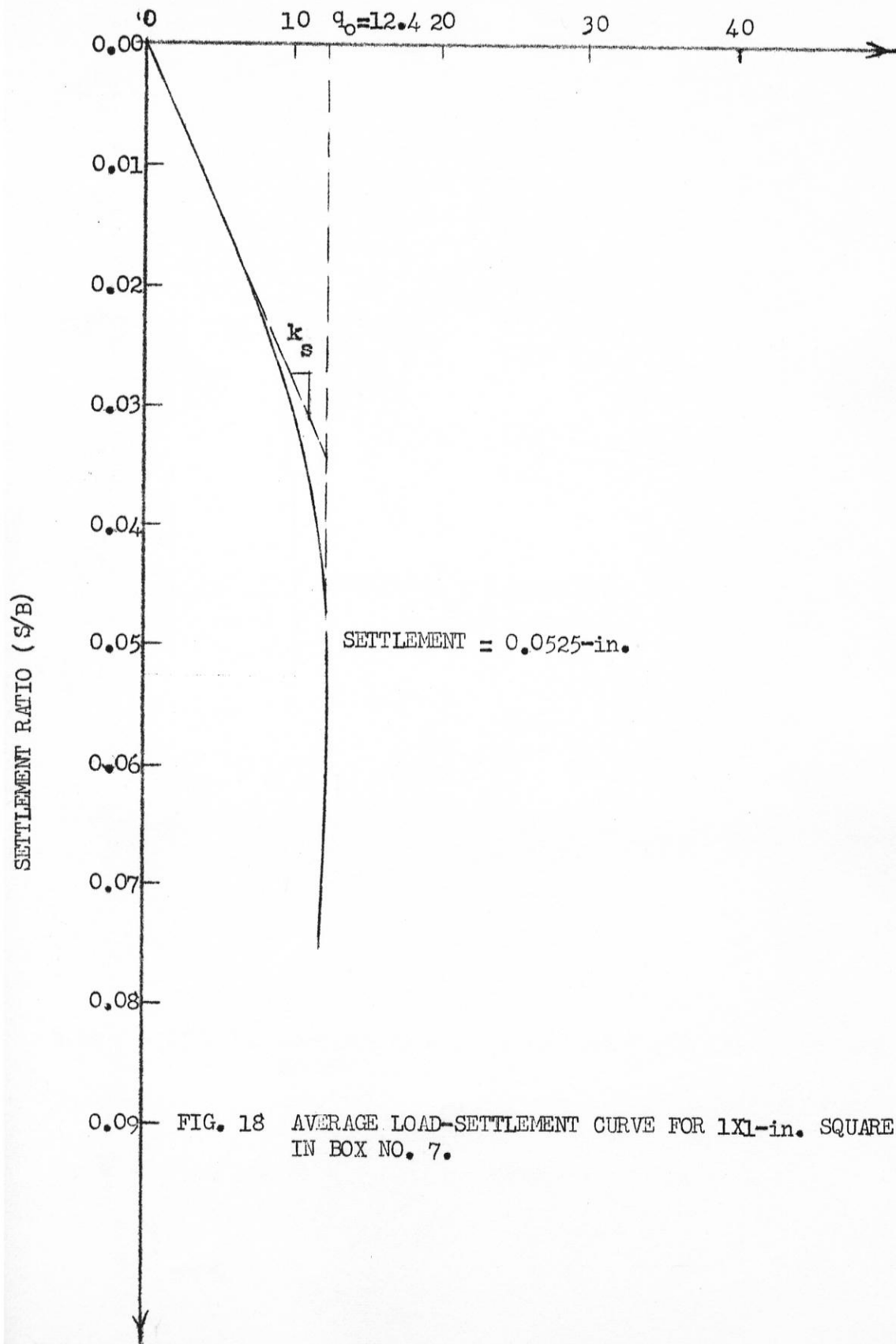


FIG. 18 AVERAGE LOAD-SETTLEMENT CURVE FOR 1X1-in. SQUARE PLATE IN BOX NO. 7.

BEARING PRESSURE (psi)

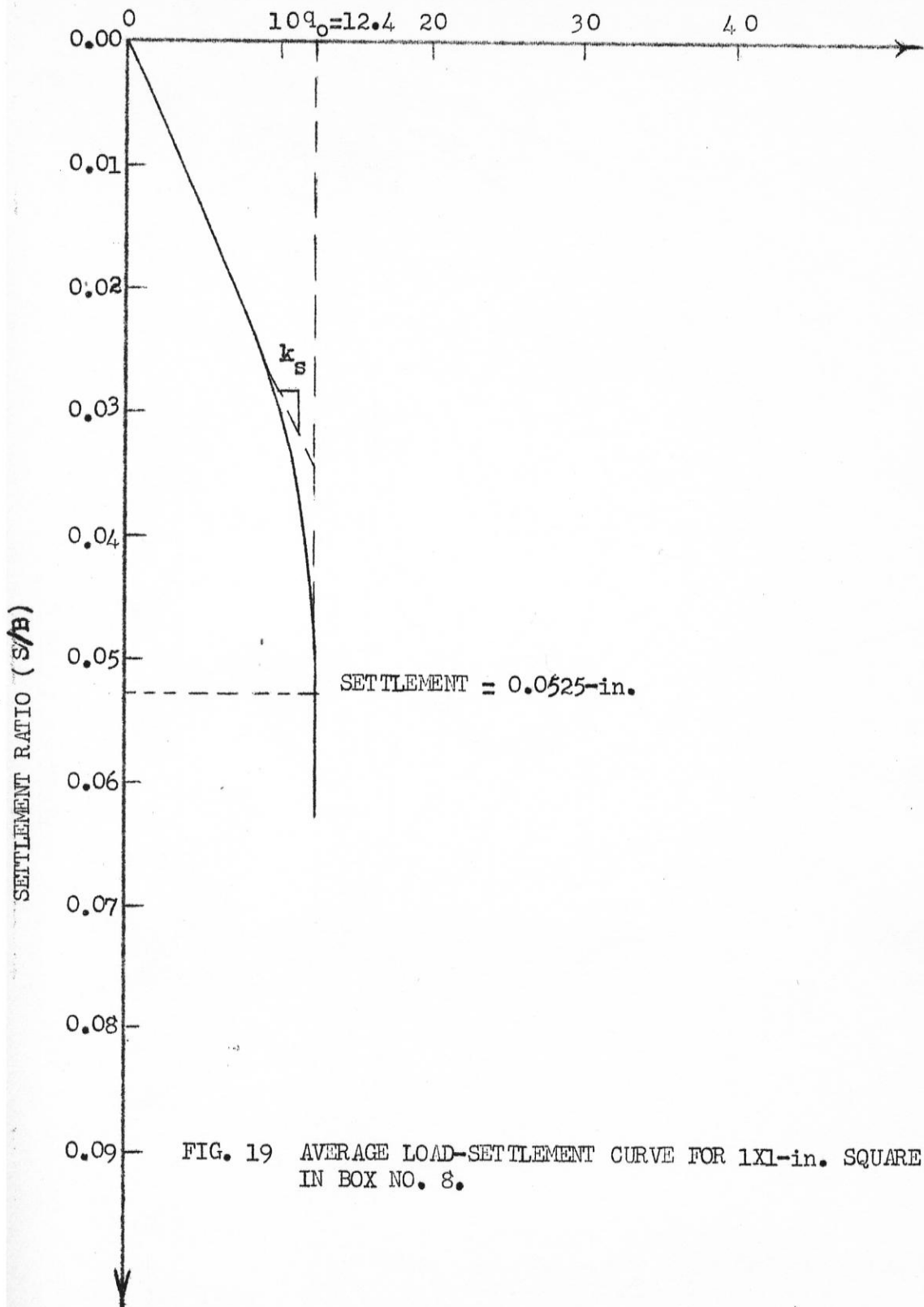
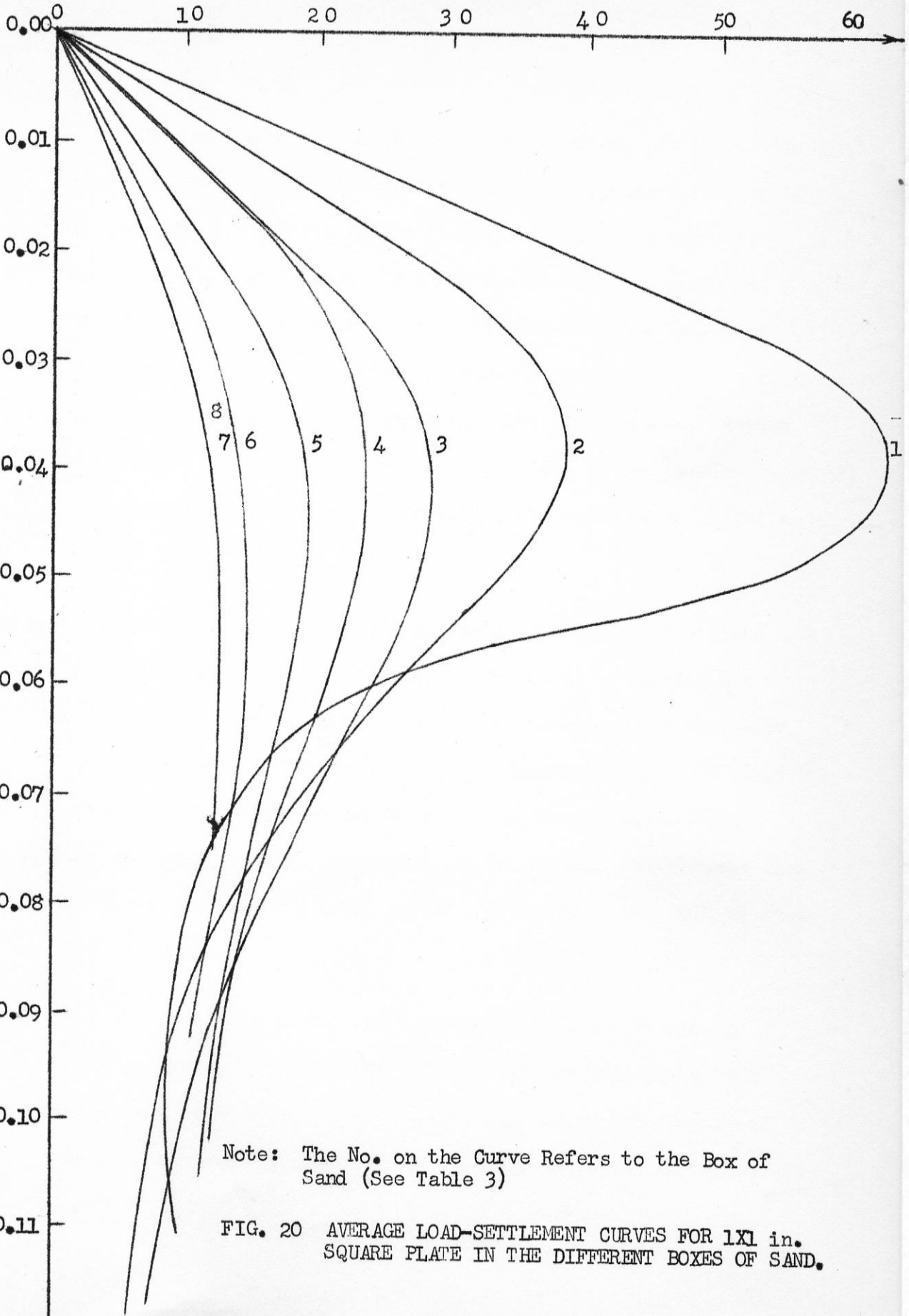


FIG. 19 AVERAGE LOAD-SETTLEMENT CURVE FOR 1x1-in. SQUARE PLATE IN BOX NO. 8.

BEARING PRESSURE (psf)

45



Note: The No. on the Curve Refers to the Box of Sand (See Table 3)

FIG. 20 AVERAGE LOAD-SETTLEMENT CURVES FOR 1x1 in. SQUARE PLATE IN THE DIFFERENT BOXES OF SAND.

Considering box 1, where the sand dimensions are three times the size of the plate, the bearing capacity increases rapidly to 62 psi. As the box dimensions increase the bearing capacity decreases indicating that the interference from the sides and bottom of the box is decreasing. This interference decreases at a decreasing rate with the increase in the size of the box until the box is about ten times the size of the plate. Beyond this limit the box dimensions have no effect on the bearing capacity, and the analysis may be carried out on the basis of an infinite foundation medium.

For clays Skempton (17) considers 4 to 6 times the plate dimensions as sufficient for model studies to be carried out without interference from the sides and bottom of the container. This, however, may be due to the high compressibility and plastic flow of clay. Even for loose sand where large volume changes may be expected, such dimensions may be enough. But for the case of dense sand where a small volume change may occur, such dimensions are not ample.

If the shear failure in sand follows exactly Prandtl's theory then the minimum width of the container has to be 18.2 times the width of the strip footing and the minimum depth has to be 2.4 times the width of the footing, while the corresponding

ratios according to Terzaghi's theory are 13.5 and 1.7 respectively. (Appendix A) However, Taylor (11) states: "Because of their compressibility, soils do not show close agreement with Prandtl's hypothesis, which was originally set up for metals, and in actual cases of footings loaded to failure the region corresponding to Zone III is much narrower than that shown in Fig. (4)". How much narrower he does not say but it is implied from the reasoning he gives that Zone III depends on the relative density of the sand under consideration. It is this phenomenon that made Meyrhooff (5, 33, 34) and others (16, 18) look for a modified failure surface.

Figure 21, curve A, shows the effect of the box dimensions on the bearing capacity. As seen from the curve, when the box dimensions are 10 times the plate size, the bearing capacity becomes constant indicating no interference from the box dimensions. The following equation which was derived empirically by a trial and error procedure to fit the experimental data of this investigation approximates the ultimate bearing capacity within less than 10 percent:

$$q_0 = 12.4 + \frac{434}{0.358r}$$

re

Table 4.

Significant Results of Loading Tests With a Square
Plate in Different Containers

Plate	Box No. *	Ultimate Bearing Capacity (psi)	** Settlement (in.)	K_s (lb/in ³)
1 x 1-in. Square	1	62.0	0.0390	1865
	2	38.4	0.0380	1330
	3	28.3	0.0415	872
	4	23.3	0.0412	896
	5	19.1	0.0437	580
	6	14.8	0.0523	442
	7	12.4	0.0525	360
	8	12.4	0.0525	360

*See Table 3

** Values read off the average curve of the points corresponding to the ultimate bearing capacity.

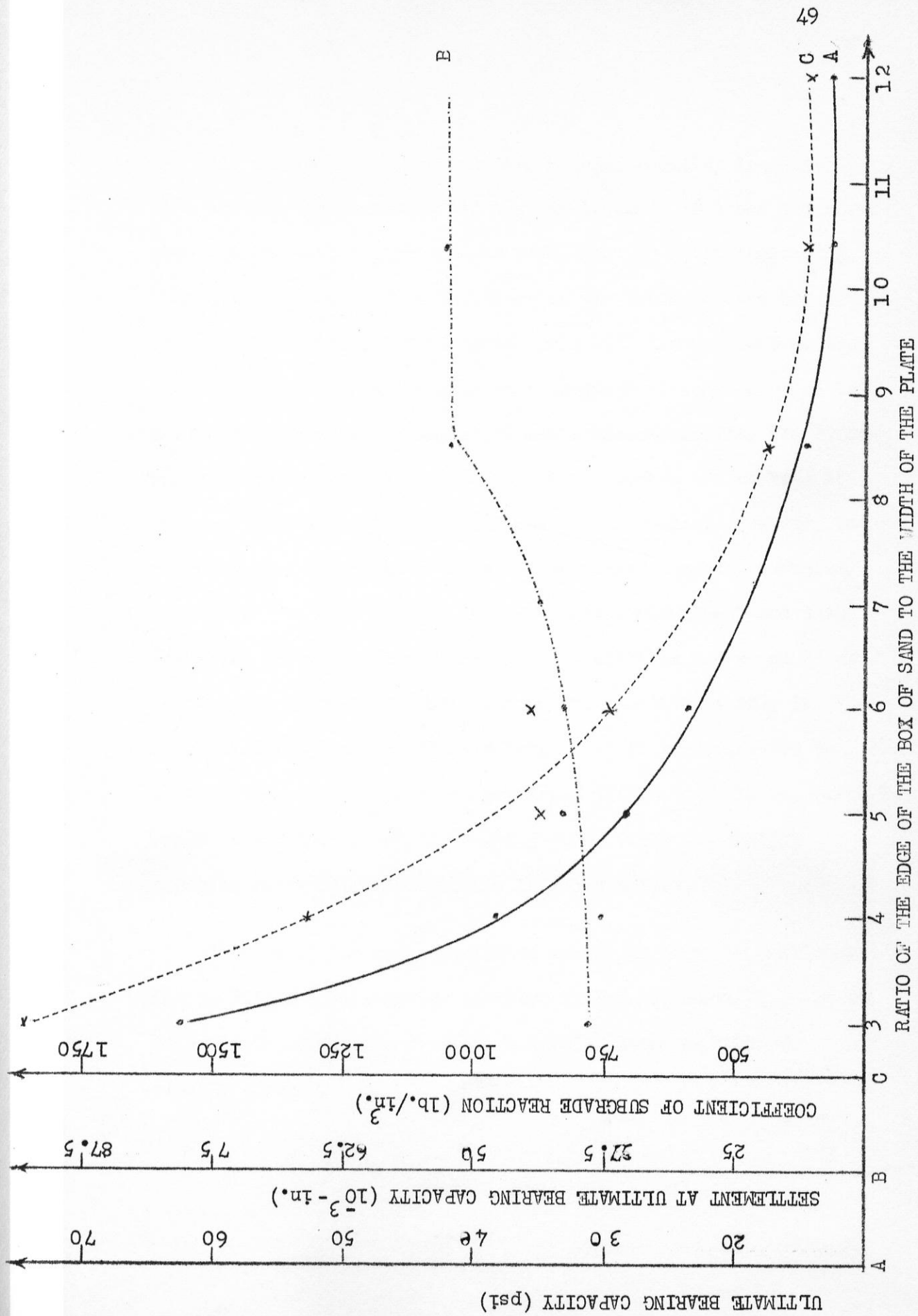


FIG. 21 INFLUENCE OF DIMENSIONS OF SOIL CONTAINER ON ULTIMATE BEARING CAPACITY (A), SETTLEMENT AT ULTIMATE BEARING CAPACITY (B), & COEFFICIENT OF SUBGRADE REACTION (C),

The settlement at the ultimate bearing capacity increases with the size of the box until the box is about 10 times the plate size. After that no increase in settlement is noted indicating that no interference from the sides or the bottom of the box is affecting the plate. This agrees well with the previous conclusion from the bearing capacity consideration although here it is less obvious due to the low settlements encountered and the difficulty in detecting the instant the plate touches the surface of the sand indicating the initial settlement reading. However, the general trend illustrates the above mentioned conclusion (Fig.21, curve B). The high rate of increase beyond abscissa 7 and then the rapid smoothing out of the curve at abscissa 8.5 seems to me to have no explanation other than errors committed mainly in starting taking settlement readings. Had it been possible to overcome completely the above mentioned difficulty, Fig.21, curve B, would be a smooth gradually varying curve since the bearing capacity curve (Fig.21) exhibits this property.

In spite of the above mentioned source of error in settlement, the coefficient of subgrade reaction in Fig.21, curve C, looks to be a smooth curve of more or less similar shape as that of Fig.21, curve A.

The early portion of a load-settlement curve is a straight line regardless of the starting point. The slope of that line and consequently the coefficient of subgrade reaction can be determined by considering any two points on that line. It may be argued that the real starting point can be exactly determined by extending the straight portion of the curve to meet the abscissa axis. This however is not a rule since the layer at the surface may not be as compacted as the other layers, and this condition produces a rather appreciable settlement without much effect on the bearing capacity or the straight portion (hence the coefficient of subgrade reaction) of the load settlement curve.

$$\text{The following equation } k_s = 360 + \frac{5200}{0.009325 r^{2.5}}$$

approximates the coefficient of subgrade reaction within less than 10 per cent. It was derived empirically by a trial and error procedure to fit the experimental data obtained in this investigation.

5.2 Influence of Plate Dimensions

Although it was suggested in Art. 5.1 that the ratio of the dimensions of the cubical box of sand to the width of the square plate used in model studies has to be at least ten if side and bottom interferences of the box are to be neglected, yet a ratio of six was used in the following tests of the investigation. This choice was made to avoid large volumes of sand and to keep weights within the carrying ability of two men. Even with such sizes the weight of sand to carry reached 107 lb. in addition to the weight of the box. This weight will increase in proportion to the cube of the edge of the box and if the ratio ten was used a weight of sand of 495 lb., excluding the weight of the box, would have resulted which is beyond the available facilities of the laboratories. Of course for the sizes of the boxes chosen there will be interference from the sides and bottom of the boxes and the ultimate bearing capacities will appear to be more than they will be in infinitely large boxes (Art. 5.1); but since this ratio of 6 is kept constant for all the square plates used in this part of the investigation it is felt that results are comparable among themselves and it is this comparison that is carried out here (Art. 5.2).

The foundation elements: 1 x 1 - in., $\sqrt{2} \times \sqrt{2}$ - in., $\sqrt{3} \times \sqrt{3}$ - in., and 2 x 2 - in. square plates, were loaded in this part of the investigation. Boxes 4, 6, 7 and 8 with sand dimensions as shown in table 3, vibrated and loaded according to the procedure in Art. 4.3, were used. Load-settlement curves for the preceding four square plates appear in figures 15, 22, 23, and 24.

For comparison purposes these four load-settlement curves are shown in Fig. 25. The ultimate bearing capacity, the settlement at the ultimate bearing capacity, and the coefficient of subgrade reaction, all versus the side of the plate are plotted on Fig. 26*.

Figure 26, curve A, shows a straight-line relationship between ultimate bearing capacity and side of the plate. This agrees well with Terzaghi's theory which states that the ultimate bearing capacity for a surface footing on a cohesionless soil is directly proportional to the width of the footing (1). Also this finding agrees well with results obtained by: Iliya (24), Selig and Mckee (35), Meyerhoff (33) and Vesic (2) for different shapes and sizes of footings. Tables 8 through 12 (Appendix C) are extracts from the above mentioned references where the influence of the size of footing on the ultimate bearing capacity is indicated. Goodman, Hegedus and Liston (26) approached the influence

*See Table 5

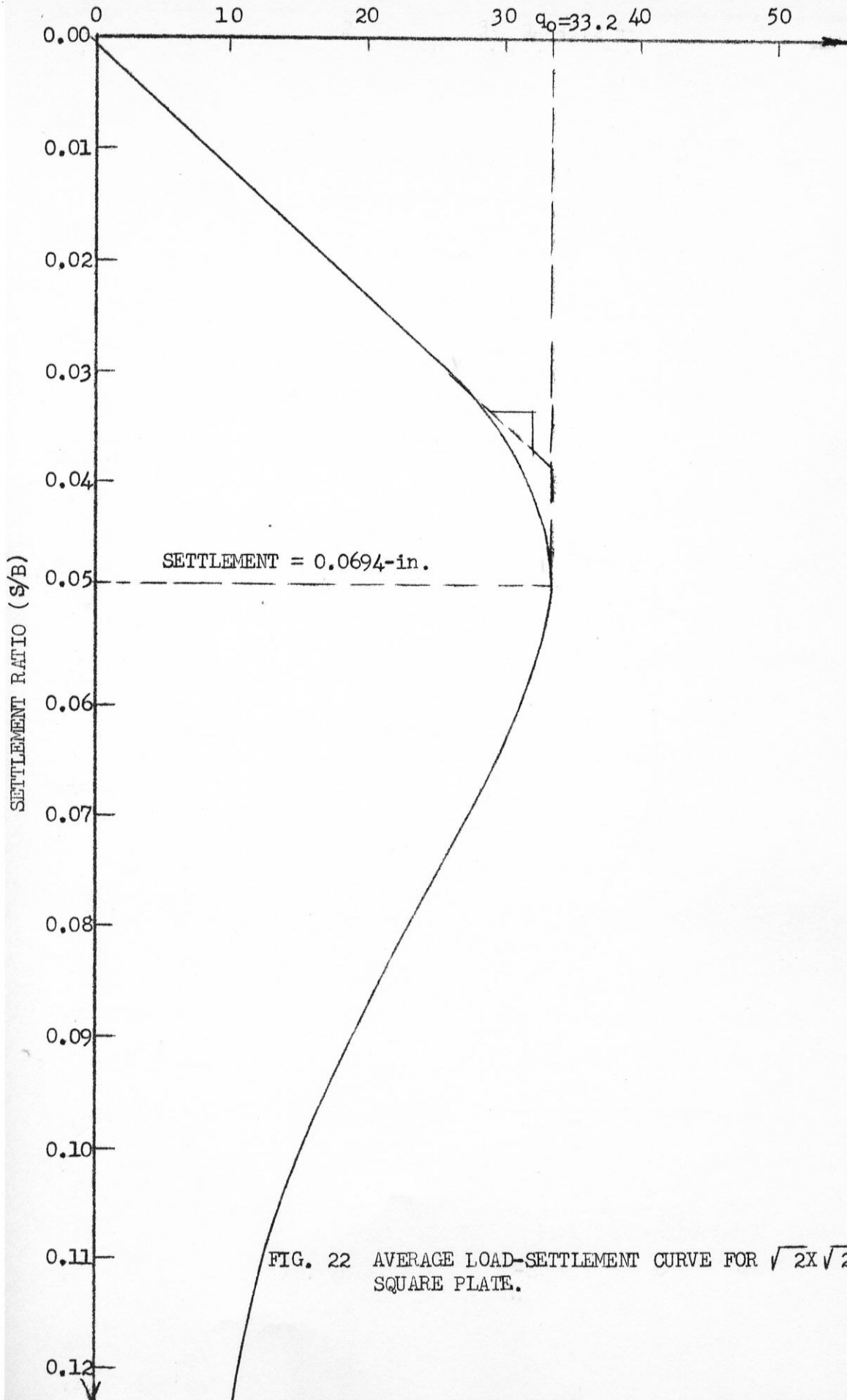


FIG. 22 AVERAGE LOAD-SETTLEMENT CURVE FOR $\sqrt{2} \times \sqrt{2}$ -in. SQUARE PLATE.

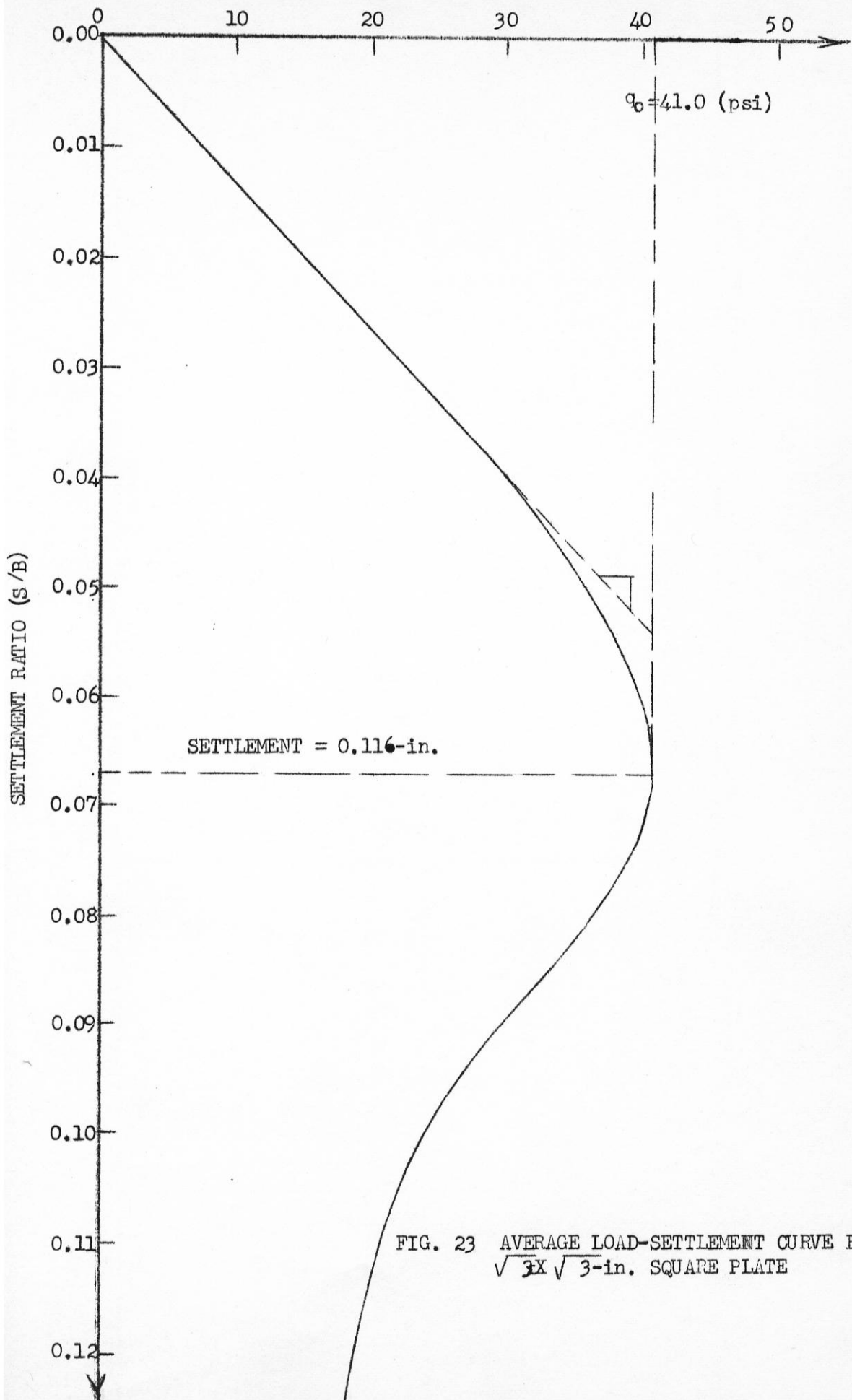


FIG. 23 AVERAGE LOAD-SETTLEMENT CURVE FOR $\sqrt{3} \times \sqrt{3}$ -in. SQUARE PLATE

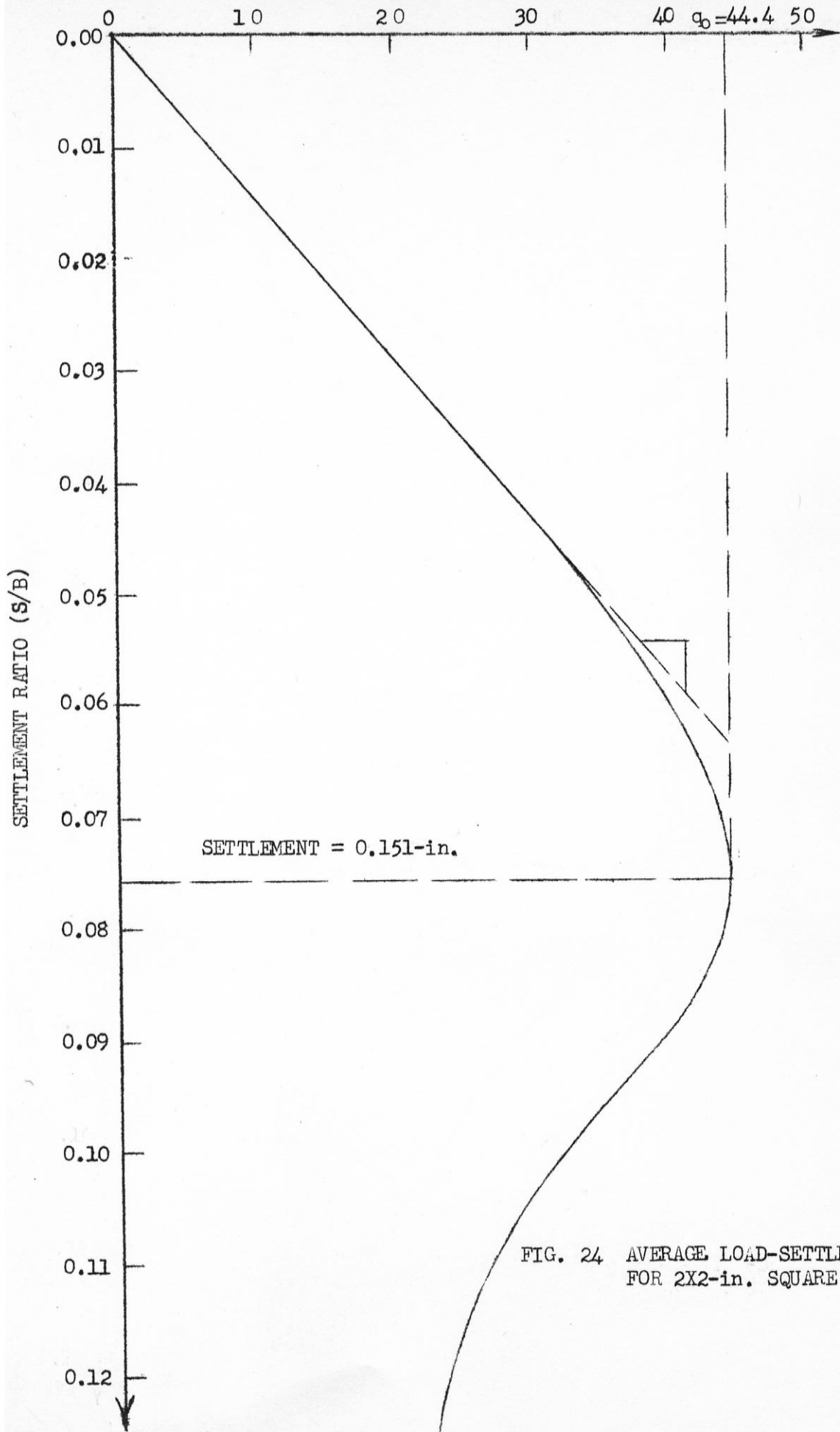


FIG. 24 AVERAGE LOAD-SETTLEMENT CURVE FOR 2X2-in. SQUARE PLATE.

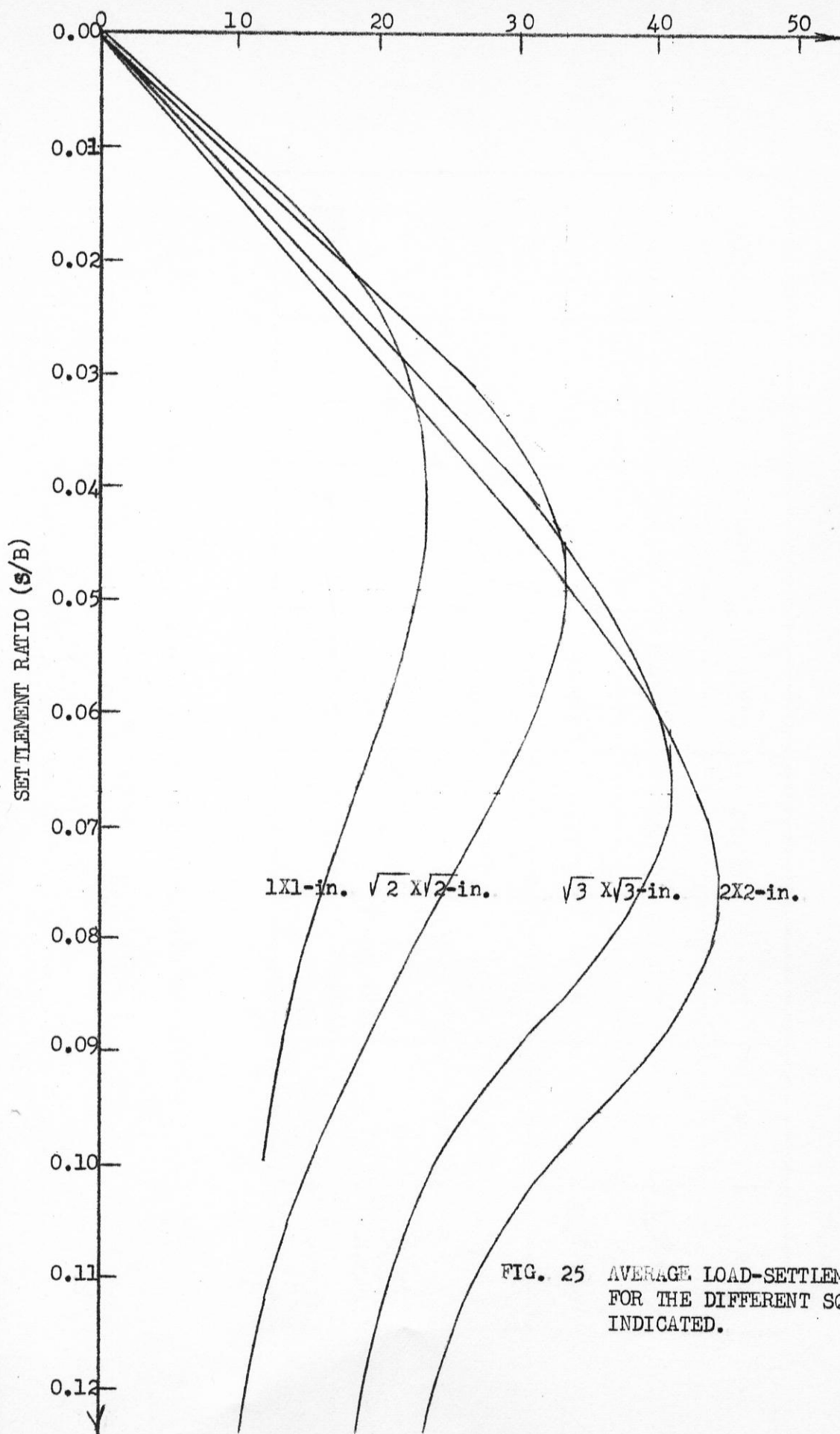


FIG. 25 AVERAGE LOAD-SETTLEMENT CURVES FOR THE DIFFERENT SQUARE PLATES INDICATED.

Table 5.

Significant Results of Loading Tests With Square Plates

Square Plate (in.)	Box No.*	Ultimate Bearing Capacity, q_0 psi	** Ratio of q_0	*** Settlement (P _c) (in.)	** Settlement Ratio	K _s (lb/in. ³)	** K _s Ratio
1 x 1	4	23.3	1.000	0.0412	1.000	896	1.000
$\sqrt{2} \times \sqrt{2}$	6	33.2	1.425	0.0694	1.684	614	0.685
$\sqrt{3} \times \sqrt{3}$	7	41.0	1.760	0.1160	2.815	438	0.490
2 x 2	8	44.5	1.910	0.1510	3.660	350	0.391

* See Table 3

** The 1 x 1 - in square is taken as a basis for comparison

*** Values read off the average curve at the points corresponding to the ultimate bearing capacity.

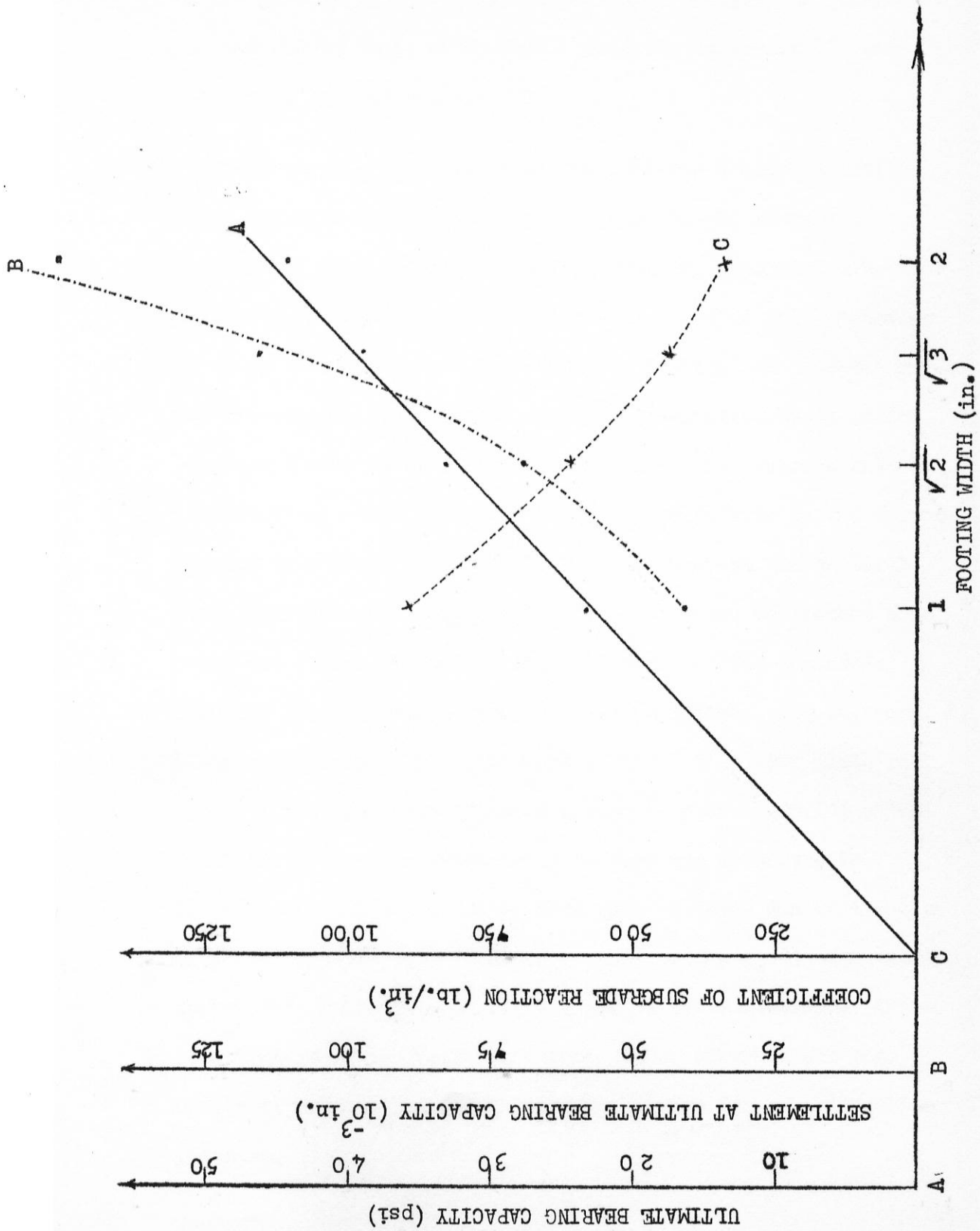


FIG. 26 INFLUENCE OF FOOTING DIMENSIONS FOR SQUARE FOOTINGS

of the size of the plate by dimensional analysis and their results showed that dimensional analysis is applicable with frictional type of soils.

However, the settlement at the ultimate bearing capacity increases more rapidly than the increase in the size of the footing and when the size of the footing is doubled the settlement is more than doubled. Taylor (11) explains this phenomenon in terms of the pressure bulbs below a footing and that of n -times its dimension. Settlements depend on a summation based on the vertical direct strains over the height of the pressure bulb for each footing. The height of the pressure bulb below the second footing is n -times that below the first, whereas the vertical average direct strain is slightly greater below the second than below the first. Therefore the settlement of the second is somewhat greater than n -times that of the first. Fig.26, curve B, illustrates this. The settlement of the 1 x 1 - in. plate is 0.0412 - in., and that of the 2 x 2 - in. plate is 0.151 - in. The ratio of the two settlements is 3.66 and it serves to illustrate a principle rather than give a value due to a source of error (previously mentioned) in starting the settlement readings. Anyhow this ratio is not constant and no curve fitting is tried here because of the above mentioned source of error and the number of points (4 points) being not enough for generalization purposes.

By doubling the diameter of a circular plate the settlement at the ultimate bearing capacity became four times according to Iliya's experiments (Appendix C, Table 8), while according to Vesic's experiments (Appendix C, Table 11) this ratio is 2.9. These differences are due to the methods and rates of loading, experimental errors and differences in the properties of the sand used in the different investigations.

According to Terzaghi's theory (4) the coefficient of subgrade reaction varies with the width of the footing according to the relation $k_s = \bar{k}_s \frac{(1 + B)^2}{4B^2}$ (page 21). Figure 26, curve C, illustrates that the experimental values are not close to the theoretical values and if plates 1 x 1 - in. and $\sqrt{2} \times \sqrt{2}$ - in. are considered, the experimental values are 6 percent less than the theoretical values. This difference tends to increase with the increase in the dimensions of the plates and for the plate 2 x 2 - in. it reaches 30 percent. The values of the coefficient of subgrade reaction obtained by Iliya (Table 8) illustrate the same general trend. Such a deviation may be due to experimental errors and the various simplifying assumptions made by Terzaghi in deriving the above mentioned relation. This point has still to be investigated further for definite conclusions on the coefficient of subgrade reaction.

5.3 Influence of Footing Length

In this article the influence of the ratio of the length of the footing to its width on the ultimate bearing capacity, settlement at the ultimate bearing capacity and coefficient of subgrade reaction is studied. Four rectangular plates having the following dimensions 1 x 1 - in., 1 x 2 - in., 1 x 3 - in. and 1 x 4 - in. were used.

The boxes with the sand dimensions (length x width x height) used for the respective footings appear below in Table 6.

Table 6

<u>Box No.</u>	<u>Sand Dimensions (Length x Width x Depth, inches)</u>
4	6 x 6 x 6
9	12 x 6 x 6
10	18 x 6 x 6
11	24 x 6 x 6

Vibration and loading procedures follow Art. 4.3 and the load-settlement curves for the respective footings appear in figures 15, 27, 28 and 29. For direct comparison, these curves are shown together in Fig.30. Curves A, B, and C of Fig. 31^{*} study the variation with the length to the width ratio of the ultimate bearing capacity, the settlement at the ultimate bearing capacity and the coefficient of subgrade reaction respectively.

Figure 31, curve A, shows that the ultimate bearing capacity for a rectangular footing increases at a decreasing rate with the increase in the length to width ratio. For a length to width ratio of 3, the ratio of the ultimate bearing capacities is 1.32. From the trend of curve A (Fig.31), it looks as if the ultimate bearing capacity flattens after a length to width ratio of 3 and apparently when the length to width ratio becomes equal to 4 the rectangular plate passes into the strip category footing. However, this is not the case. Although the dimensions of the box of the sand were always kept equal to 6 times the corresponding dimensions of the plate yet the interference from the sides and bottom of the boxes affected the different plates differently. This interference became more and more pronounced as the length to width ratio increased. For the case of the square plate

*See Table 7

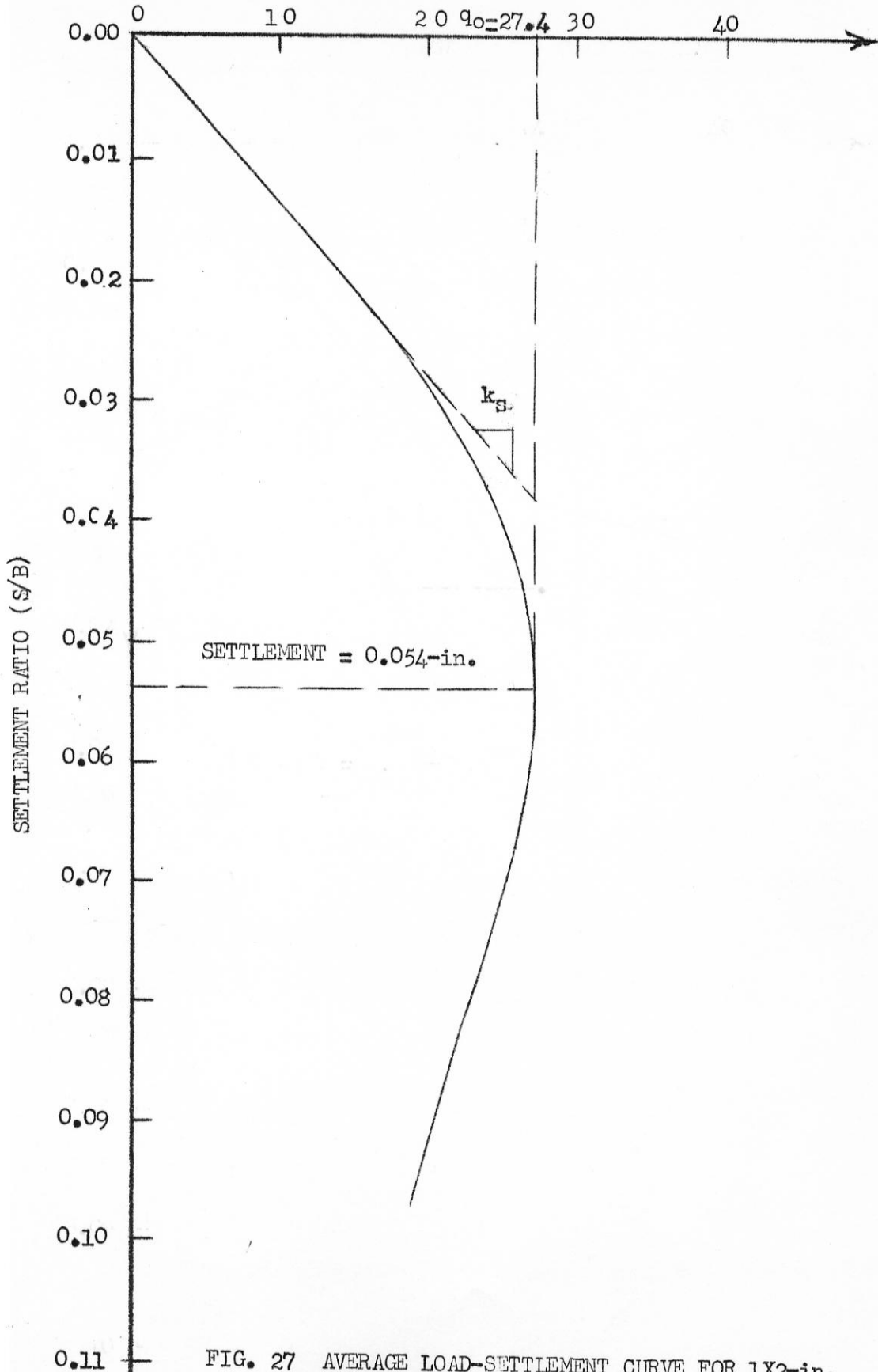


FIG. 27 AVERAGE LOAD-SETTLEMENT CURVE FOR 1X2-in. RECTANGULAR PLATE.

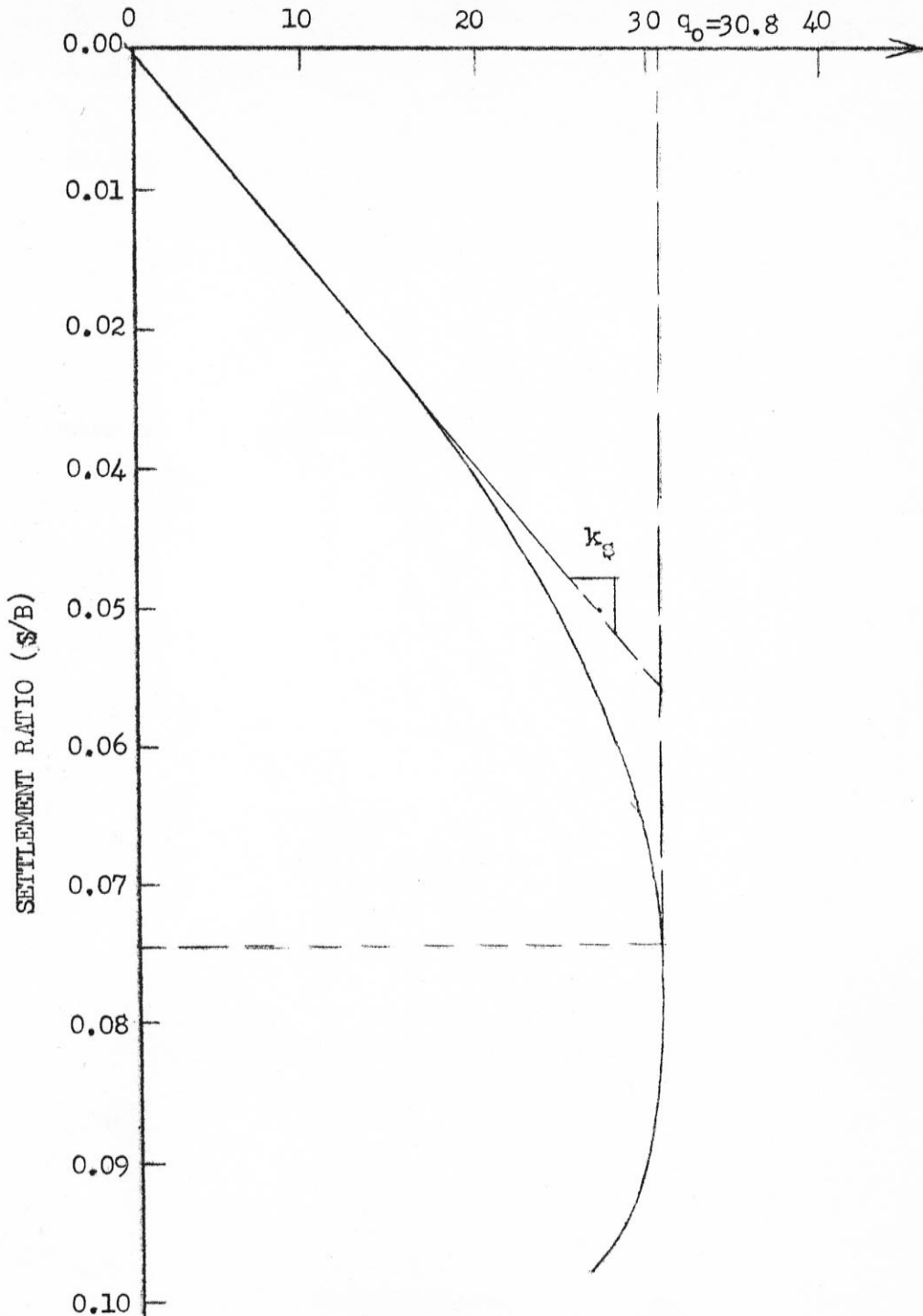


FIG. 28 AVERAGE LOAD-SETTLEMENT CURVE FOR 1X3-in. RECTANGULAR PLATE.

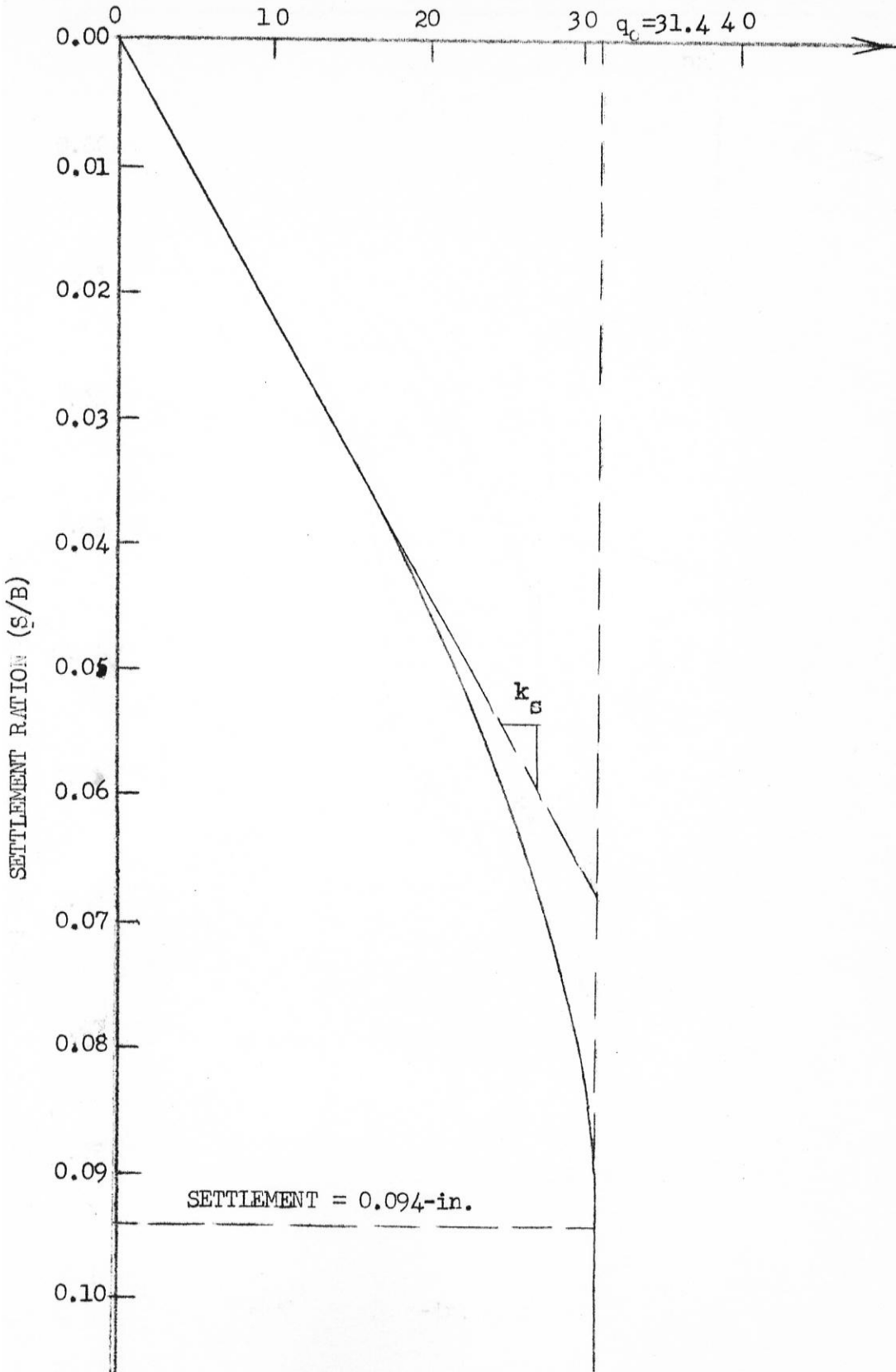


FIG. 29 AVERAGE LOAD-SETTLEMENT CURVE FOR 1x4-in. RECTANGULAR PLATE.

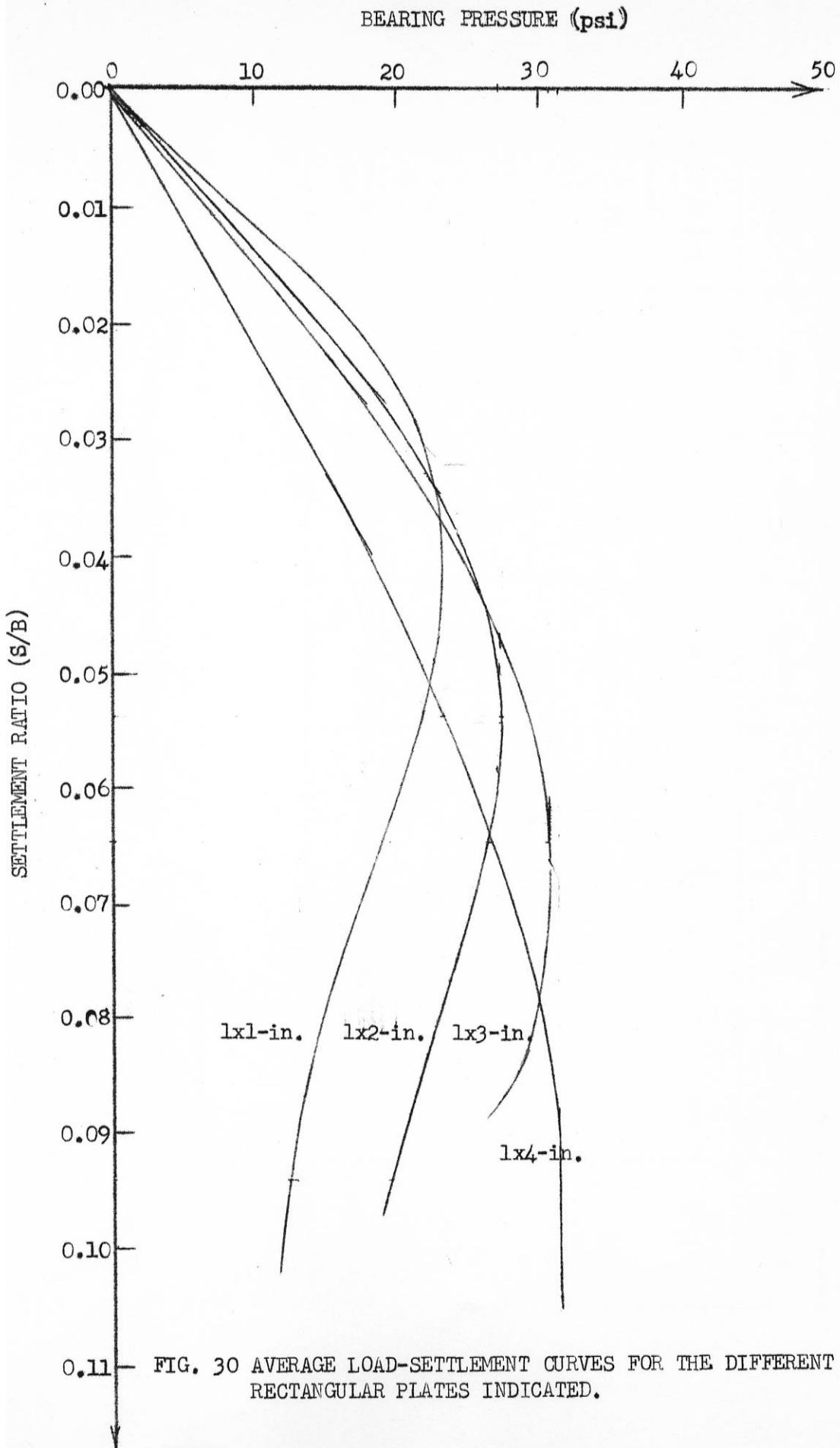


FIG. 30 AVERAGE LOAD-SETTLEMENT CURVES FOR THE DIFFERENT RECTANGULAR PLATES INDICATED.

Table 7

Significant Results of Loading Tests With Rectangular Plates

Rectangular Plate (in.)	Box No.*	Ultimate Bearing Capacity q (psi)	** Ratio of Settlement q_0	*** Settlement per (in.)	** Settlement Ratio	k_s (1 ¹ / _{in.} ³)	** K_s Ratio
1 x 1	4	23.3	1.000	0.0412	1.000	896	1.000
1 x 2	9	27.4	1.175	0.054	1.310	721	0.805
1 x 3	10	30.8	1.320	0.0645	1.505	670	0.748
1 x 4	11	31.4	1.347	0.0940	2.280	462	0.516

* See Table 4

** The 1 x 1-in. plate is taken as a basis for comparison

*** Values read off the average curve at the points corresponding to the ultimate bearing capacity.

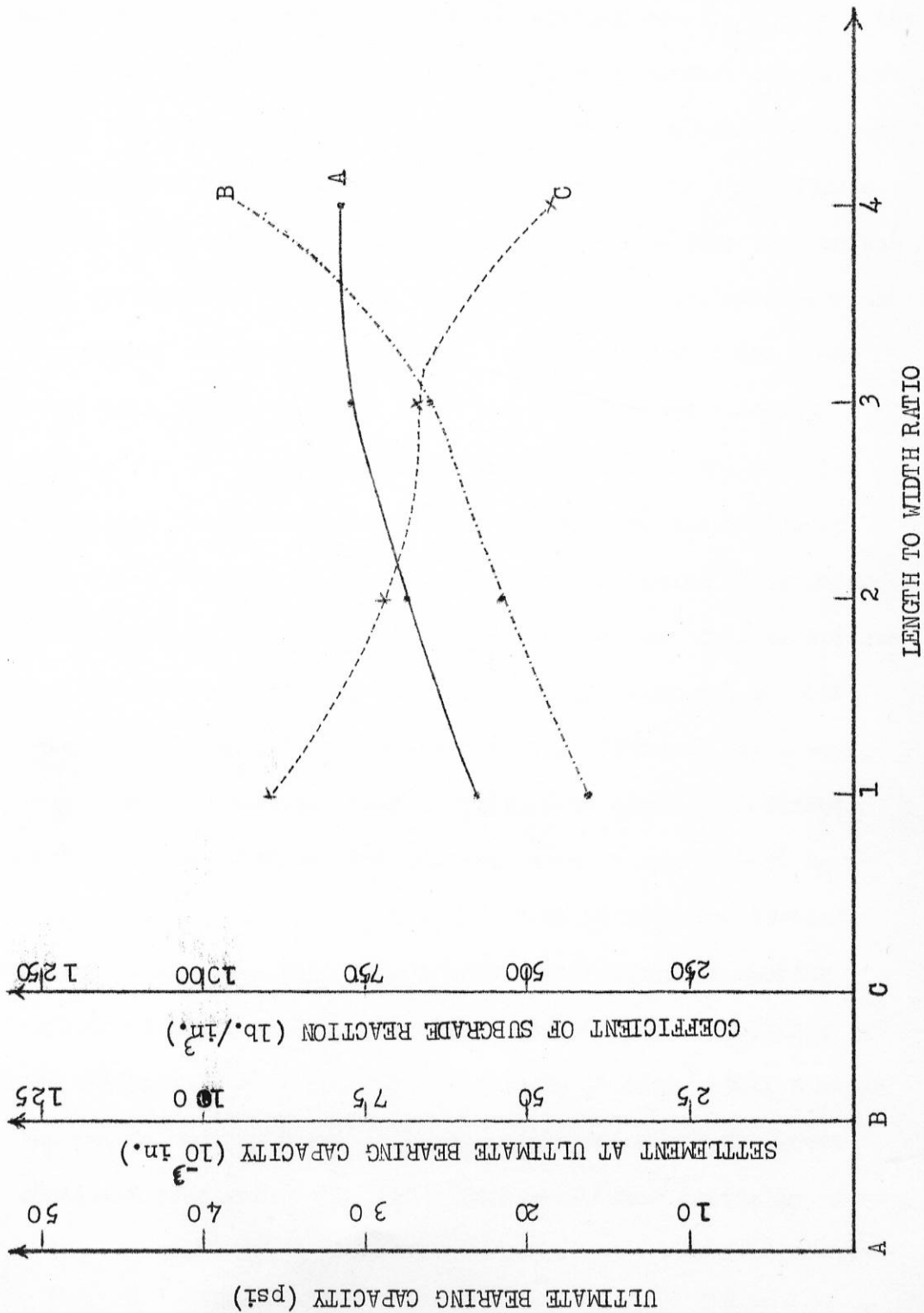


FIG. 31 EFFECT OF FOOTING LENGTH

(1 x 1 - in.), the failure surface developed within the box and so, after reaching the peak load, the bearing capacity began to decrease smoothly to reach a certain minimum value. But when the length to width ratio reached 3, the failure surface was seen to touch the sides of the box. Not far after the ultimate load was reached, the bearing capacity dropped suddenly to a negligible value. With length to width ratio of 4, the failure surface was seen to intersect the faces of the box and the ultimate bearing capacity of the sand was reached, in the sense that the load settlement curve reached a value and then dropped suddenly. This is due to the fact that the inside faces of the box are smooth and the instant the failure surface reaches obliquely such faces slippage occurs almost instantaneously. This phenomenon leads to the important conclusion that the failure surface is a function of the shape of the footing, being of greater extent (at least sidewise since this was observed) for a strip than a square footing. Such an indication gives an indirect partial explanation why the bearing capacity coefficient N_{ϕ} for a strip footing is greater than that of a square footing. As the length to width ratio increases the ultimate bearing capacity increases at a decreasing rate until it approaches the ultimate bearing capacity of a strip footing. Such a value can not be obtained from this investigation due to the above mentioned phenomenon and, aside from this, four points on curve A

Fig.31) are not sufficient to determine when a rectangular footing can be considered a strip one.

Results obtained by Selig and Mckee (Table 9) indicate that there is still an increase in the ultimate bearing capacity when the length to width ratio reaches seven. Their experiments (Table 9) indicate that for surface footing on cohesionless soils, the ultimate bearing capacity of a square footing is 0.65 times that of a rectangular footing with a length to width ratio of seven (whereas they report this ratio as 0.69, reference 35) and thus if a strip footing instead of a rectangular one is used for comparison purposes that ratio will be even lower than the above mentioned value. Meyerhoff (5) considers that a rectangular footing on sand of $\phi = 45^{\circ}$ can be dealt with as a strip footing when the length to width ratio is equal to or exceeds 20. He also gives the value of this ratio for different values of the angle of internal friction ϕ .

In this investigation the ultimate bearing capacity of a square footing was found to be 0.76 that of a rectangular footing of a length to width ratio of 3. Terzaghi (1) gives the ratio of the ultimate bearing capacity of a square footing on the surface of a cohesionless soil to that of a strip footing of the same width as 0.80.

Hence if the strip footing is used as a basis (as is usually done) for determining the value of the N_{ϕ} to be used in the design, the 0.80 coefficient for a square footing leads to an unsafe result.

A comparison of curves A and B of Fig.31 shows that these curves are more or less parallel until the abscissa of 3. From that point on, curve A tends to flatten rapidly while curve B shoots up quickly. This is a consequence of the fact that at the abscissa of 4, the failure surface reached obliquely the smooth faces of the container resulting in slippage and giving an appreciable settlement with very little increase in the ultimate bearing capacity. Before the abscissa of 3, curve B was rising smoothly showing that as the length to width ratio increases, the settlement at the ultimate bearing capacity increases to approach that for the case of strip footing. The parallelism between curves A and B before the abscissa of 3 is not exact because the curves approach each other more and more (but at a slow rate) as the ratio increases. This indicates that the failure surface goes deeper (but at a slow rate) as the length to width ratio of the footing increases to approach the strip case, while the rapid increase in curve B (or the smoothing out of curve A) after the abscissa of 3 indicates that the horizontal extension of the failure surface is rapid.

Curve C (Fig.31) exhibits consistent results with curves A and B. Before the abscissa of 3, the ultimate bearing capacity increases with the increase in the ratio of the length to the width of the footing and consequently the increase in the settlement is expected (curve B discussed above). Therefore, from the definition of the coefficient of the subgrade reaction, K_s is expected to decrease. This is clear from curve C. But after the abscissa of 3, slippage of the sand on the faces of the container occurs resulting in relatively large settlements with negligible increase in the ultimate bearing capacity and hence a drop in K_s (curve C) after the abscissa of 3 is expected. Such consistent results indicate the validity of the above mentioned conclusions.

5.4 Influence of Depth of Soil Bed

The load-settlement curves for square plates, 1 x 1 - in. and $\sqrt{2} \times \sqrt{2}$ - in. were investigated in boxes Nos. 4 and 6 respectively to study the influence of the soil bed on the ultimate bearing capacity, settlement at the ultimate bearing capacity, and the coefficient of subgrade reaction. As seen in Table 2, the lengths and widths of these boxes are 6 times the corresponding dimensions of the investigated plates. However, the depths of sand in these boxes were varied, always being exact multiples of the sides of the plates. Vibration and loading procedures appear in Art. 4.3. The load-settlement curves were plotted as discussed in Art. 5.1, and the ultimate bearing capacities, the settlements at the ultimate bearing capacities and the coefficients of subgrade reaction for the different soil beds were taken from such graphs and plotted separately in Figures 32, 33 and 34, with the ratio of the depth of soil bed to the width of the plate as ordinate.

Figure 32 shows that the ultimate bearing capacity increases with the increase in the soil depth until the ratio of the soil depth to the width of the plate is about 10. After that the graphs tend to be vertical indicating that further increases in depth have little or no effect on the ultimate bearing capacity. This result is of practical importance when the sand beds are underlain by

ULTIMATE BEARING CAPACITY (psi)

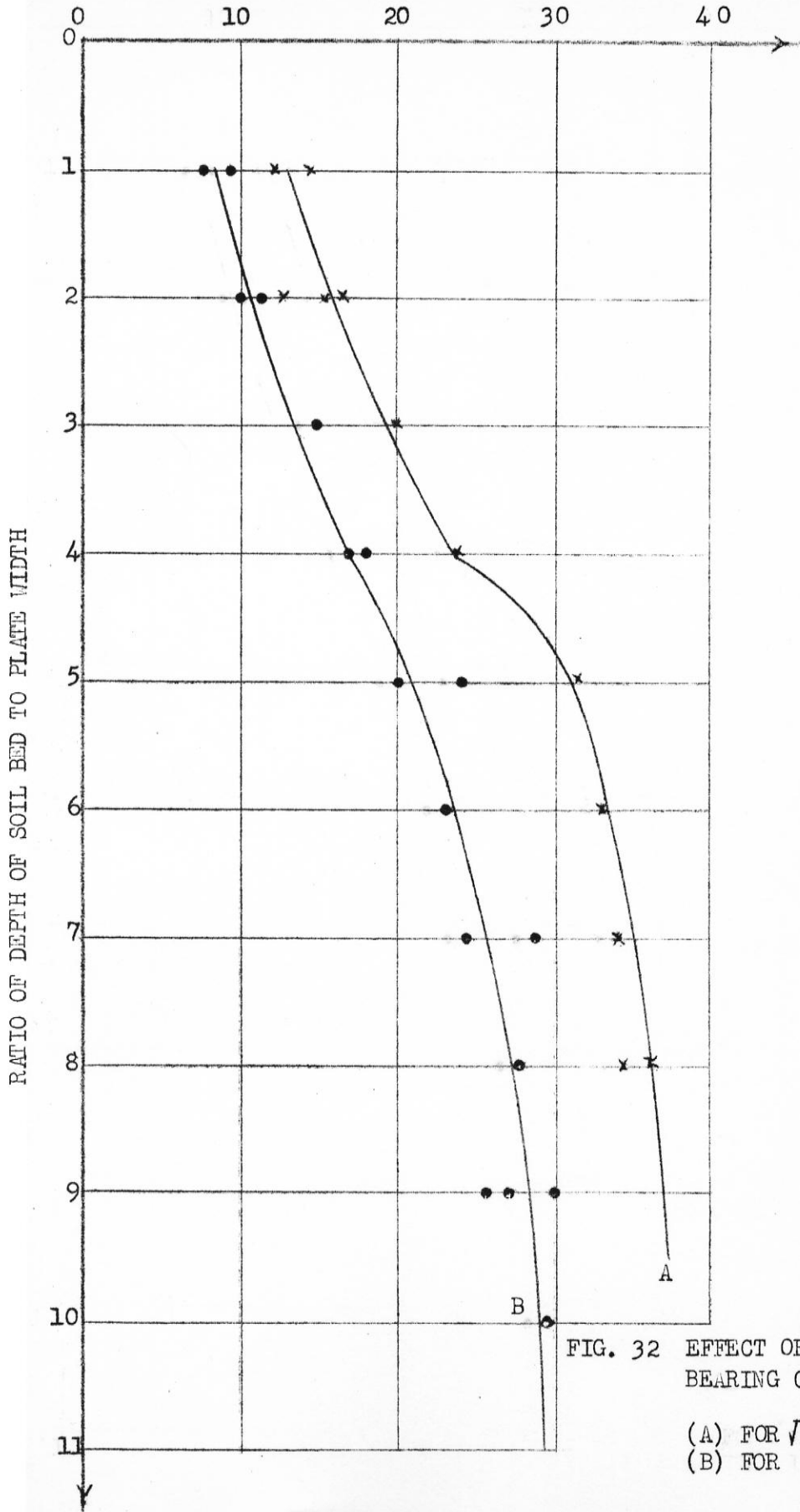


FIG. 32 EFFECT OF SOIL DEPTH ON ULTIMATE BEARING CAPACITY:

- (A) FOR $\sqrt{2} \times \sqrt{2}$ -in. SQUARE PLATE
- (B) FOR 1 X 1-in. SQUARE PLATE

RATIO OF SETTLEMENT AT ULTIMATE BEARING CAPACITY TO WIDTH OF PLATE

0.00 0.01 0.02 0.03 0.04 0.05 0.06

RATIO OF DEPTH OF SOIL BED TO PLATE WIDTH

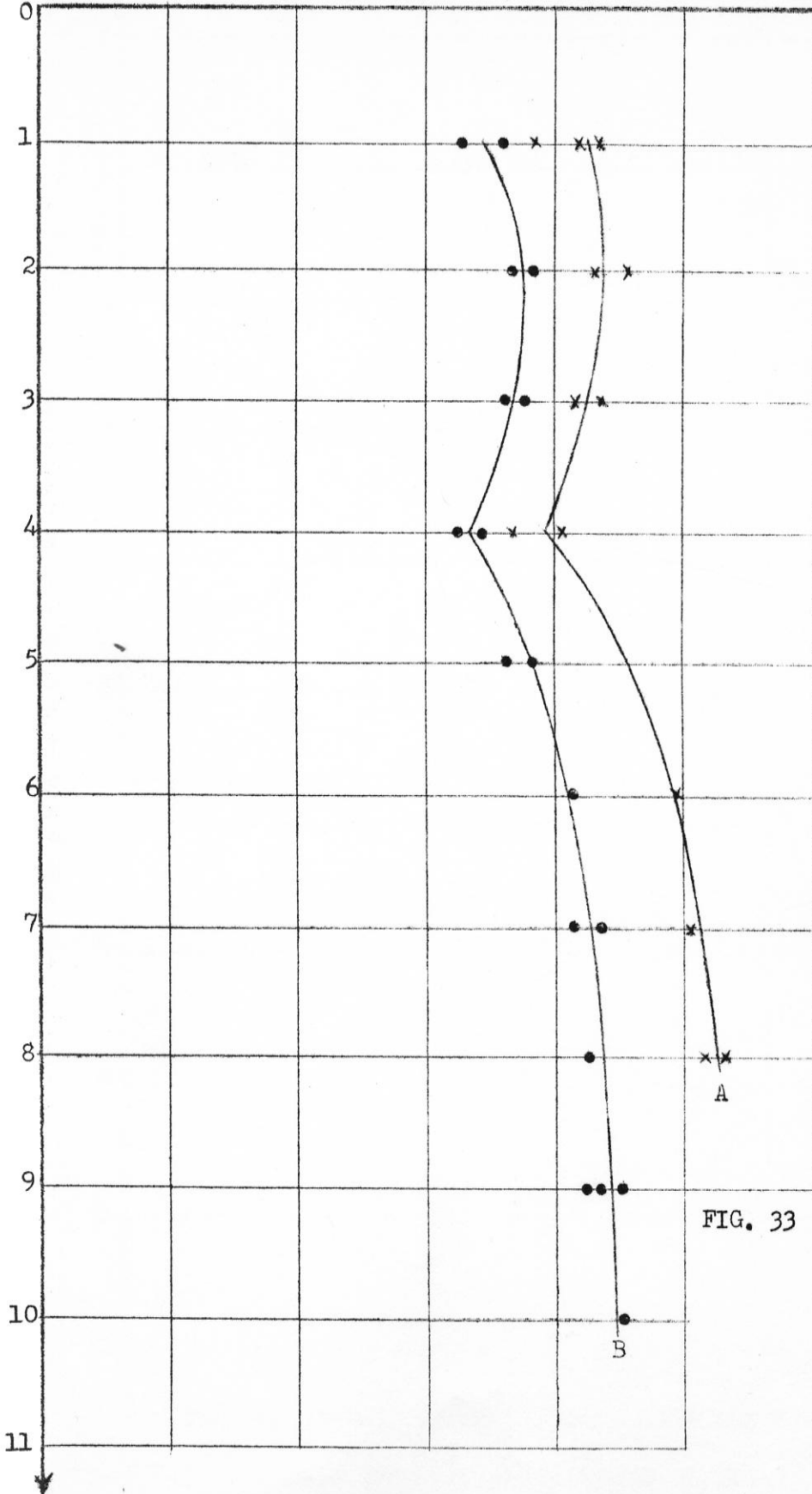


FIG. 33 EFFECT OF SOIL DEPTH ON THE SETTLEMENT AT ULTIMATE BEARING CAPACITY:

- (A) FOR $\sqrt{2} \times \sqrt{2}$ -in. SQUARE PLATE
- (B) FOR 1x1-in. SQUARE PLATE

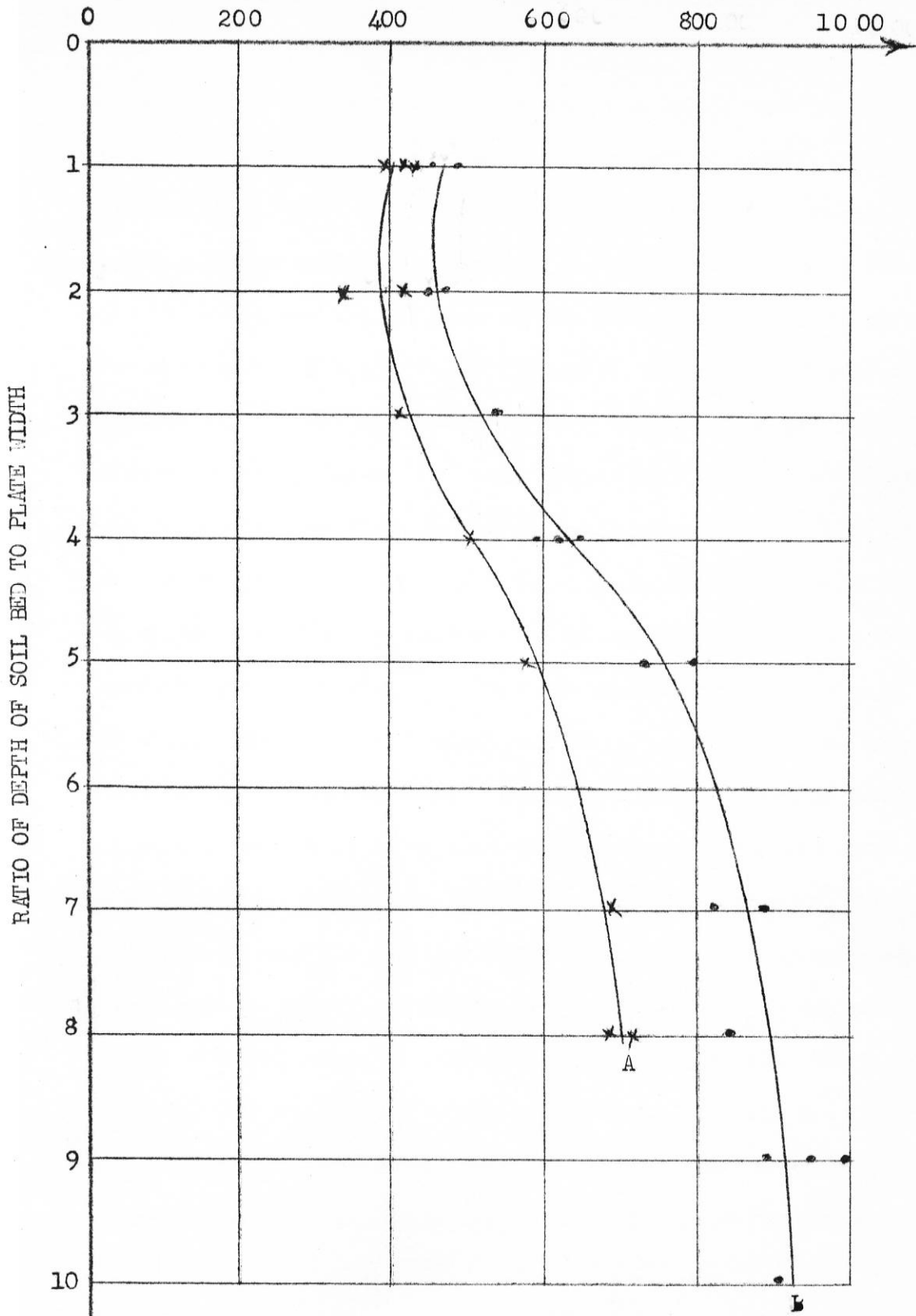


FIG. 34 EFFECT OF SOIL DEPTH ON COEFFICIENT OF SUBGRADE REACTION

(A) FOR $\sqrt{2} \times \sqrt{2}$ -in. SQUARE PLATE
 (B) FOR 1 X 1-in. SQUARE PLATE

rock since it allows to study how the presence of such rock affects the ultimate bearing capacity. Also it is important when designing model experiments to find the minimum size of the box where analysis can be carried out on infinite basis (Art. 5.1). Since the inner faces of the boxes are smooth, slippage of the sand on these faces, especially for low depths of sand, causes failure to result with low bearing capacities. As the depth of the sand increases the confining effect for the layer at the bottom increases. This, coupled with the lower stresses reaching the bottom layer, decreases the slippage effect thus resulting in higher bearing capacities. However, for an ordinate of 4 the graphs in Fig. 32 exhibit a kink and the second derivative changes sign. No thorough explanation has yet been presented; but it could be that the failure surface may go deeper than is represented by Prandtl's solution of the ultimate bearing capacity, especially if we realize that the real failure surface does not extend sidewise as the theory states. This, however, does not invalidate Prandtl's approach to the problem. In this approach (13), certain simple solutions are fitted together to conform to the external boundary conditions (real or assumed) of the problem, but usually the "mechanism" devised controls the internal boundaries or lines of discontinuity between the zone of plastic equilibrium and that in which predominantly elastic

stresses exist. Furthermore, it is assumed that the material is incompressible, giving rise to the continuity equation in the plasticity theory. This is not strictly true in the case of sand. In any example studied, the investigator has, of course, no certainty that the mechanism for which he has determined the lowest failure load among those he has examined is, in fact, the actual failure mechanism, but he can be sure that he has calculated at least an upper boundary to the load or stress. If the hypothesis of extension of the real failure surface deeper than Prandtl's failure mechanism is accepted as being true, then the explanation of the "Kink" and the different curves on both sides of it can be attributed to different failure surfaces and the intersection of the bottom of the box with these surfaces at different points.

The same anomaly seen in Fig.32 may also be seen in Figs. 33 and 34. As may be noted from an examination of the plotted points in Figs.33 and 34, the unusual results were not due to experimental errors since multiple tests with different plates yielded practically the same results.

Data concerning the influence of soil depth on the ultimate bearing capacity, the settlement at ultimate bearing capacity and the coefficient of subgrade reaction, are limited.

Goodman, Hegedus & Liston (26) realised the depth of the soil layer influence but they chose a soil depth to produce semi-infinite conditions and so they eliminated the soil depth from their dimensional analysis of size effect. Iliya (24) studied the depth of the soil layer influence for a circular plate in a rectangular box. His results are in close agreement with the general shapes of the curves presented in Figs.32 through 34 if we consider the smooth inside faces of boxes in this study as compared with the rough inside faces of the box he used. However, he reports that the influence is felt until the depth of the soil layer becomes 8-times the width of the plate as compared with the 10-times in this study. This difference in the results may be due to the different sands and different vibrating procedures employed in both investigations. Also the lengths and widths of the boxes in this study, being smaller than his corresponding dimensions (6-times the plate width in this investigation as compared with 8-times the plate diameter in his case) will produce a more confining effect to the horizontal extension of the failure surface and hence forcing it to go deeper. In addition, the shape of the plate may also have its effect in both investigations.

However, due to the limited number of experiments related to this problem, conclusions drawn are not definite and it is suggested that further research along this line be carried.

5.5 Experimental Versus Theoretical Results

Having discussed the interference of the sides and bottom of the boxes and the influence of the sizes and shapes of the plates on the ultimate bearing capacity, the settlement at ultimate bearing capacity and the coefficient of subgrade reaction in the preceding articles, it now remains to compare the experimental results with theoretical values. For the purpose of this comparison and as mentioned in chapter 2, Terzaghi's approximate formulas for the bearing capacity of footings will be used. Square plate 1 x 1 - in. in box No.8 (Table 3) is chosen for this comparison because interference from the sides and bottom is negligible (Art. 5.1).

According to Terzaghi: $q_0 = 0.8 \times B N_f$ for a square footing.

For a friction angle of 45.2° , N_f is equal to 331 for a smooth footing and 322 for a rough one (Appendix A). Hence q_0 is equal to 8.20 psi and 7.98 psi for the smooth and rough cases respectively.

The experimental value of q_0 is 12.4 psi (Fig.19). This value is 1.55 to 1.51 the theoretical value depending on the smoothness of the base of the footing, being nearer to 1.51 (Art. 1.3).

Tables 8 through 12 (Appendix C) show that the observed bearing capacities are 0.95 to 4.1 times the corresponding theoretical values. It is to be observed that the 0.95 value

exists only in the case of Davis and Woodward's experiments; otherwise this value is greater than 1. Vesic reports that this value generally varies from 1.2 to 4.0. A fully satisfactory explanation of this phenomenon has not yet been found. But in the conditions of plane strain, with one principal stress intermediate in value between the other two, the actual angle of internal friction may be somewhat higher than that indicated in the triaxial tests. This may be one of the reasons that the values of N_{γ} measured in model tests on long footings exceed the theoretical values. Such a reasoning fails in the case of square or circular footings.

Thus, although the 0.8 coefficient for a square footing in Terzaghi's equation is too high (Art.5.3) for local sand, the bearing capacity obtained from that equation is quite conservative for design.

CHAPTER SIX

CONCLUSIONS

From the results of this investigation the following observations may be made:

- 1- The ratio of the cubical soil bed to the width of the square plate used in model studies of bearing capacity must be at least ten where side effects are to be neglected.
- 2- The ultimate bearing capacity for square plates placed on the surface of dense cohesionless soils varies directly with the width of the plate.
- 3- The ultimate bearing capacity for rectangular plates placed on the surface of dense cohesionless soils increases with the increase in length to width ratio.
- 4- The equation of Terzaghi for the ultimate bearing capacity of square plates placed on the surface of cohesionless soils can be safely applied to Khalde¹ sand.
- 5- The settlement at the ultimate bearing capacity for square plates placed at the surface of dense cohesionless soils increases at a higher rate than the increase in the side of the plate.
- 6- The settlement at the ultimate bearing capacity for rectangular plates increases with the increase in the length to the width ratio.

- 7- For a relative density D_r of 0.798 Khalde¹ sand exhibits general shear failure usually occurring at settlements not exceeding 10 percent of the foundation width.
- 8- The coefficient of subgrade reaction k_s is a constant for any one square plate on any particular cohesionless soil up to a contact pressure slightly above one-half the value of the ultimate bearing capacity of the soil for that plate.
- 9- The coefficient of subgrade reaction k_s is a constant for any one rectangular plate on any particular cohesionless soil up to a contact pressure not exceeding one-half the value of the ultimate bearing capacity of the soil for that plate.
- 10- The value of the coefficient of subgrade reaction for a square plate on the surface of a cohesionless soil decreases with the increase in the side of the plate but at a higher rate.
- 11- The value of the coefficient of subgrade reaction for a rectangular plate on the surface of a cohesionless soil decreases with the increase in the length to width ratio of the plate.

- 12- The thickness of the sand layer must be at least ten times the width of the foundation plate so as not to have any effects from the bottom of the container on the ultimate bearing capacity, the settlement at the ultimate bearing capacity, and the coefficient of subgrade reaction.
- 13- The minimum settlement at the ultimate bearing capacity of a footing resting on sand occurs when a solid stratum exists at a depth equal to four times the width of the footing.

APPENDICES

APPENDIX A

APPENDIX A

Steps Used in the Calculations of the Bearing Capacity Coefficient N_γ for a Strip Footing.

(Refer to freebody diagram, Fig. 35)

Typical steps to be carried out for all failure surfaces assumed for trial.

- 1- Compute the passive force F from the relation

$$F = \frac{1}{2} \gamma h^2 N_\gamma$$

where h is in terms of B and $N_\gamma = \tan^2 (45 + \phi/2)$

- 2- Compute the moment arm r , of the force F , which is assumed to act at $\frac{2}{3}$ the height h ($r = \frac{2}{3} h$)
- 3- Compute the weight W_1 of the triangle adf from the relation

$$W_1 = \frac{1}{2} \gamma h l$$

where l is in terms of B

- 4- W_1 acts at a distance of $n = x + \frac{2}{3} l$ from the center of the spiral, O
- 5- Compute the weight W_2 of the triangle abo from the relation:

$$\begin{aligned} W_2 &= \frac{1}{2} \gamma (ao)(ab) \sin \hat{aob} \\ &= \frac{1}{2} \gamma (ao)(ab) \sin (45 - \phi/2 + \psi) \end{aligned}$$

where ao and ab in terms of B

- 6- Find the center of gravity of the triangle abo and consequently arm m .

where m is in terms of B .

- 7- Compute the moment of the weight of soil obd, bounded by ob, od and the spiral bd, about the center of the spiral O from the relation.

$$M_s = \frac{r_o^3}{3(9 \tan^2 \phi + 1)} \left[\frac{e^{3B \tan \phi} (\sin B + 3 \tan \phi \cos B) - e^{3\alpha \tan \phi} (\sin \alpha + 3 \tan \phi \cos \alpha)}{3} \right]$$

where α and B are directed angles in radians, $r = r_o e^{\theta \tan \phi}$ and r_o is in terms of B.

- 8- The passive force P acts at $\frac{1}{3}$ rd of ab and makes an angle ϕ with the normal to ab as shown.
- 9- Find the arm S of the force P from the center of the spiral "O" where S is in terms of B.
- 10- Compute the force P from the relation

$$P = \frac{1}{S} (F \times r + W_1 \times n - W_2 \times m + M_s)$$

note that x and y are directed segments and P thus computed is a function of ϕ and B^2

- 11- Repeat steps 1 through 10 for the various assumed failure surfaces and plot the results of the values of P. The minimum value of P will be the controlling value to be used in determining N_s .

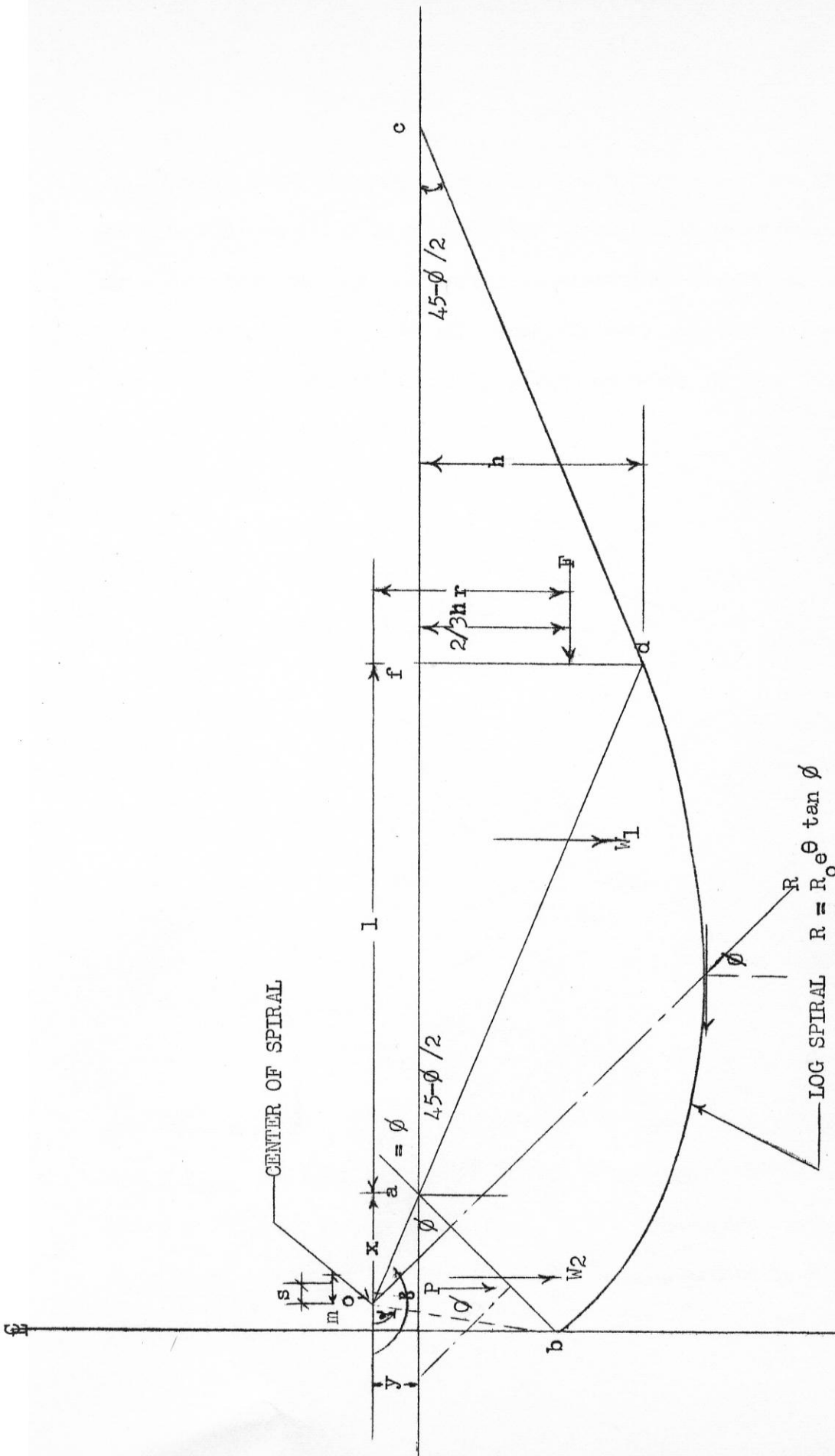


FIG. 35 FREE BODY DIAGRAM *

* TERZAGHI'S SOLUTION OF THE BEARING CAPACITY COEFFICIENT N_q .

Having determined $P_{\min.}$ and considering only surface footings on cohesionless soils we isolate the footing with sand below it as a free body and add the forces in a vertical direction. The equilibrium of the mass of soil requires that the sum of these vertical forces should be equal to zero as shown in Fig. 36.

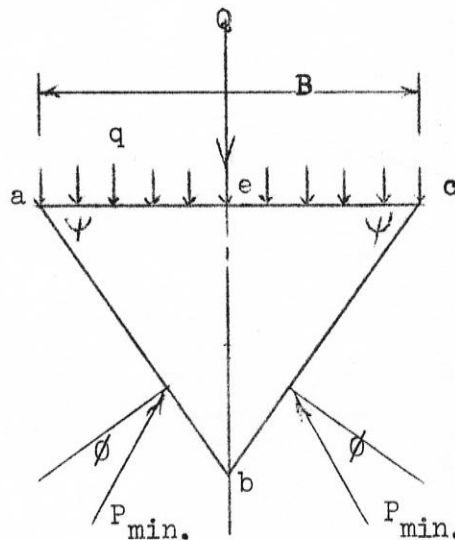


FIG. 36

$$Q + \frac{\gamma B^2}{4} \tan \psi = 2 P_{\min.} \cos (\psi - \phi) \quad \text{and}$$

$$Q = 2 P_{\min.} \cos (\psi - \phi) - \frac{\gamma B^2}{4} \tan \psi \quad \text{also}$$

$$Q = B \times \frac{\gamma B}{2} N_\phi = \frac{\gamma B^2}{2} N_\phi. \quad \text{Therefore}$$

$$N_\phi = \frac{2}{\gamma B^2} \left[2 P_{\min.} \cos (\psi - \phi) - \frac{\gamma B^2}{4} \tan \psi \right] \text{ which is dimensionless.}$$

Calculations of the Bearing Capacity Coefficient N_{ϕ} for a Plate
for $\psi = \phi$

(Refer to Fig. 37)

$$N_{\phi} = \tan^2(45 + \phi/2) = \tan^2(45 + \frac{45.2}{2}) = 5.886$$

$$\sin(45 - \frac{\phi}{2} + \psi) = \sin(67.6) = 0.925$$

$$B = 157.6^{\circ}$$

$$ab = \frac{\sqrt{2}}{2} B$$

Surface - 1 -

$$h = 0.90 B$$

$$F = \frac{1}{2} \gamma h^2 N_{\phi} = 2.39 \gamma B^2$$

$$r = \frac{1}{20}(3 + \frac{2}{3} \times 18) B = 0.75 B$$

$$M = F \times r = 1.795 \gamma B^3$$

$$l = 2.2 B$$

$$W_1 = \frac{1}{2} \gamma h l = 0.99 \gamma B^2$$

$$n = \frac{1}{20}(7 + \frac{2}{3} \times 44) B = 1.815 B$$

$$M = W_1 \times n = 1.796 \gamma B^3$$

$$a_0 = 0.375 B$$

$$W_2 = 0.125 \gamma B^2$$

$$m = 0.06 B$$

$$M = W_2 \times m = 7.375 \times 10^{-3} \gamma B^3$$

$$\alpha = 78^{\circ}$$

$$r = 0.675 B$$

$$r_0 = 0.172 B$$

$$M = 1.675 \gamma B^3$$

$$S = 0.01 B$$

$$\sum M = 5.2589 \gamma B^3$$

hence

$$P = \frac{1}{0.01B} \times 5.2589 \gamma B^3 = \underline{\underline{525.89 \gamma B^2}}$$

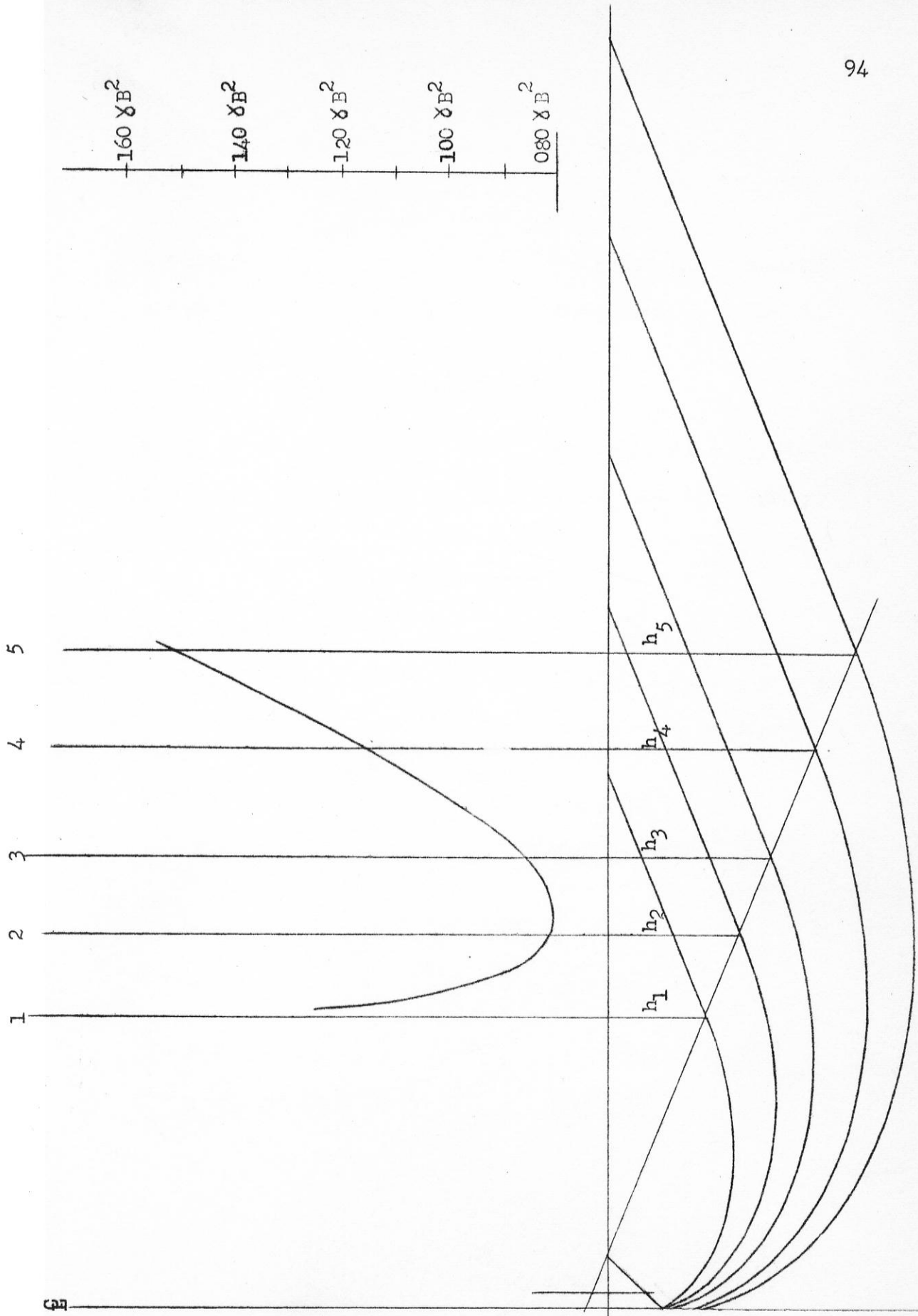


FIG. 37 FAILURE SURFACES FOR A STRIP FOOTING FOR A RISE ANGLE γ EQUAL TO ϕ .

Surface - 2 -

$$h = 1.2 B$$

$$F = \frac{1}{2} \gamma h^2 N_b = 4.24 \gamma B^2$$

$$r = \frac{1}{20} \left(2 + \frac{2}{3} \times 24 \right) B = 0.90 B$$

$$M = F \times r = 3.81 \gamma B^3$$

$$l = 2.97 B$$

$$W_1 = \frac{1}{2} \gamma L \times h = 1.78 \gamma B^2$$

$$n = \frac{1}{20} \left(4 + \frac{2}{3} \times 59.4 \right) B = 2.18 B$$

$$M = W_1 \times n = 3.89 \gamma B^3$$

$$a_0 = 0.225 B$$

$$W_2 = 0.075 \gamma B^2$$

$$m = 0.04 B$$

$$M = W_2 \times m = 3 \times 10^{-3} \gamma B^3$$

$$\alpha = 64^\circ$$

$$r = 0.655 B$$

$$r_0 = 0.2125 B$$

$$M = 3.15 \gamma B^3$$

$$S = 0.1335 B$$

$$\sum M = 10.847 \gamma B^3$$

hence

$$P = \frac{1}{0.1335B} \times 10.847 \gamma B^3 =$$

$$\underline{81.25 \gamma B^2}$$

Surface - 3 -

$$h = 1.5 B$$

$$F = \frac{1}{2} \gamma h^2 N_{\phi} = 6.625 \gamma B^2$$

$$r = \frac{1}{20} \left(1 + \frac{2}{3} \times 30 \right) B = 1.05 B$$

$$M = F \times r = 6.95 \gamma B^3$$

$$l = 3.675 B$$

$$W_1 = \frac{1}{2} \gamma h l = 2.75 \gamma B^2$$

$$n = \frac{1}{20} \left(2 + \frac{2}{3} \times 73.5 \right) B = 2.55 B$$

$$M = W_1 \times n = 7.03 \gamma B^3$$

$$a_0 = 0.11 B$$

$$W_2 = 0.036 \gamma B^2$$

$$m = 0.09 B$$

$$M = W_2 \times m = -3.25 \times 10^{-3} \gamma B^3$$

$$\alpha = 53.5^\circ$$

$$r = 0.675 B$$

$$r_0 = 0.2635 B$$

$$M = 5.9625 \gamma B^3$$

$$S = 0.2335 B$$

$$\sum M = 19.9405 \gamma B^3$$

hence

$$P = \frac{1}{0.2335B} \times 19.9405 \gamma B^3 = \underline{85.5 \gamma B^2}$$

Surface - 4 -

$$h = 1.925 B$$

$$r = \frac{1}{20} \left(0 + \frac{2}{3} \times 38.5 \right) B = 1.3 B$$

$$F = \frac{1}{2} \gamma h^2 N_\phi = 10.9 \gamma B^2$$

$$M = F \times r = 14.16 \gamma B^3$$

$$l = 4.675 B$$

$$n = \frac{1}{20} \left(\frac{2}{3} \times 93.5 \right) B = 3.115 B$$

$$W_1 = \frac{1}{2} \gamma h l = 4.5 \gamma B^2$$

$$M = W_1 \times n = 14.06 \gamma B^3$$

$$a_0 = 0$$

$$m = \text{---}$$

$$W_2 = 0$$

$$M = W_2 \times m = 0$$

$$\alpha = 45.2^\circ$$

$$r_0 = 0.32 B$$

$$r = 0.707 B$$

$$M = 10.125 \gamma B^3$$

$$S = 0.3335 B$$

$$\sum M = 38.9375 \gamma B^3$$

hence

$$P = \frac{1}{0.3335B} \times 38.9375 \gamma B^3 = \underline{\underline{116.75 \gamma B^2}}$$

Surface - 5 -

$$h = 2.3 B$$

$$F = \frac{1}{2} \gamma h^2 N_\phi = 15.55 \gamma B^2$$

$$r = \frac{1}{20} (-0.6 + \frac{2}{3} \times 46) B = 1.5 B$$

$$M = F \times r = 23.343 \gamma B^3$$

$$l = 5.57 B$$

$$W_1 = \frac{1}{2} \gamma h l = 6.4 \gamma B^2$$

$$n = \frac{1}{20} (-2 + \frac{2}{3} \times 111.4) B = 3.62 B$$

$$M = W_1 \times n = 23.175 \gamma B^3$$

$$a_0 = 0.10 B$$

$$W_2 = 0.0325 \gamma B^2$$

$$m = 0.235 B$$

$$M = W_2 \times m = + 7.75 \times 10^{-3} \gamma B^3$$

$$\alpha = 38^\circ$$

$$r = 0.75 B$$

$$r_0 = 0.385 B$$

$$M = 18.6125 \gamma B^3$$

$$S = 0.4335 B$$

$$\sum M = 65.139 \gamma B^3$$

hence

$$P = \frac{1}{0.4335B} \times 65.139 \gamma B^3 = \underline{150.5 \gamma B^2}$$

From the graph $P_{\min.}$ is equal to $80.6 \gamma B^2$,

$$\text{Now } \psi = \phi = 45.2^\circ \text{ and } \tan \phi = 1.007 \text{ and } \frac{\gamma B^2}{4} \tan \psi = 0.252 \gamma B^2$$

$$\text{So } N\gamma = \frac{2}{\gamma B^2} (2 \times 80.6 \gamma B^2 - 0.252 \gamma B^2) = 2 \times 160.948 = 321.896$$

$$\text{Say } N\gamma = 322.$$

Calculations of the Bearing Capacity Coefficient N_o for a Plate
for $\psi = 45 + \phi/2$

(Refer to Fig. 38)

$$N_o = \tan^2 (45 + \phi/2) = 5.886$$

$$\sin (45 - \phi/2 + 45 + \phi/2) = 1.0$$

$$B = 157.6^\circ$$

$$ab = 1.22 B$$

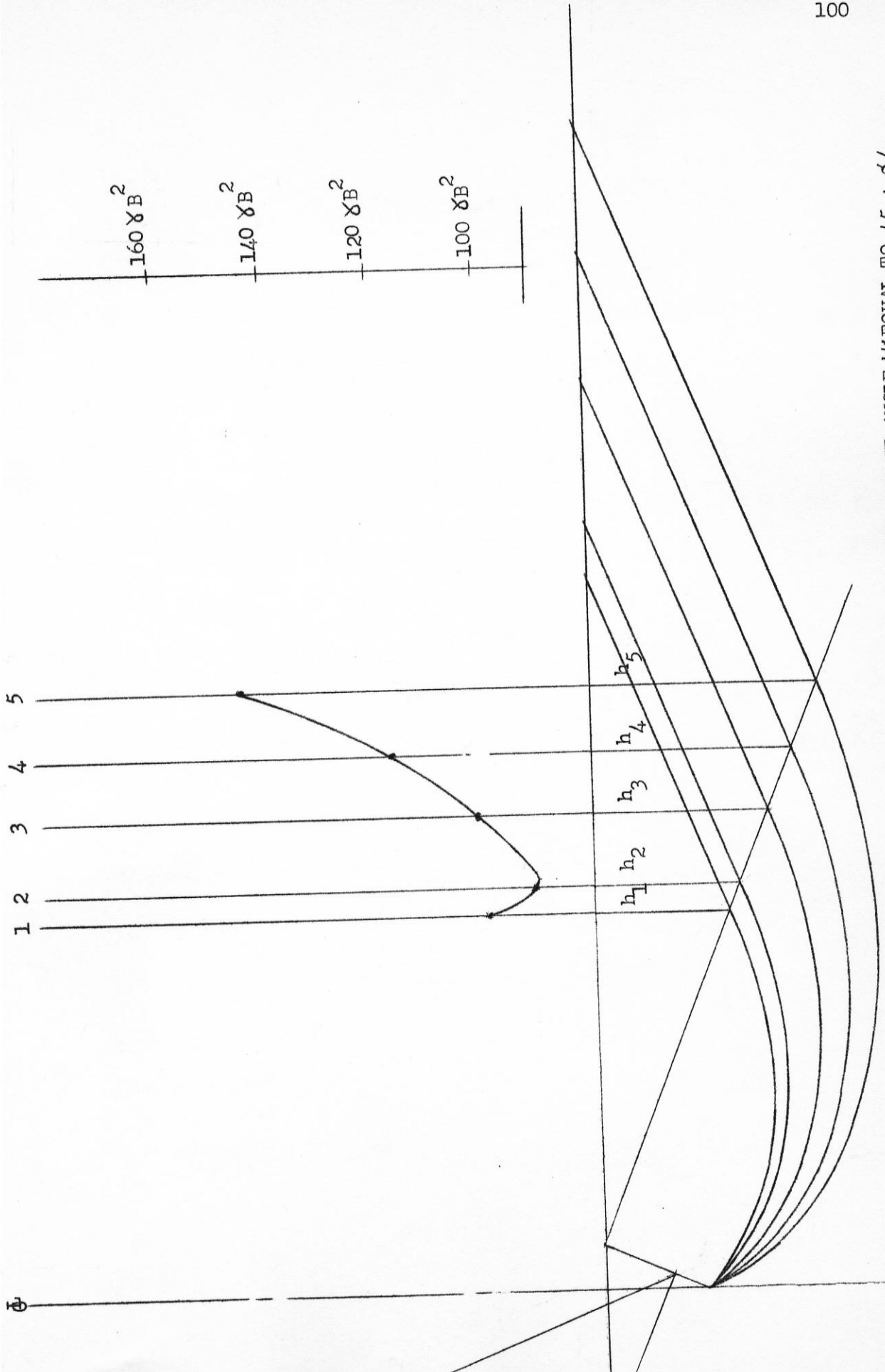


FIG. 38 FAILURE SURFACES FOR A STRIP FOOTING FOR A RISE ANGLE ψ EQUAL TO $45 + \phi/2$

Surface - 1 -

$$h = 1.595 B$$

$$F = \frac{1}{2} \gamma h^2 N_{\phi} = 7.475 \gamma B^2$$

$$r = \frac{1}{16} \left(3 + \frac{2}{3} \times 25.5 \right) B = 1.25 B$$

$$M = F \times r = 9.35 \gamma B^3$$

$$l = 3.88 B$$

$$W_1 = \frac{1}{2} \gamma h l = 3.085 \gamma B^2$$

$$n = \frac{1}{16} \left(7 + \frac{2}{3} \times 62 \right) B = 3.02 B$$

$$M = W_1 \times n = 9.33 \gamma B^3$$

$$a_0 = 0.50 B$$

$$W_2 = 0.305 \gamma B^2$$

$$m = 6.25 \times 10^{-2} B$$

$$M = W_2 \times m = 9.05 \times 10^{-3} \gamma B^3$$

$$\alpha = 87.5^\circ$$

$$r = 1.405 B$$

$$r_0 = 0.3025 B$$

$$M = 9.13 \gamma B^3$$

$$S = 0.278 B$$

$$\sum M = 27.8 \gamma B^3$$

hence

$$P = \frac{1}{0.278B} \times 27.8 \gamma B^3 = \underline{\underline{99.914 \gamma B^2}}$$

Surface - 2 -

$$h = 1.72 B$$

$$r = \frac{1}{16} (2 + \frac{2}{3} \times 27.5) B = 1.27 B$$

$$F = \frac{1}{2} \gamma h^2 N_\phi = 8.30 \gamma B^2$$

$$M = F \times r = 10.80 \gamma B^3$$

$$l = 4.18 B$$

$$n = \frac{1}{16} (5 + \frac{2}{3} \times 67) B = 3.106 B$$

$$W_1 = \frac{1}{2} \gamma h l = 3.595 \gamma B^2$$

$$M = W_1 \times n = 11.20 \gamma B^3$$

$$a_0 = 0.344 B$$

$$m = 3.125 \times 10^{-2} B$$

$$W_2 = 0.2095 \gamma B^2$$

$$M = W_2 \times m = -6.54 \times 10^{-3} \gamma B^3$$

$$\alpha = 82^\circ$$

$$r_0 = 0.325 B$$

$$r = 1.385 B$$

$$M = 11.55 \gamma B^3$$

$$S = 0.375 B$$

$$\sum M = 33.78 \gamma B^3$$

hence

$$P = \frac{1}{0.375B} \times 33.78 \gamma B^3 = \underline{90.000 \gamma B^2}$$

Surface - 3 -

$$h = 2.0925 B$$

$$F = \frac{1}{2} \gamma h^2 N_{\phi} = 12.55 \gamma B^2$$

$$r = \frac{1}{16} \left(1 + \frac{2}{3} \times 33\right) B = 1.438 B$$

$$M = F \times r = 18.04 \gamma B^3$$

$$l = 5.03 B$$

$$W_1 = \frac{1}{2} \gamma h l = 5.18 \gamma B^2$$

$$n = \frac{1}{16} \left(2 + \frac{2}{3} \times 80.5\right) B = 3.48 B$$

$$M = W_1 \times n = 18.1 \gamma B^3$$

$$a_0 = 0.1375 B$$

$$W_2 = 0.084 \gamma B^2$$

$$m = 9.375 \times 10^{-2} B$$

$$M = W_2 \times m = -7.86 \times 10^{-3} \gamma B^3$$

$$\alpha = 74^\circ$$

$$r = 1.344 B$$

$$r_0 = 0.366 B$$

$$M = 16.175 \gamma B^3$$

$$S = 0.5125 B$$

$$\sum M = 52.31 \gamma B^3$$

hence

$$P = \frac{1}{0.5125B} \times 52.31 \gamma B^3 = \underline{\underline{101.945 \gamma B^2}}$$

Surface - 4 -

$$h = 2.375 B$$

$$F = \frac{1}{2} \gamma h^2 N_\phi = 16.20 \gamma B^2$$

$$r = \frac{1}{16} \left(\frac{2}{3} \times 38 \right) B = 1.58 B$$

$$M = F \times r = 25.64 \gamma B^3$$

$$l = 5.75 B$$

$$W_1 = \frac{1}{2} \gamma h l = 6.84 \gamma B^2$$

$$n = \frac{1}{16} \left(\frac{2}{3} \times 92 \right) B = 3.835 B$$

$$M = W_1 \times n = 26.22 \gamma B^3$$

$$a_0 = 0$$

$$W_2 = 0$$

$$m = \underline{\quad}$$

$$M = W_2 \times m = 0$$

$$\alpha = 67.6^\circ$$

$$r = 1.312 B$$

$$r_0 = 0.40 B$$

$$M = 21.02 \gamma B^3$$

$$S = 0.625 B$$

$$\sum M = 72.94 \gamma B^3$$

hence

$$P = \frac{1}{0.625B} \times 72.94 \gamma B^3 = \underline{\underline{116.560 \gamma B^2}}$$

Surface - 5 -

$$h = 2.655 B$$

$$F = \frac{1}{2} \gamma h^2 N_\phi = 20.75 \gamma B^2$$

$$r = \frac{1}{16} (-1 + \frac{2}{3} \times 42.5) B = 1.705 B$$

$$M = F \times r = 35.4 \gamma B^3$$

$$l = 6.50 B$$

$$W_1 = \frac{1}{2} \gamma h l = 8.64 \gamma B^2$$

$$n = \frac{1}{16} (-2 + \frac{2}{3} \times 104) B = 4.21 B$$

$$M = W_1 \times n = 36.3 \gamma B^3$$

$$a_0 = 0.1375 B$$

$$W_2 = 0.084 \gamma B^2$$

$$m = 0.25 B$$

$$M = W_2 \times m = + 20.95 \times 10^{-3} \gamma B^3$$

$$\alpha = 61.75^\circ$$

$$r = 1.344 B$$

$$r_0 = 0.454 B$$

$$M = 30.65 \gamma B^3$$

$$S = 0.71 B$$

$$\sum M = 102.43 \gamma B^3$$

hence

$$P = \frac{1}{0.71B} \times 102.43 \gamma B^3 = \underline{143.900 \gamma B^2}$$

From the graph $P_{\min.}$ is equal to $89.85 \gamma B^2$

Now $\psi = 45 + \phi/2 = 67.6^\circ$ and $\tan \psi = 2.4262$

and $\frac{\gamma B^2}{4} \tan \psi = 0.60655 \gamma B^2$

So $N_\phi = \frac{2}{\gamma B^2} (2 \times 89.85 \times 0.9245 - 0.60655) \gamma B^2$

Say $N_\phi = 331$

APPENDIX B

APPENDIX B

Steps Used in the Calculation of Relative Density of Sand.

- 1- Determine the specific gravity of sand
- 2- Determine the maximum void ratio
- 3- Determine the minimum void ratio
- 4- Determine the void ratio e of sand used in the investigation
- 5- Determine the relative density D_r from the relation

$$D_r = \frac{e_{\max.} - e}{e_{\max.} - e_{\min.}}$$

1- Specific Gravity Determination

Determination No.	1	2	3
WT. Bottle + Water + Soil, W_1 , in g	784.45	748.40	723.75
Temperature, T in $^{\circ}\text{C}$	18.30	18.30	18.30
WT. Bottle + Water, W_2 , in g	628.132	623.232	630.032
WT. Bottle + Dry Soil in g	378.55	323.70	280.50
WT. Bottle in g.	128.85	123.95	130.75
WT. Soil, W_s , in g	249.70	199.75	149.75
Specific Gravity of Water at T , G_T	0.998563	0.998563	0.998563
Specific Gravity of Soil, G_s	2.674	2.671	2.6722

$$G_s = \frac{G_T W_s}{W_s - W_1 + W_2}$$

$$G_s = \underline{2.672}$$

2- Determination of e_{\max} .

Dry sand is poured gently into a one litre capacity container through a funnel one centimeter in diameter. The tip of the funnel is kept always about one inch above the level of the sand. The experiment was repeated thrice and comparable results were obtained. The density of the sand in its loosest state is 87.5 lb/ft^3 .

$$\gamma_d = \frac{G}{1 + e} \gamma_w \quad \text{and}$$

$$e = G \frac{\gamma_w}{\gamma_d} - 1$$

$$\therefore e_{\max.} = 2.672 \times \frac{62.5}{87.5} - 1 = \underline{0.908}$$

3- Determination of e_{\min} .

Different methods are employed to obtain the most compact state of the sand. The sand was vibrated for different times in rectangular and wide boxes to avoid arching. The densest state of the sand in this investigation was obtained by tamping the sand gently in a cylindrical mould in shallow layers. The maximum density obtained was 113.1 lb/ft^3 .

$$e = G \frac{\gamma_w}{\gamma_d} - 1$$

$$e_{\min.} = 2.672 \times \frac{62.5}{113.1} - 1 = \underline{0.475}$$

4- Determination of e

The sand used in this investigation has a unit weight of 107 lb/ft³. Hence

$$e = 2.672 \times \frac{62.5}{107} - 1 = \underline{0.561}$$

5- Determination of relative density

$$D_r = \frac{e_{\max} - e}{e_{\max} - e_{\min.}}$$

$$= \frac{0.908 - 0.561}{0.908 - 0.475} = \frac{0.347}{0.435} = \underline{0.798}$$

APPENDIX C

Table 8 (24)

Experimental Versus Theoretical Results

(From R. Iliya)

Footing Shape	Plate Diameter (in.)	Ultimate Bearing Capacity q_u (lb/ft ²)	Theoretical Value Using Tezaghi's E_c (lb/ft ²) *	Ratio of Experimental to Theoretical	Settlement (in.) **	Ratio of Settlement to Plate Diameter	K_s (tor./ft ³)	Ratio of K_s ***
Circular	2.22	650	538	1.21	0.194	0.0875	65	$\frac{65}{65} = 1$
	3.14	910	761	1.20	0.39	0.125	46	$\frac{46}{65} = 0.708$
	4.44	1290	1076	1.20	0.78	0.175	32.5	$\frac{32.5}{65} = 0.5$

*Values calculated are based on an average angle of internal friction of 38.75 degrees and a mean density of 101 pcf.

**Values read off the average curves at the points corresponding to the ultimate bearing capacity.

***Values are calculated by A. Najm.

EXPERIMENTAL VERSUS THEORETICAL RESULTS

(From Selig and McKee)

Footing Shape	Dimensions In.	Average Bearing Capacity Load lb/in. ²	Theoretical* Value Using Terzaghi's Equations lb/in. ²	Ratio of Experimental Theoretical
Square	2 x 2	9.3	9	1.03
	3 x 3	15.1	13.5	1.12
	4 x 4	19.1	18	1.06
Circular	2.26 diameter	9.3	5.3	1.75
	3.39	14.1	7.95	1.77
Rectangular	3 x 6	15.9	11.7	1.36
	3 x 9	17.5	11.7	1.50
	3 x 12	22.5	11.7	1.92
	3 x 15	22.5	11.7	1.92
	3 x 18	21.7	11.7	1.85
	3 x 21	23.1	11.7	2.06

*Values calculated by R.A. Iliya based on an average angle of internal friction of 39.5 degrees and a mean density of 112.3 lb/ft³.

TABLE 10 (33)

EXPERIMENTAL VERSUS THEORETICAL RESULTS

(From Meyerhoff)

Footing Shape	Dimensions	Average Bearing Capacity lb/ft ²	Theoretical* Value Using Terzaghi's Equation lb/ft ²	Ratio of Experimental Theoretical
Square	1/2 x 1/2	720	388	1.85
	1 x 1	1200	775	1.55
Rectangular	1/2 x 1 1/2	700	486	1.44
	1/2 x 3	1080	486	2.22
	1/2 x 4 1/2	1560	486	3.2
	1/2 x 6	1240	486	2.56
	1 x 3	1640	972	1.69

* Values calculated by R.A. Iliya based on an angle of internal friction of 30.5 degrees, and a density of 106 lb/ft³.

Table 11 (2)

Significant Results of Loading Tests With
Circular Plates at the Surface

(From Vesic)

Plate Diameter B (in.)	Ultimate Pressure q_o (psi)	Theoretical [*] q_o (psi) Terzaghi	Ratio of Experimen- tal q_o to Theo- retical	Ultimate Settlement (P_o) (in.)	$\frac{P_o}{B}$ (%)
2.13	33.8	8.25	4.1	0.126	5.9
3.94	53.8	15.25	3.53	0.227	5.8
6.00	73.4	23.3	3.14	0.425	7.1
8.00	79.2	31.0	2.55	0.667	8.3

* Values calculated by A.S. Najm based on an average angle of internal friction of 43.4 degrees and a mean density of 96.2 lb/ft³.

EXPERIMENTAL VERSUS THEORETICAL RESULTS

(From Davis and Woodward)

Footing Shape	Dimensions In.	Average Bearing Capacity Load lb/in. ²	Theoretical* Value Using Terzaghi's Equation lb/in.	Ratio of Experimental Theoretical
Rectangular	1 x 24	16.0	14.7	1.09
		16.0	14.7	1.09
		14.0	14.7	0.95
		18.0	14.7	1.23
	1 x 10	22.0	14.7	1.49
		20.0	14.7	1.49
		14.0	14.7	0.95
		16.0	14.7	1.09
		22.0	14.7	1.09
	Circular	2 diameter	21	17.7
22			17.7	1.24
23			17.7	1.30

*Values calculated by R.A. Iliya based on an angle of internal friction of 36 degrees and a density of 102 lb/ft³.

BIBLIOGRAPHY

1. Terzaghi, K., "Theoretical Soil Mechanics," Chapter 8, John Wiley and Sons, Inc., New York, 1948
2. Vesic, A.B., "Bearing Capacity of Deep Foundations in Sand," Highway Research Record No.39, (1963).
3. De Beer, E.E., and Vesic, A.B., "Etude Experimentale de la Capacite Portante du Sable sous des Fondations Directes Etablies en Surface." Annales des Travaux Publics de Belgique, 59: 3,5-58 (1958).
4. Terzaghi K., "Evaluation of Coefficients of Subgrade Reaction," Geotechnique, pp. 297-326, Vol. 5, No.4, December 1955.
5. Meyerhoff, G.G., "The Ultimate Bearing Capacity of Foundations," Geotechnique, pp. 301-332, Vol. 2, December 1951.
6. Prandtl, L., "Uber die Harte platisher Korper." Nachrichten Kon. Gesell. der Wissenschaften, Math. Phys. Klasse, 74-85, Gottingen (1920).
7. Prandtl, L., "Uber die Eindringungsfestigkeit plastischer Baustoffe und die Festigkeit von Schneiden." Zeitschrift fur Angewandte Mathematik und Mechanik, 1:1, 15-20 (1921).
8. Reissner, H., "Zum Erddruckproblem." Proc. First Intern. Conf. Applied Mech., 295-311, Delft (1924).
9. Caquot, A., "Equilibre des massifs a frottement interne." Gauthier-Villars, Paris (1934).
10. Buisman, A.S.K., "De weerstand van paalpunten in zand." De Ingenieur, 50: 25-28, 31-35 (1935).
11. Taylor, D.W., "Fundamentals of Soil Mechanics," Chapter 19, John Wiley and Sons, Inc., New York, 1962.
12. Tschebotarioff, G.R., Soil Mechanics, Foundations and Earth Structures," pp. 136-137, McGraw-Hill Book Company, Inc., New York, 1951.
13. Scott, R.F., "Principles of Soil Mechanics," Chapter 9, Addition-Wesley Publishing Company, Inc., Massachusetts, 1963.

14. Sokolovski, V.V., "Statics of Soil Media," London: Butterworth, 1956.
15. Berezantsev, V.G., "Osesimetricznaia Zadacha Teorii Nogo Ravnovesia Sypuchei Sredy," Gostechizdat, Moscow (1952).
16. Jumikis, A.R., "Soil Mechanics," pp. 618-640, Van Nostrand Company, Inc., New York, 1962.
17. Skempton, A.W., "The Bearing Capacity of Clays," Proceedings of Building Research Congress, Division I, Part II, pp. 180-189, London 1951.
18. De Beer, E.E., "Etude des Fondations sur Pilotis et des Fondations Directes," Annales de Travaux Publics des Belgique, 46:1-78 (1945).
19. Meyerhoff, G.G., "Recherches sur la Force Portante des Pieux," Annales de l'Institut Technique du Batiment et des Travaux Publics, 6: 63-64, 371-374 (1953).
20. Bishop, R.F., Hill, R., and Mott, N.F., "The Theory of Indentation and Hardness Test." Proc. of the Physical Soc., 57: 147-159 (1945).
21. Skempton, A.W., Yassin, A.A., and Gibson, R.E., "Theorie de la force portante des pieux." Annales de l'Institut Rechnique du Batiment et des Travaux Publics, 6: 63-64, 285-290 (1953).
22. Ladanyi, B., "Etude theorique et experimentale de l'expansion dans un sol pulverulent d'une cavite presentant une symetrie spherique ou cylindrique." Annales des Travaux Publics de Belgique, 62: 105-148, 365-406 (1961).
23. Mayerhoff, G.G., "The Tilting of a large Tank on Soft Clay," Proceedings of the South Wales Institute of Engineers, Vol. L XVII, No.2, pp. 53-71, 1951.
24. Iliya, R., "Static Load Versus Settlement for Geometric Shapes on Cohesionless Soil," Department of Civil Engineering, University of Texas, Austin, pp. 16-23, 1965.

25. Yoder, E.J., Principles of Pavement Design, pp. 53-54, 1965.
26. Goodman, L.J., Hegedus, E., and Liston, R.A., "Scaling Considerations in Plate-Sinkage Tests," Highway Research Record No.145, (1966).
27. Skempton, A.W., "An Investigation of the Bearing Capacity of Soft Clay Soil," Jour. Inst. of Civil Eng., 1942.
28. Lambe, T.W., "Soil Testing For Engineers," Triaxial Compression Test on Cohesionless Soil (1954).
29. Kedzi, A., "The Effect of Inclined Loads on the Stability of a Foundation," Proc. 5th Int. Conf. Soil Mech. and Found. Eng. I, 699, 1961.
30. Meyerhoff, G.G., "The Bearing Capacity of Footings Under Eccentric and Inclined Loads," Proc. 3rd Int. Conf. Soil Mech. and Found. Eng. 1,440, 1953.
31. Meyerhoff, G.G., "Discussion of Paper by Jumikis, A.," "Rupture Surfaces in Sand Under Oblique Loads," Proc. ASCE, Paper No.861, 1956.
32. Casagrande, A., and Shannon, W.L., "Stress Deformation and Strength Characteristics of Soils Under Dynamic Loads," Proc. 2nd Int. Conf. Soil Mech., Vol. 5, Paper II & 10, pp. 29-34, 1948.
33. Meyerhoff, G.G., "An Investigation of the Bearing Capacity of Shallow Footings on Dry Sand," Proc. 2nd Int. Conf. Soil Mech. 1:237, 1948.
34. Meyerhoff, G.G., "The Bearing Capacity of Sand," Ph.D.(Eng.) Thesis, Univ. of London, 1950.
35. Selig, E.T., and McKee, K.E., "Static and Dynamic Behavior of Small Footings," Proceedings of the American Society of Civil Engineers, Soil Mechanics and Foundations Division, SM6, December, 1961.
36. Davis, E.H. and Woodward, R.J., "Some Laboratory Studies of Factors Pertaining to the Bearing Capacity of Soils," Reprint No. 6, Proceedings of the Twenty-ninth Annual Meeting of the Highway Research Board, December 1949.